信州大学審査学位論文

Synchronization-Based Control of a Robotic Suit for Walking Assist

March 2012

ZHANG XIA

Contents

Figures

Tables

Tables

Chapter 1

Introduction

Chapter 1 Introduction

1.1 Background

Japan is going to be the Old Aged Society in year 2014 with the elderly population of 25%, which means there will be one person older than 65 among every four. The aging process results in the problems of physical function decline (muscle weakening) which troubles the elderly in their daily-life activities [1]. For example, the decrease in walking speed, the step length, walking ratio (the ratio of step length (m) to cadence (step/min)) and the joint torque of leg is thought the productive of muscle weakening, which also results in a failure of maintaining a position. As walking can be considered as one of the key activities in Self-Reliance life, many research projects including wearable power-assist suits have been conducted for elderly walking assist.

Since 1996, Kazerooni *et al* have begun to work on the technology of human power amplifier [19]. In 2005, Kazerooni *et al* at Berkeley made a wearable Lower Extremity Exosketeton (BLEEX) seeking to supplement solders with the significant strength. Nowadays, the same group made the Ekso which aimed to be applied to the rehabilitation training [18]. It is reported that the Ekso is the bionic exoskeleton that allows wheelchair users to stand and walk. From 1991, Sankai *et al* at Tsukuba began the development of Robot Suit. Their representative achievement is HAL, which aims to be used in medical applications, welfare and other developments. These two examples are considered have the longest history of human assist related studies. Other several exoskeletons were developed, and were limited to predefined motions. Such as the "RoboKnee" is a powered knee brace that functions in parallel to the wearer's knee and transfers load to the wearer's ankle [20].

When encountering the problem of how to control a wearable robotic suit which is designed for an assist (power-assist or motion-assist) purpose, previous studies tend to solve it in one of two ways. In the first approach, the assist suits adapt to the user. In order to get the user's move intension, the suits are commonly controlled based on measuring bio-electrical signals or the algorithm of modeling a user's dynamics and kinematics.

HAL, for example, is controlled by the Phase Sequence Control method using bio-electrical signals and floor reaction forces as control input signals [2][3]. Using Phase Sequence Control method to control the HAL, the joint moving codes are categorized into active, passive and free modes according to the characteristic of the muscle force conditions (estimated based on the

myoelectric signals that reflect the operator's intension). Angle sensors, floor sensors are adopted in order to obtain the condition of the HAL and the operator. HAL has two kinds of control systems, one of which is called voluntary control system which responds to signals originating in the brain, the other is called autonomous control system which operates based on stored movement patterns and provides human movement sequences [3]. The voluntary control system is mostly used for assisting purpose, and the autonomous control system mostly for supporting rehabilitation. It is reported that those whose bio-electrical signals couldn't be easily or clearly obtained are exclusive of the assisting targets of the HAL system.

Another example is the BLEEX. The BLEEX project developed an exoskeleton capable of carrying its own weight plus an external payload. Using the information from the sensors in the sole of the foot, the controller determines which phase BLEEX operates at, and which of the three dynamic models should be applied to control the exoskeleton [4][5]. Control methods mentioned above are ways of outputting joint torque presumed by using kinematics or human muscle-activities and then supplementing the operators' insufficient force [7][8]. These systems have to deal with the system's complexity, because the bio-signals and kinematics of each user are changing from one to another. In addition, the sensors attached on the user's body for obtaining move intension are extra payload to the user. Furthermore, people who have severe damage in motor neuron are not the targets of the robotic suit controlled based on bio-signals.

In the second approach, the user adapts to the assist suit. For example those assist suits designed for the movement reeducation (rehabilitation training) or mobility of those whose legs are severe injured or almost completely disabled are controlled based on pre-defined trajectories. A reeducation device called the WalkTrainer, which has been developed for walk rehabilitation training of spinal cord injuries, relies on the combination of predefined robotic trajectory and muscle stimulation [9]. The standing-transfer ABLE, designed to improve mobility including several kinds of movements, implements movements with predefined trajectories [10].

Recently, a new control method based on Central Pattern Generation (CPG) for walking support is recently beginning to be studied and utilized with a viewpoint of mimicking human mutual interaction. Y. Miyake *et al.* have developed a cooperative walking system named walk-mate for walking support using rhythmic sounds [13]. The walk-mate uses a nonlinear phase oscillator to get information (the step timing of human) of mutual entrainment between human and robot, an another controller is use to adjust the phase difference between the step timing of human and robot's output to converge on a target phase difference. The results indicate the importance of mutual entrainment of rhythmic motion for walking support. The Honda Assist device is also based on CPG control and it has been designed for rhythmic assist and amplifying step-length [21].

However, in the real life, a nurse assisting a patient has to assist in a way to meet the specific

demand and physical condition of the patient [11]. For example, where the movement assistance is required, the nurse synchronizes herself in a timely manner to help passively according to the patient's need; for the rehabilitation training, the nurse will not be synchronous but actively provide a certain movement to reeducate the patient. The conceptualization of synchronization phenomenon in human-human interaction is shown in Fig. 1.1.1. Here comes the problem: how to realize the human-like assist action (active/passive assist action) with a robotic suit?

Our primary study on human-robot handshaking used neural oscillators to control each joint of a handshaking robot, and simulation and experiments have verified that neural oscillators had enabled the human-robot handshaking to be conducted in active/passive way according to the synchronization level of the robot [17]. The results of our primary study on human-robot handshaking inspired us to use the neural oscillators to control a wearable robotic suit. Thus, we proposed the synchronization-based control using neural oscillators for a robotic suit, which could be able to learn to synchronize with user's movement through interacting with the user. The natural assistant behavior of a robotic suit stemmed from synchronization-based control could be considered as a potential alternative to realize a more human-like assistance. We distinguish our study from previously mentioned approaches by coming up with a third way of developing a robotic suit for walking assistance using the interaction approach-synchronization-based control.

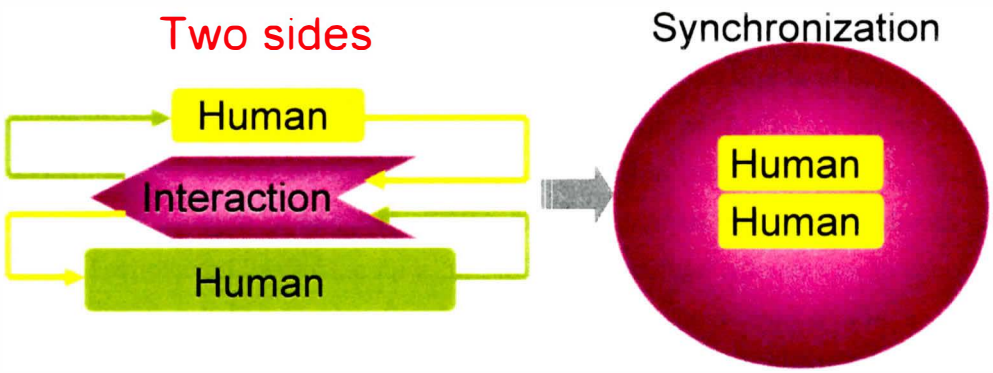

Fig. 1.1. 1 Synchronization phenomenon in human assist activities

Our inspiration of using the neural oscillator for a walking assist robot is also from neurophysiological studies. Neurophysiological studies of animal locomotion have revealed that the basic rhythm of movement is controlled by rhythm-generating networks in the nervous system, which are called central pattern generators (CPG). G. Taga *et al.* verified that a CPG for human walking probably exists in some form by simulating a biped walking robot, and they have shown that the walking movement of the simulated robot emerges from dynamic interaction through global entrainment among neural oscillators and the musculo-skeletal

system and the environment [15][16]. Locomotion emerged from the real-time interaction between the neural and mechanical dynamics without a priori limitations on prescribed trajectories of movements. Prior studies helped us to explore a neurophysiology-based vision related to the control of a walking assist robot.

The neural oscillator discussed in this study is a mathematic model of a network of two or more neurons responsible for the production of the timing cues of a rhythmic motor output pattern [12]. Over the last two decades, neural oscillators have been applied to control rhythmic movement via robots to generate rhythmic movement through interacting with the environment. M.M. Williamson *et al.* have used neural control for rhythmic arm movements which can interact with external forces [14]. Results of those aforementioned studies indicate that neural oscillators are able to implement great plasticity (the ability of a system to adapt to a changing environment) to the application objects. This plasticity is also necessary for a robotic suit to adapt in a way that enables synchronization and natural interaction, thus providing better assistance or rehabilitation training.

1.2 Study purpose

In this study, we proposed synchronization-based control using neural oscillators for a wearable robotic suit, which learns to synchronize with the user's movement through interacting with the user. By implementing the synchronization phenomenon using a wearable robotic suit, a natural assist behavior could be obtained.

In order to realize synchronization between a human user and the wearable robotic suit, we connect a neural oscillator to each joint of the suit to synchronize the robotic suit's motion with that of human user. The reason why we use neural oscillator is that it has extraordinary ability to synchronize its basic frequency with that of the periodic input signal. As human walk is considered as a kind of periodic motion, the application of neural oscillator to walking assist could be a potential solution to realize the human-like assist action with a robotic suit. In addition, we introduce a gain to switch the neural oscillator to be synchronous and non-synchronous status, thus the robotic suit could switch its assist model to be synchronous or non-synchronous for different assist requirement. Furthermore, coordination movement among the suit's multiple joints is achieved by the incorporation among neural oscillators.

Our approach is divided into three steps: first, we applied the synchronization-based control to a simpler one-degree-of-freedom (DOF) system, and investigated the mechanism of the proposal which enables synchronization and assist effect by conducting extensive simulations and experiments; second, we evaluated the feasibility of the proposal for walking assist with a

two-DOF robotic suit designed for supporting hip joint movement in walk; third, we designed a four-DOF robotic suit for walking assist by supporting the whole lower limb. Now we are working towards implementing the proposal to the four-DOF robotic suit.

This thesis is arranged as follows:

In chapter 2, we proposed the synchronization-based control for walking assist. In chapter 3, we explained the neural oscillator and its features in detail. In chapter 4, we proposed two kinds of control methods to realize the synchronization-based control: one is motion assist and the other is power assist, and compared these two kinds of methods. In chapter 5, we conducted preliminary computer simulations on a human-movement assist system and experiments with a joint torque sensing assist suit. In chapter 6, we depicted the four-DOF robotic suit designed for walking assist. In chapter 7, we conducted walk experiments with a two-DOF robotic suit by supporting the hip joint. In chapter 8, we implemented the proposal to the four-DOF robotic suit to investigate the validity. In chapter 9 we concluded this study.

References

[1] http://www.tyojyu.or.jp/hp/page000000500/hpg000000436.htm (in Japanese)

[2] Hiroaki Kawatoto, Yoshiyuki Sankai, "Power assist method based on Phase Sequence and muscle force condition for HAL,"*Advanced Robotics*, Vol.19, No.7,pp.717—734,2005.

[3] Suwoong LEE, Yoshiyuki SANKAI, "Minimizing the Physical Stress by Virtual Impedance of Exoskeletal Robot in Swinging Motion with Power Assist System for Lower Limb" *Journal of the Japan Society of Mechanical Engineers*, Vol.71, No.707,pp.274—282,2005.

[4] H.Kazerooni, Jean—Louis Racine,Lihua Huang, Ryan Steger, "On the Control of the Berkeley Lower Extremity Exoskeleton(BLEEX),"*IEEE Int. Conf. on Robotics and Automation,* Barcelona, pp.4364-4371, April 2005.

[5] Andrew Chu, H.Kazerooni, and Adam Zoss, "On the Biomimetic Design of the Berkeley Lower Extremity Exoskeleton(BLEEX),"*IEEE Int. Conf. on Robotic and Automation*, Barcelona, pp.4356-4363, April 2005.

[6] Kyoungchul Kong, Hyosang Moon, Beomsoo Hwang, Doyoung Jeon, Masayoshi Tomizuka, "Robotic Rehabilitation Treatments: Realization of Aquatic Therapy Effects in Exoskeleton Systems," *IEEE Int. Conf. on Robotic and Automation*, Japan, pp.1923-1928, May 2009.

[7] Takahiko Nakamura, Kazunari Saito, ZhiDong Wang, Kazuhiro Kosuge, and Masya Tajika, "Human Cooperative Motion Adapted Wearable Anti-Gravity Muscle Support System," *IEEE International Conference on Intelligent Robot and System,* pp.1843-1848, 2006.

[8] K. Kiguchi and Q. Quan,"Muscle-Model-Oriented EMG-Based Control of an Upper-limb Power-Assist Exoskeleton with a Neuro-Fuzzy Modifier", Proc. of IEEE World Congress of Computational Intelligence, pp. 1179-1184, 2008.

[9] Stauffer Yves, Mohamed Bouri Reymond Clavel, Yves Allemande and Roland Brodard, "A novol verticalized reeducation device for spinal cord injuries: the WalkTrainer, from defign to clinical trials" *Robotics 2010: Current and Future Challenges*, pp.194-209.

[10] Yoshikazu Mori, Ken Maejima and Katsuya Nagase, "ABLE: A Standing Style Transfer System for a Person with Disabled Lower Limbs-Chair and a Step Motions-," *JRSJ* Vol.27 pp.334-342,2009.

[11] http://www.limbach.org/ (in Japanese)

[12] U. Bässler, "On the Definition of Central Pattern Generator and its Sensory Control," *Biol. Cybern.*, Vol.54, pp.65-69,1986.

[13] Yoshihiro Miyake, "Interpersonal Synchronization of Body Motion and the Walk-Mate Walking Support Robot" *IEEE Transactions on Robotics*, Vol.25, No.3, pp. 638-644.

[14] Matthew M.Williamson, "Neural control of rhythmic arm movement," *Neural Networks 11*,pp.1379-1394.

[15] Gentaro Taga, "A model of the neuro-musulo-skeletal system for human location I. Emergence of basic gait," *Biological Cybernetics*, 73,pp.97-111,1995.

[16] Gentaro Taga, "A model of the neuro-musulo-skeletal system for human location II. Real-time adaptability under various constraints," *Biological Cybernetics*, 73,pp.113-121,1995.

[17] Tomofumi Kasuga, Minoru Hashimoto, "Human—Robot Handshaking using Neural Oscillators," *IEEE Int. Conf. on Robotics and Automation, Barcelona*, pp3813-3818, April 2005.

[18] http://www.eksobionics.com/ekso

[19] Kazerooni, H., "The Human Power Amplifier Technology at the University of California, Berkeley," *Journal of Robotics and Autonomous Systems*, Elsevier, Vol.19, 1996, pp.179-187

[20] Pratt, J., Krupp, B., Morse, C., Collins, S., "The RoboKnee: An Exoskeleton for Enhancing Strength and Endurance During Walking," *IEEE Conf. on Robotics and Automation*, New Orleans, 2004

[21] http://www.honda.co.jp/news/2008/c080422.html

Chapter 2

Synchronization-based control for walking assist

Chapter 2 Synchronization-based control for walking assist

2.1 Synchronization/non-synchronization phenomena in assist activity

When people interact with each other, such as nursing a patient, walking side by side or shaking hands, they are able to adapt to make one synchronized motion. Where a walking assistance is required, a nurse synchronizes herself in a timely manner to help according to the needs and physical conditions (balance maintenance and muscular strength) of the person she is assisting [1]. In the case of elderly people, they might be with weakened muscular strength or weakened balance maintaining ability, and they might need a crutch to support walking. Where a walking assist is required for the elderly people mentioned above, a nurse needs to stand at the patient's one side which is opposite to the side holding the crutch, and the nurse grasps the patient's arm and walks simultaneously side by side to support [2]. We refer this case to as synchronization-based assist. Figure 2.1.1 shows an example of the synchronization-based assist. In the case of severely injured people or motor neuron damaged people, they couldn't move without the help from other people or a mobility device. In order to assist those patients severely injured, a nurse needs to stand at the patient's back to hold up the patient's waist, and the nurse actively takes the patient to move [2]. We refer this case to as non- synchronized-movement assist. Figure 2.1.2 shows an example of the non-synchronization-based assist.

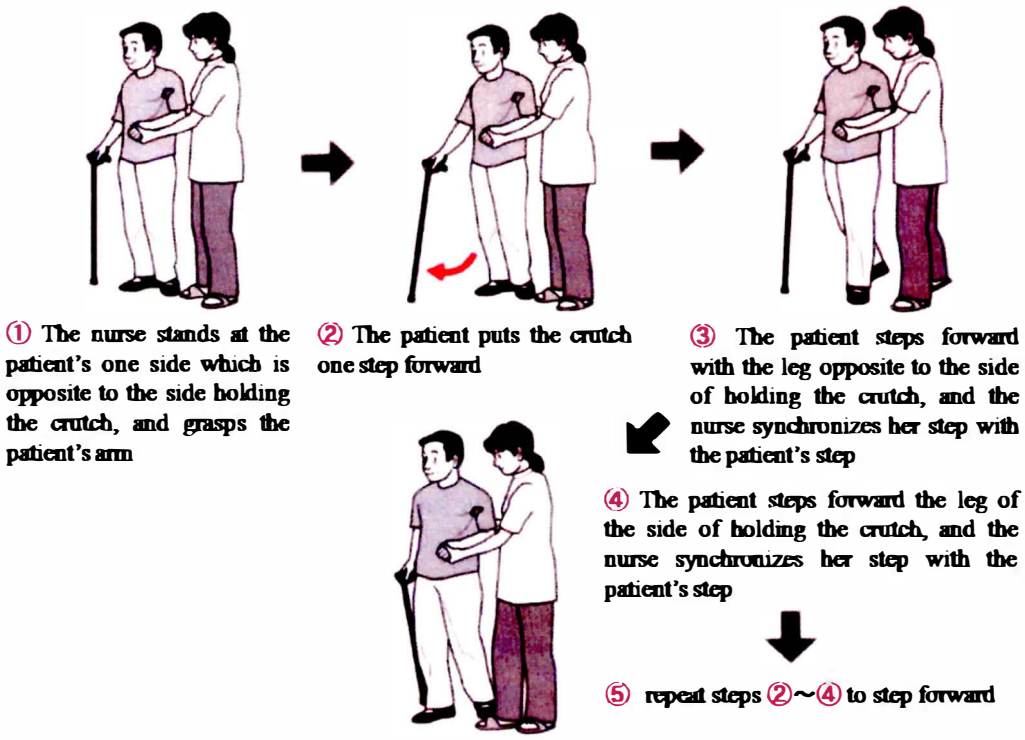

Fig. 2.1. 1 One example of synchronization-based assist

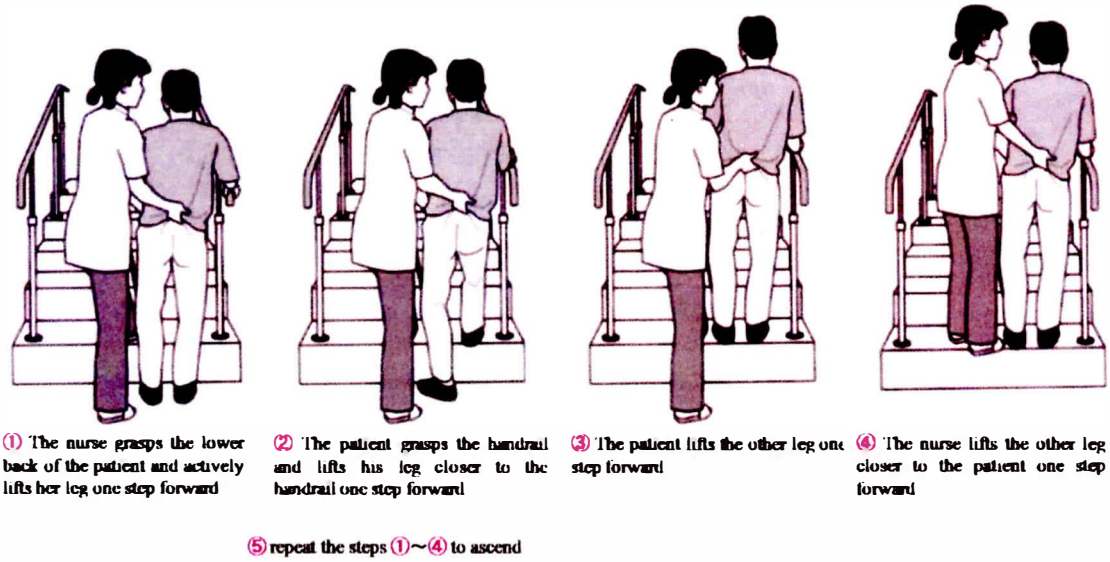

Fig. 2.1. 2 One example of non-synchronization-based assist

2.2 Neural oscillator for walking assist

As mentioned in the last section, a nurse decides to give synchronization-based assist or non-synchronization assist according to the patient's physical ability. We come with an idea of implementing the synchronization-based assist behavior with a robotic suit by using neural oscillators, because neural oscillator is known for its strong ability of frequency entrainment. The neural oscillator is able to synchronize its basic frequency with that of the periodic input signal. As human walk is considered as a kind of periodic motion shown in Fig.2.2.1 [3], the application of neural oscillator to movement assist could be a potential solution to realize the human-like assist action with a robotic suit.

In addition, we introduce a gain to switch the neural oscillator to be synchronous and non-synchronous status. This technique will be discussed in section 3.3.1.

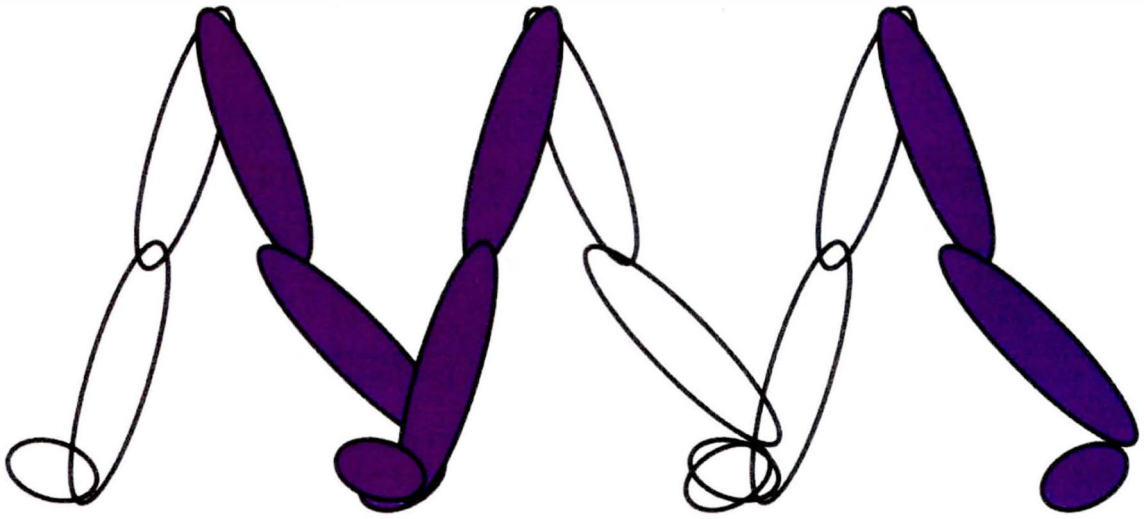

Fig. 2.2. 1 Periodic pattern of human walking

2.3 Synchronization-based control design

First, summarize the traditional control methods of wearable robotic suits. The control methods commonly used for wearable robotic suits can be generally summarized as one-way adaption, one of which is the robotic suit adapts to the user, the other is the user adapts to the robotic suit. The first approach, shown in Fig. 2.3.1, is that the assist suits are controlled to adapt to follow the user's intension, which is presumed by modeling the user's kinematics or by measuring bio-signals. This approach is ways of outputting joint torque presumed and then supplementing the operators' insufficient force. The second approach, shown in Fig. 2.3.2, is that the assist suit

with pre-defined motion takes the patient to move. That is, the user adapts to the assist suit's movement. The former control method is mainly adopted for power assistance purpose, and the latter is mainly adopted for mobility and rehabilitation training purpose. For different assisting purpose, different control strategy should be chosen thereof.

Although there are many research have been done in the field of lower limb assist, it is still far away saying there is a best solution.

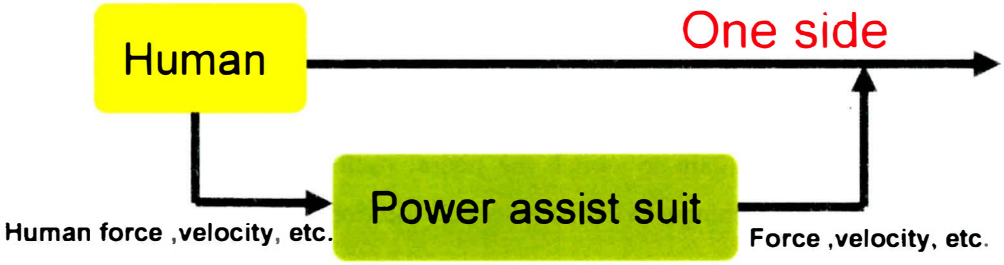

Fig. 2.3. 1 Conventional control method

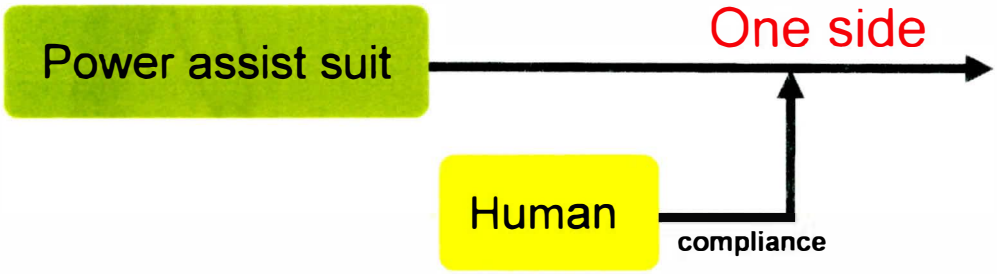

Fig. 2.3. 2 Compliance control method

In this study, a more universal control method aiming at mimicking human assist behavior is proposed. We refer it to as the synchronization-based control, of which the outline is shown in Fig. 2.3.3. Even though the suit and user have different patterns of motions initially, along with the user's moving intension being fed back into the controller of the assist suit, the motion of the assist suit is the timely synchronization with human motion and entrained to the same period. The user's move intension can be obtained by measuring mutual joint torque, which will be generated once there is any difference between the human motion and robot motion. Also, the user's move intension can be obtained by presuming the joint torque using the dynamics and kinematics.

We proposed two approaches using neural oscillator to enable a robot be both synchronous and assistive. One is using mutual joint torque between the user and the robot as input to the neural

oscillator, and the output of neural oscillator as the desired angle of the robot. We referred this proposal to as the synchronization-based motion assist. The second approach is using the human joint torque as input to the neural oscillator and the output of the neural oscillator as robot joint torque. We referred the second approach to as the synchronization-based power assist.

We analyzed the mechanism of synchronization-based motion and synchronization-based power assist in Chapter 4.

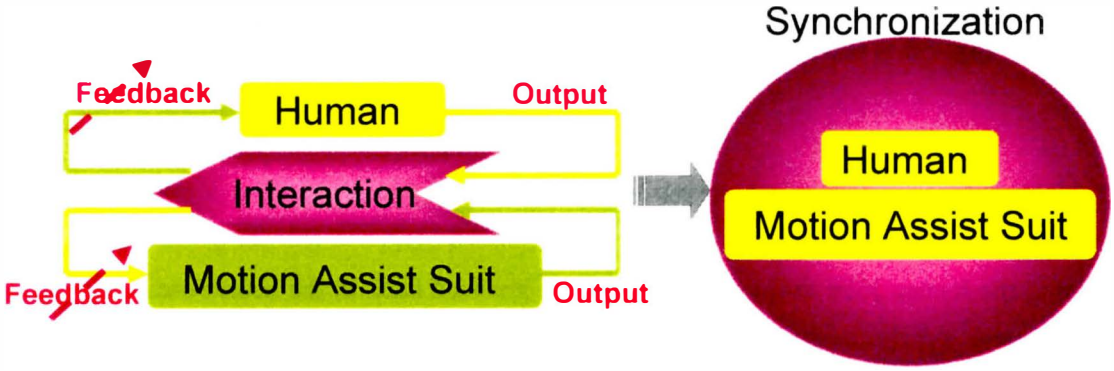

Fig. 2.3. 3 Proposed control method

2.3.1 Synchronization-based motion assist

The specific framework of the synchronization-based motion assist method is shown in Fig.2.3.4.

The mutual joint torque generated is used as input signals for neural oscillators and synchronized output signals of neural oscillators as desired joint angles. A proportional integral differential (PID) feedback controller generates a control signal for each joint of the robotic suit to follow the desired joint movement, and new locomotion is thus generated and again mutual joint torque is used as the input signal of the neural oscillator. These flows are repeated to achieve a series of entrained and synchronized movements between a user and a robotic suit. The PID control gains have been decided to make the joint angle follow the desired angle accurately and quickly. Here, the mutual joint torque means the interaction torque generated by human-robot interaction, and it doesn't mean the interaction torques in multi-joints of an object [4].

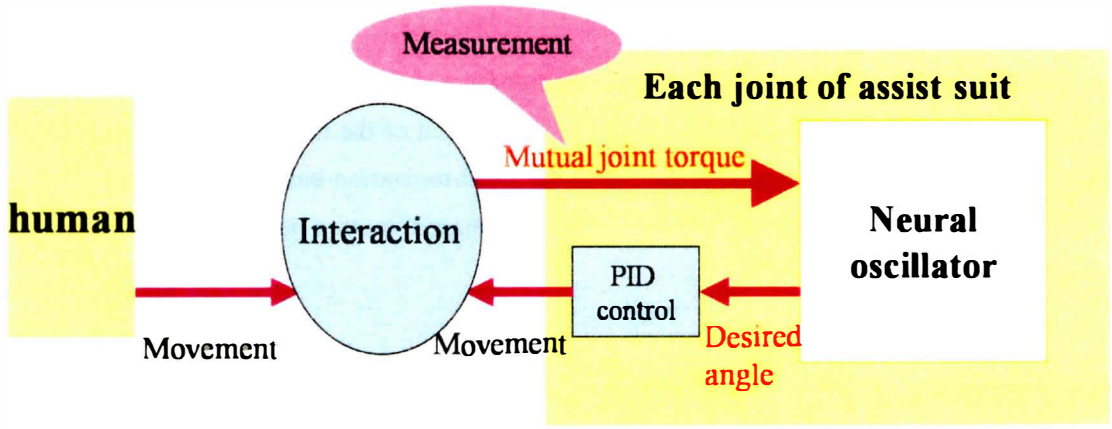

Fig. 2.3. 4 Block diagram of synchronization-based motion assist method

2.3.2 Synchronization-based power assist

Using the human joint torque as the external signal fed back to the neural oscillator, we also can achieve synchronization of the robot with the human using the approach described as follows: firstly, use the human joint torque as the input signals to the neural oscillator, then use the synchronized output signals of the neural oscillator as the robot joint torque. Figure 2.3.5 shows the framework of the synchronization-based power assist.

We discuss the feasibility of the two kinds of approaches of synchronization-based control in Chapter 4.

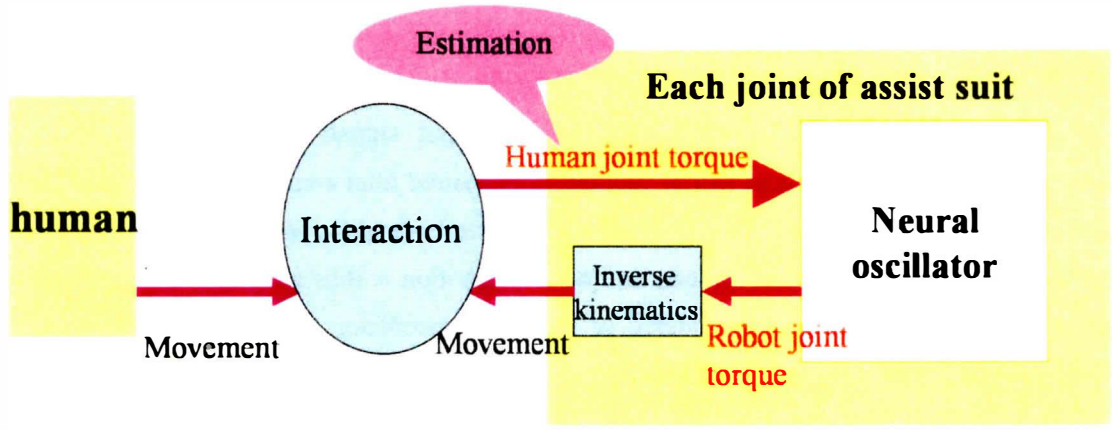

Fig. 2.3. 5 Block diagram of synchronization-based power assist method

References

[1] http://www.limbach.org/ (in Japanese)

[2] http://www.ryokuseikan.ac.jp/center/pdf/190222.pdf#search='歩行介助仕方' (in Japanese)

[3] K. Kong and M. Tomizuka, "Control of Exoskeletons Inspired by Fictitious Gain in Human,"IEEE/ASME Transactions on Mechatronics, Vol. 14, No. 6, pp. 689-698, 2009

[4] Hiroshi Nagasaki, "Movement Coordination and the Interaction Torque in Multijoint Motion," Rigakuryoho Kagaku, Vol.21(1),pp.75-79,2006

Chapter 3

Neural oscillators

Chapter 3 Neural oscillators

There are commonly two types of neural oscillators that are used in human-robot interaction. One is called phase oscillator and the other is called inhibitory oscillator (i.e. Matsuoka model). In the case of phase oscillator, phase differences among oscillators are easily designed by giving a desired phase as input to the current oscillator. However, it is known as difficult to calculate the phase relationships among multiple-joints of human during walking, and it lacks of flexibility in amplitude in trajectory control. Comparatively, Matsuoka model has been found effective in generating trajectory that controls a robot. The model consisting of two neurons with inhibitory connections in-between has been commonly used in controlling biped robot walking, because the inhibitory connections enable each neuron activate alternatively, and the alternation is similar to the flexion-extension motion in walking. M. M. Williamson reported the successful research of using the output of Matsuoka model to control the robot joint interacting with its input, and the input to the Matsuoka model could be either the force, or the position at the actuated-joint [5]. Our prior study on human-robot handshaking also used the Matsuoka model, and the study results showed that flexible handshaking was achieved using the output of Matsuoka model as the desired joint angle of robot [6]. For walking assist, one of the key factors that we need to consider is the flexible trajectory design. Therefore, we used Matsuoka model as the controller of a robot for walking assist.

3.1 Matsuoka model

Kiyotoshi Matsuoka presented some patterns of oscillations generated by cyclic inhibition networks consisting of two to five neurons [1]. Also he suggested that the oscillation generated by mutual inhibition network consisting of two neurons could be considered as a model for bipedal locomotion, and neurons rings consisting of four neurons as a model for quadrupeds, etc. In this paper, we use the network consisting of two neurons based on Matsuoka's model [2]. Equations (3.1) and (3.2) represent the structure of the neural oscillator adopted in this study. The structure of one neuron of neural oscillator is shown in Fig. 3.1.1. The structure consisting of two neurons is shown in Fig. 3.1.2. The black circles correspond to inhibitory connections, white circles to excitatory

$$T_r \frac{dx_i}{dt} + x_i = -\sum_{j \neq i} a_{ij} g(x_j) + S_i - b_i x_i' + (-1)^{i-1} Input_k \quad (3.1)$$

$$T_a \frac{dx_i'}{dt} + x_i' = g(x_i) \qquad g(x_i) = \max(0, x_i) \qquad (3.2)$$

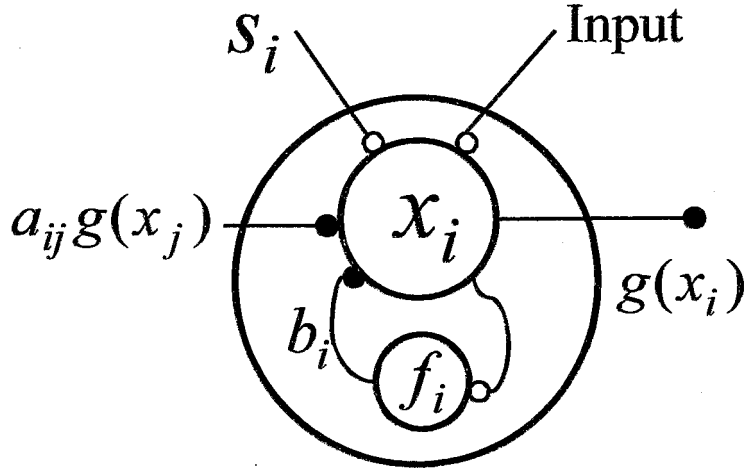

Fig.3.1. 1 Structure of a neuron

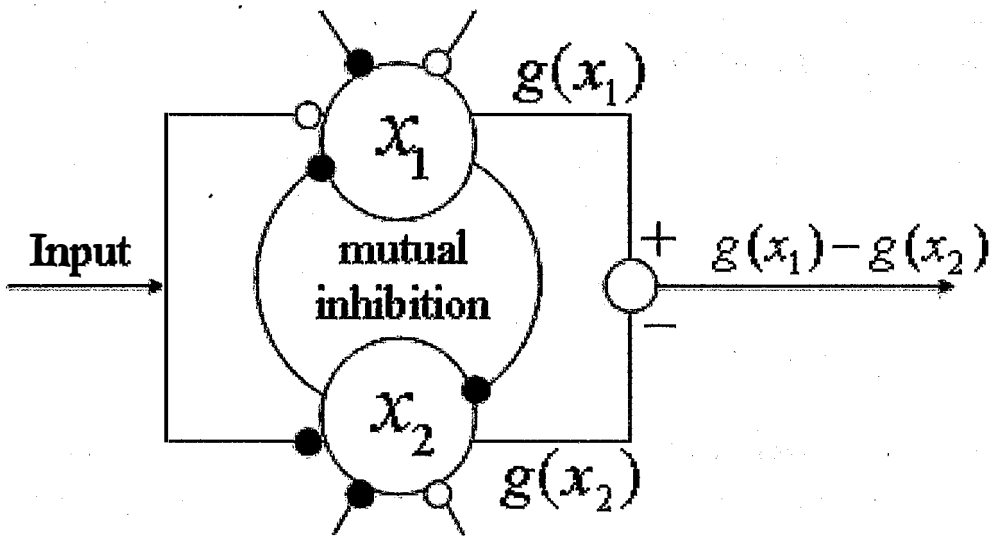

Fig.3.1. 2 Structure of a neural oscillator

x_i denotes the firing rate representing the potential of the i th neuron. x_i' is a variable representing the self-inhibition of the i th neuron, b_i is a constant representing the degree of self-inhibition on the inner state of the i th neuron, T_r and T_a are time constants of the inner state and adaptation of the i th neuron, a_{ij} is the connecting weight from the j th to i th neurons, s_i is steady-state input of the i th neuron.

3.2 Features of Matsuoka model

In this section, we recited the features of Matsuoka model's each parameters summarized by our former study [3]. The features were discussed with standard value of each parameter assigned as following: $a_{12} = a_{21}$ =1.2, $b_1 = b_2$ =2.5, $S_1 = S_2$ =2.0, T_r =0.2, T_a =2.0. The standard value of parameters are determined allowing stable oscillating referring to [2][3]. The initial state of each variable was determined by trial and error as follows: $x_1(0)$=3, $f_1(0)$=1, $x_2(0)$=2, $f_2(0)$=2. The frequency of neural oscillator without any response to external signal is called basic frequency.

- The value of S_i affects the oscillation's amplitude.

The amplitude of oscillation changes according to the value of the steady state S_i. The larger the value of S_i, the larger the amplitude is.

- The value of b_i affects the oscillation's amplitude, the time of getting steady, and the basic frequency.

Assign a larger value to b_i, the amplitude will get smaller, and the basic frequency will get higher, and the time of getting steady will become longer.

- The value of a_{ij} affects the shape of the oscillation and the basic frequency.

Change the value of connecting weight a_{ij}, the shape and the basic frequency of the oscillation will change. The larger the value of a_{ij}, the lower the frequency is. When $a_{12} = a_{21}$ =0.8, no oscillation is found to occur. Therefore, it is concluded that a specific range of a_{ij} existed to allow oscillation.

- The value of T_r, T_a affects the oscillation's amplitude and frequency

Fix the T_r and decrease the T_a, the amplitude will get smaller and the oscillation will eventually attenuate to zero, and the frequency will get higher.

Fix the T_a, and increase the T_r, the frequency of oscillation will get higher. Decrease the T_r, the amplitude will get larger but never exceed a certain limit.

Change the value of T_r and T_a under a steady ratio of T_r/T_a=1/10, the amplitude will not change, but the frequency changes in proportion to $1/T_r$.

3.3 Proposed model

In this study, we proposed using the neural oscillator consisting of two neurons, one neuron counts for the flexion movement of one joint, and the other for the extension movement of the joint. The proposed model is shown in Fig. 3.3.1.

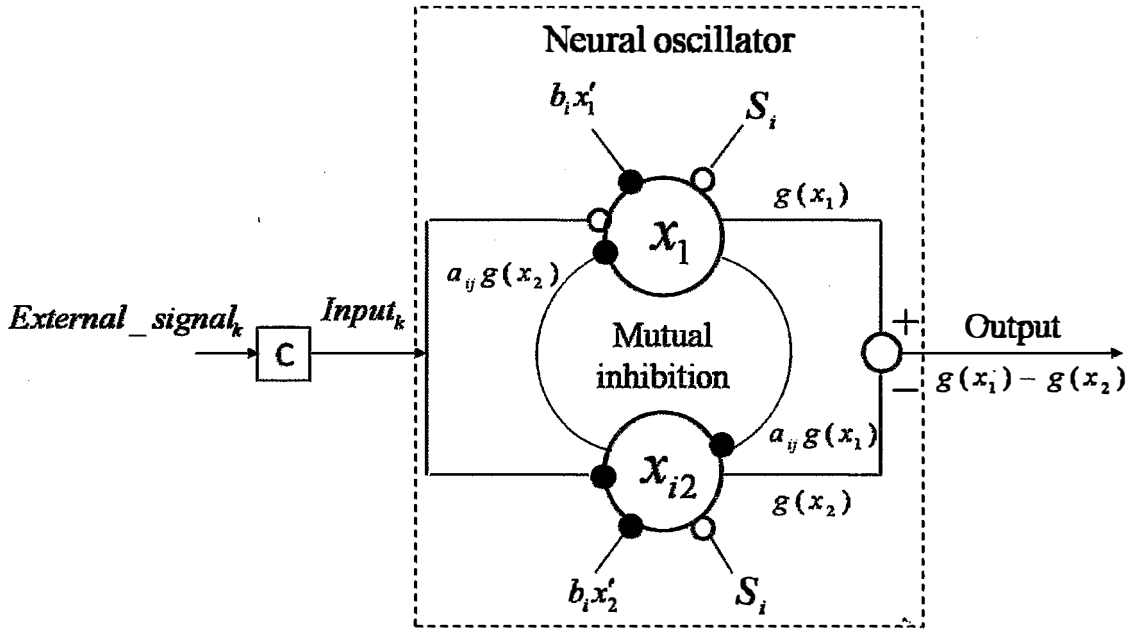

Fig.3.3. 1 Structure of proposed model

$Input_k$ is the external signal to the k th neural oscillator. The value of k is correspondent to the number of a robotic suit's joint. $Input_k$ in Fig.3.3.1 is obtained by multiplying the $Extenal\_signal_k$ by a gain C, called synchronization gain. $Extenal\_signal_k$ could be the mutual joint torque or human joint torque, depending on in which control model: motion-assist or power-assist. Synchronization gain C are determined as experiment requirements, so its value is discussed in sections that follow.

i, j represent the number of neuron, here $i = j = 1,2$. The output of one neural oscillator is calculated as max(0, x_1)-max(0, x_2). As long as the parameters mentioned above and the initial states of neurons are defined, the two neurons will be activated alternately at a certain frequency [2]. Premising stable oscillation and referring to [3], we determine the typical neural oscillator parameters as follows: $a_{12} = 1.2$, $b_i = 2.5$, $s_i = 2.0$. For T_r, T_a belongs to equations (3.1)-(3.2), and a characteristic is concluded by [3] such that when the ratio of T_r to T_a is smaller than 1/10, autonomous oscillation converges to zero. Assuming that to get autonomous oscillation, we should guarantee that the ratio of T_r to T_a is larger than 1/10, we determined

T_r by 0.12 and T_a by 0.6 for the robotic suit. If there is no input signal fed back to the neural oscillator, a sine-curve like output, shown by the red solid line in Fig. 3.3.2, will be generated. It can be found that the basic amplitude and frequency of the oscillation are 0.85 and 1Hz.

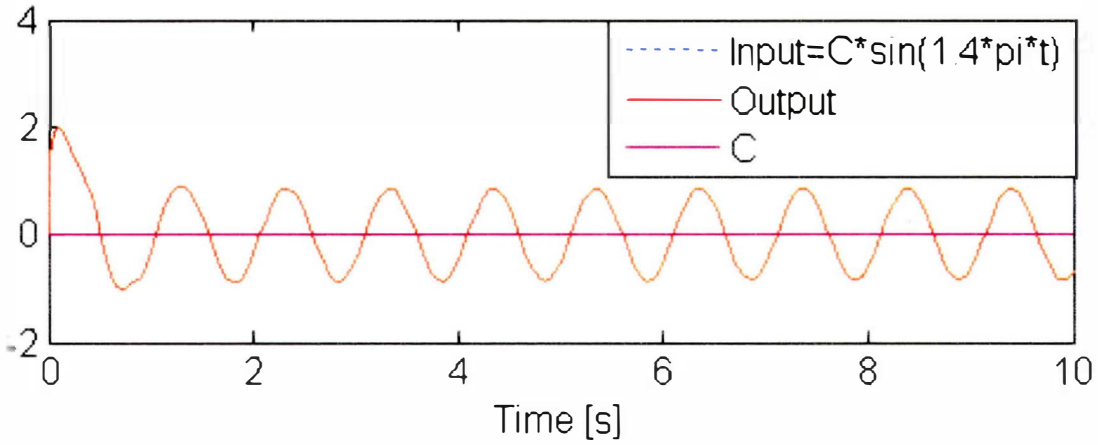

Fig.3.3. 2 Original oscillation of the neural oscillator (C=0)

3.3.1 Synchronization behavior

To investigate the effect of synchronization gain acting on the output of neural oscillator, we conducted a series of simulations by feeding back sinusoidal curve (with frequency of 0.7Hz). The value of C changed from 0 to 1 gradually along with the time cue. The output of neural oscillator and the gain C plotted against time was shown in Fig. 3.3.3. We showed the change of amplitude and frequency of outputs against the synchronization gain in Fig. 3.3.4 and Fig. 3.3.5 respectively. Along with the increase of the synchronization gain, the amplitude was found to be increasing while the frequency was entrained to that of the input (0.7Hz).

Then, we investigated the output of neural oscillators by feeding back couples of sinusoidal curves with different frequencies, of which were 0.4Hz, 0.7Hz, 0.9Hz, 1.1Hz, 1.3Hz and 1.6Hz. Each time we increased the C gradually (0.1) from 0 to 1. The frequency of output of the neural oscillator responding to each input is plotted against the synchronization gain and is shown in Fig. 3.3.6, and the amplitude is also plotted against the synchronization gain and is shown in Fig. 3.3.7.

As shown in Fig. 3.3.6, a valve value of the synchronization gain, found for each input, separates the output of neural oscillators into two groups: the first group maintains the original frequency, and the second group changes the frequency which is synchronous with that of the input signals. It can be found that the closer the basic frequency of the input signals to that of the neural oscillator, the smaller the valve values of the synchronization gain for each input. The amplitude increases along with the increase of synchronization gain for all kinds of input, shown in Fig. 3.3.7.

To conclude, different synchronization gain C brings about different outcome. With a larger gain, the neural oscillator synchronizes the frequency of its outputs with that of the inputs, and the amplitude of neural oscillators' outputs is getting increased, and vice versa. The closer the basic frequency of the input signals to that of the neural oscillator, more easily the synchronization occurs.

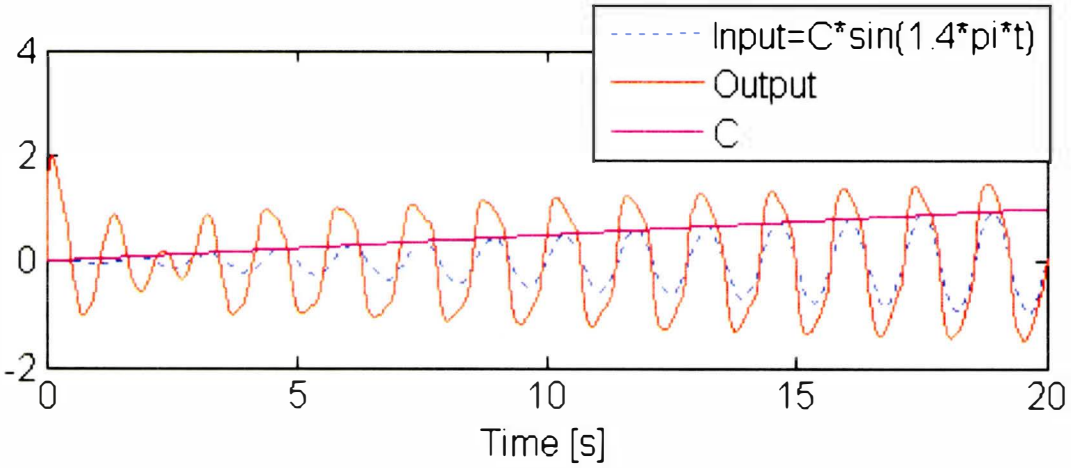

Fig.3.3. 3 Output of neural oscillator

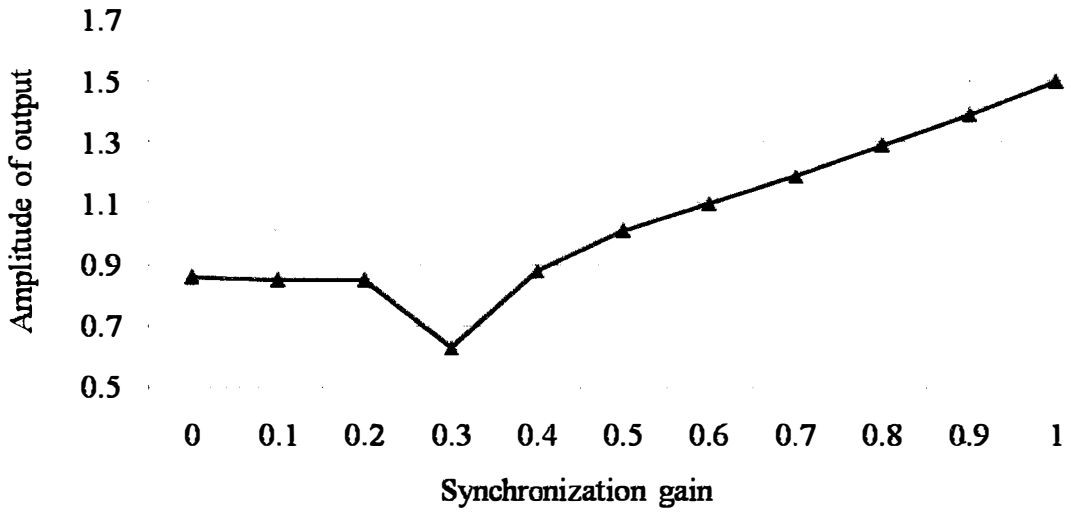

Fig.3.3. 4 Structure of a neural oscillator

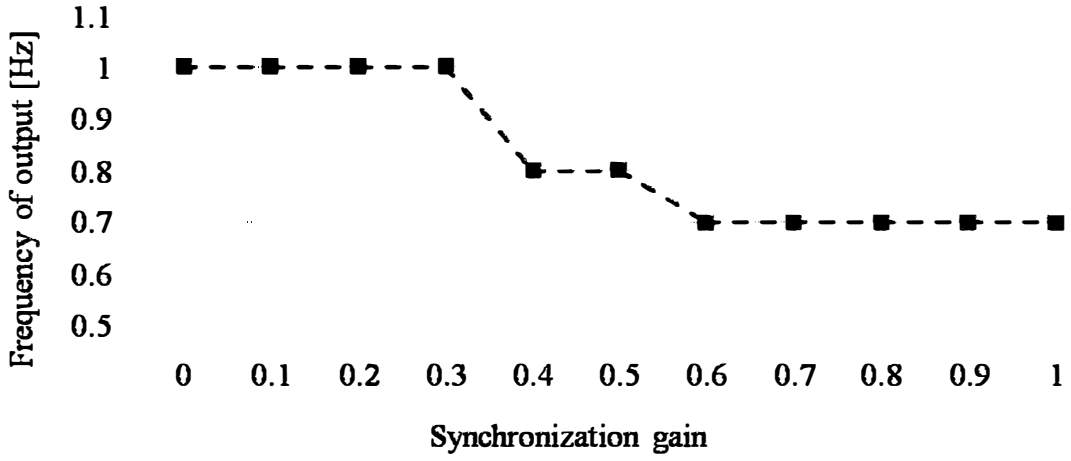

Fig.3.3. 5 Structure of a neural oscillator

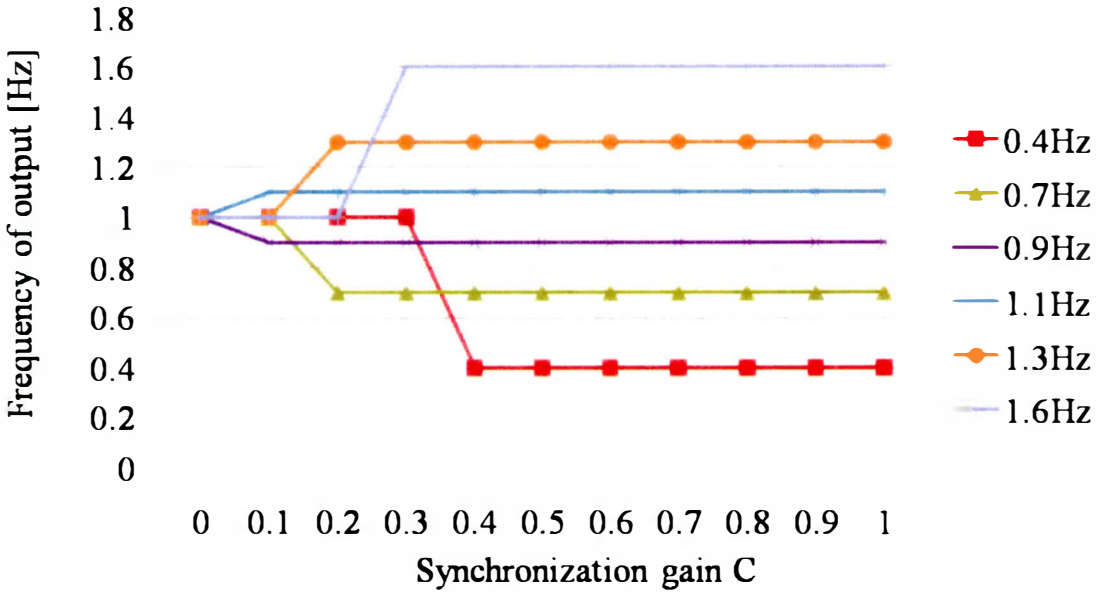

Fig.3.3. 6 frequency of output of neural oscillator responding to each input

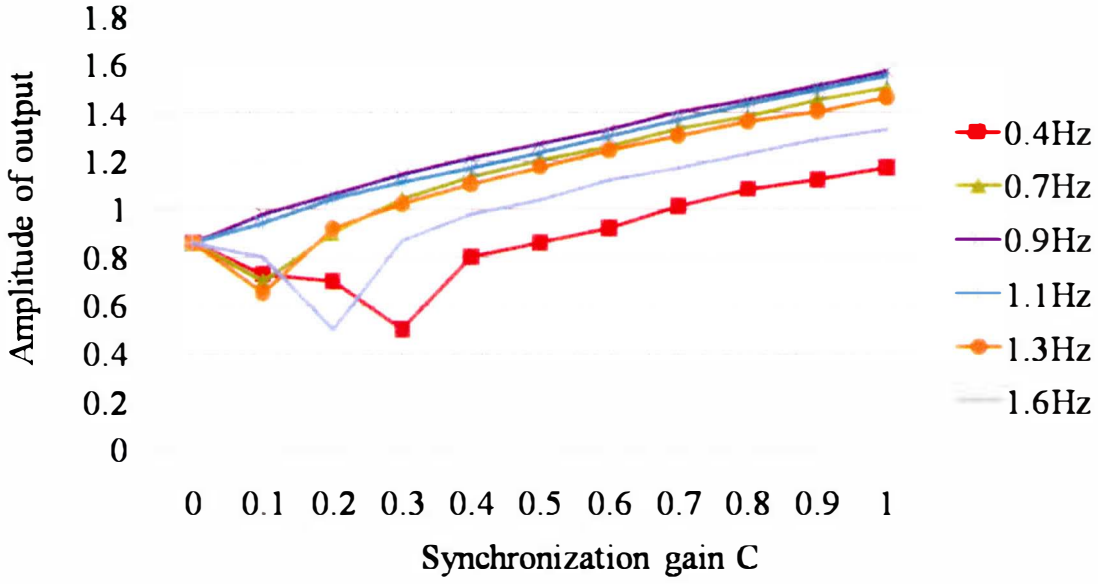

Fig.3.3. 7 Amplitude of output of neural oscillator responding to each input

3.3.2 Wide Synchronization range

The designed model is able to synchronize with a wide range of input signals with frequency varying from 0.1 Hz to 3.5Hz. Figure 3.3.8 shows the wide synchronization range. Here, $C=1$.

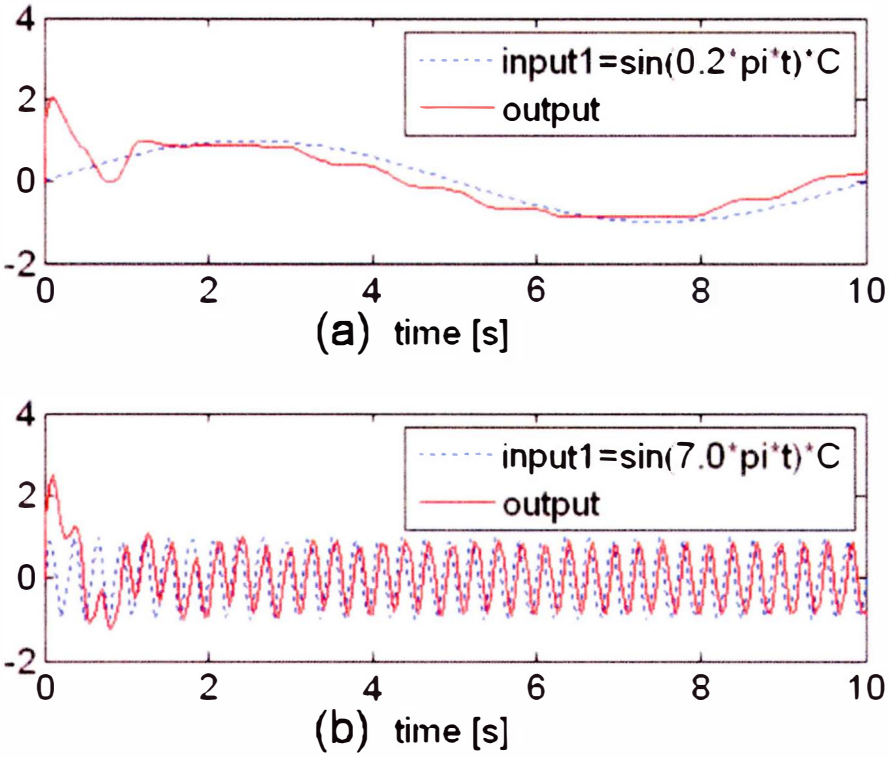

Fig.3.3. 8 The range of input able to be synchronized

The features relating to the synchronization of the designed model of neural oscillator are concludes as:

1) Synchronize the frequency of the output with the input frequency with a larger gain.
2) Increase the amplitude of the output by increasing the value of synchronization gain.
3) A wide range of frequency from 0.1Hz to 3.5Hz can be synchronized.

3.3.3 Attenuation mode

By putting the negative sign to the output of the neural oscillator and feeding it back to the neural oscillator as input signal (Outline is shown in Fig.3.3.9), we found that the oscillation was attenuating with the time cue. In addition, the higher the value of C, the quicker the attenuation speed is. We concluded that the attenuating speed was proportionate to the amplitude of input which was in opposite direction to the output of neural oscillator. The attenuation phenomena are shown in Fig. 3.3.10-Fig. 3.3.12. The unique attenuation model will be greatly helpful for motion assist. For example, the robotic suit could easily facilitate stop during walking when a user wants to make a stop, as long as the robotic suit is under motion assist control, that is the input to the neural oscillator is the mutual joint torque and the output of the neural oscillator is the desired angle of robot. The mechanism of facilitating stop is that, the mutual joint torque and the desired angle of the robot (the input and output of neural oscillator)

are becoming in opposite directions automatically when a user is making a stop. In section 5.4, section 5.5 and section 7.3, we will discuss how the attenuation mode plays a part in friendly motion assist.

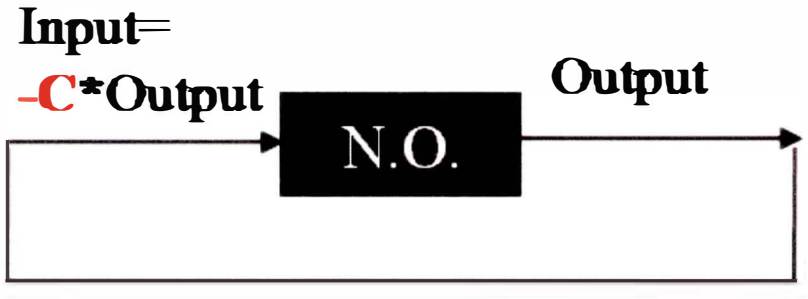

Fig.3.3. 9 Attenuation mode of the neural oscillator

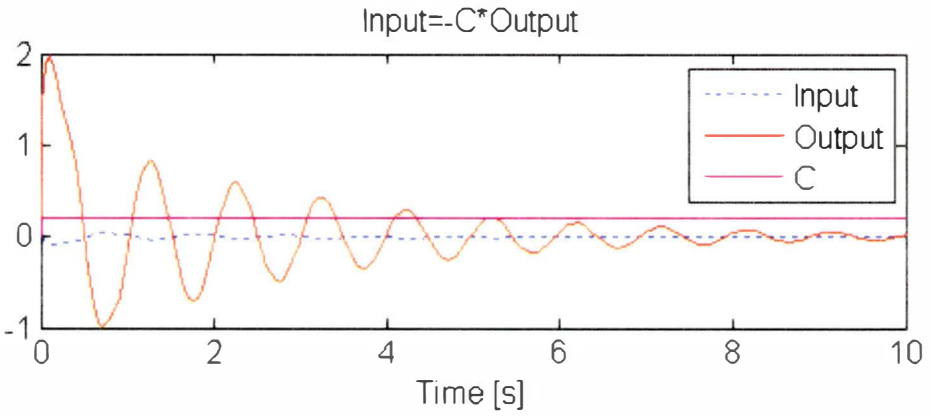

Fig.3.3. 10 Attenuation results by feeding back the output with negative sign, here, C=0.2

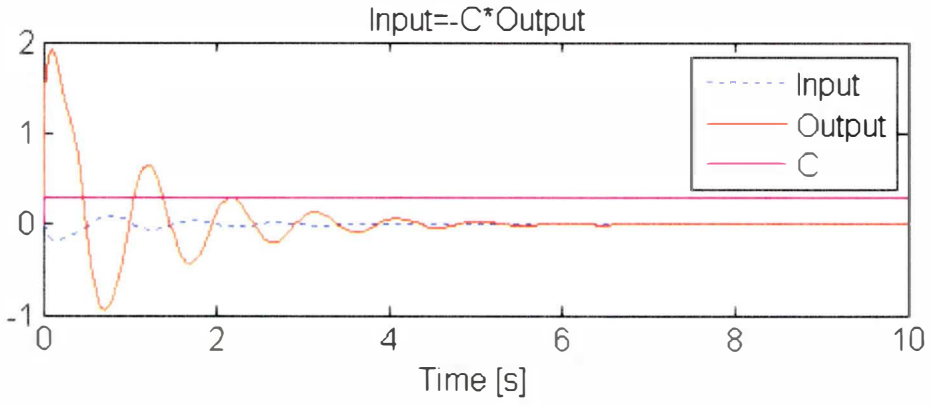

Fig.3.3. 11 Attenuation results by feeding back the output with negative sign, here, C=0.3

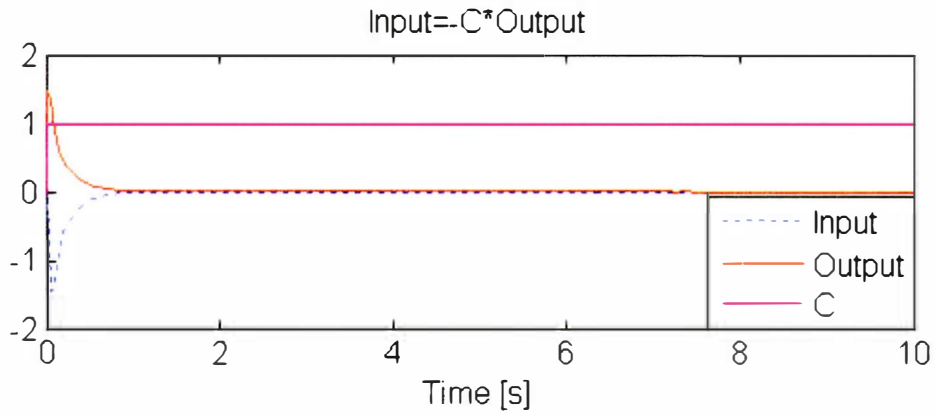

Fig.3.3. 12 Attenuation results by feeding back the output with negative sign, here, C=1

3.3.4 From Synchronization to walking assist

As specified in section 3.3.1, its feature of enlarging the output's amplitude with synchronized frequency with that of input motivates us to apply the neural oscillator to the wearable robotic suit to assist human, because for either power or motion assist, a robot is required to be both synchronous with the user and assistive. Increasing the gain will enable the robotic suit to respond to the input, and thus synchronize with the user's movement (especially the pace) easily; conversely, decreasing the gain reduces the magnitude of the input signal, which means that the robotic suit will tend to not synchronize but move following its original pattern, generated by neural oscillators with their predefined parameters, arbitrarily and regardless of the user's movement. The $Input_k$ ($C * Extenal\_signal_k$) should be scaled by C to be basically in the range of 0 and 1 to get different synchronization level (non-synchronous, lower synchronous or higher synchronous) and stable synchronized outputs. Therefore, the range of C will change if the range of the external signal changes. With a larger gain, the robotic suit is able to synchronize with the user's motion to support walking, and this pattern is considered correspondent to the case of synchronization-based assist specified in Fig.2.1.1. Conversely, with a smaller gain, the robotic suit tends to move following its original trajectory which will forcibly take the user to move, and this pattern is considered correspondent to the case of non-synchronization-based assist specified in Fig.2.1.2. The former potential, which is helpful for walking assistance for those who walk in small steps, will be verified with experiments in this thesis. The latter potential, which provides help with certain proper trajectory or proper torque, could be thought useful for rehabilitation training.

It is necessary for the robotic suit to confer stability to walking assistance as well. That is,

there should be a kind of human-like cooperative motion among each joint of the robotic suit. To solve the problem, we propose incorporating mutual inhibition between neural oscillators, which will be discussed in the next section.

3.3.5 The mutual inhibition among neural oscillators

Mutual inhibition between neurons will activate the two neurons alternately. So far, mutual inhibition between neural oscillators has been applied to control biped robots to help maintain an anti-phase relationship between the robots' left and right leg [4]. Figure 3.3.13 shows the mutual-inhibition involved structure of two neural oscillators. The number of neurons, $i, j = 1, \cdots, 4$, and the number of neural oscillators, $k = 1,2$. The pair of anti-phase output from the pair of neural oscillators is shown in Fig. 3.3.14.

In our study, not only is the mutual inhibition from other neural oscillator fed back, but the external signal representing human user's move intension needs to be fed back to the current neural oscillator. It can be predicted that once the pair of input signals to the left and right neural oscillator do not have the same frequency or are not anti-phase, the pair of neural oscillators will become confused between outer synchronization and inner-inhibition, or even worse their outputs become unstable. Therefore, the need to determine the inhibitory weight properly becomes very important. Assignment of inhibitory weight between neural oscillators, $a_{13}, a_{31}, a_{34}, a_{43}$, is discussed in detail in Chapter 6.

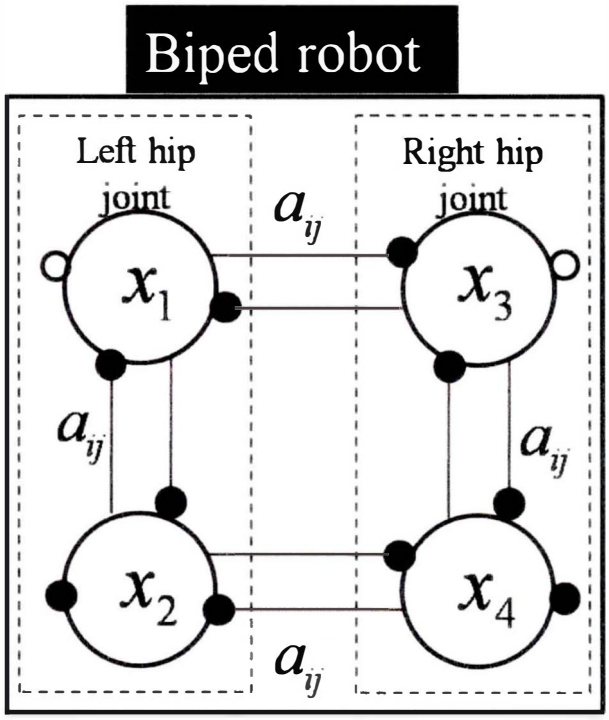

Fig.3.3. 13 Structure of two neural oscillators with mutual inhibition

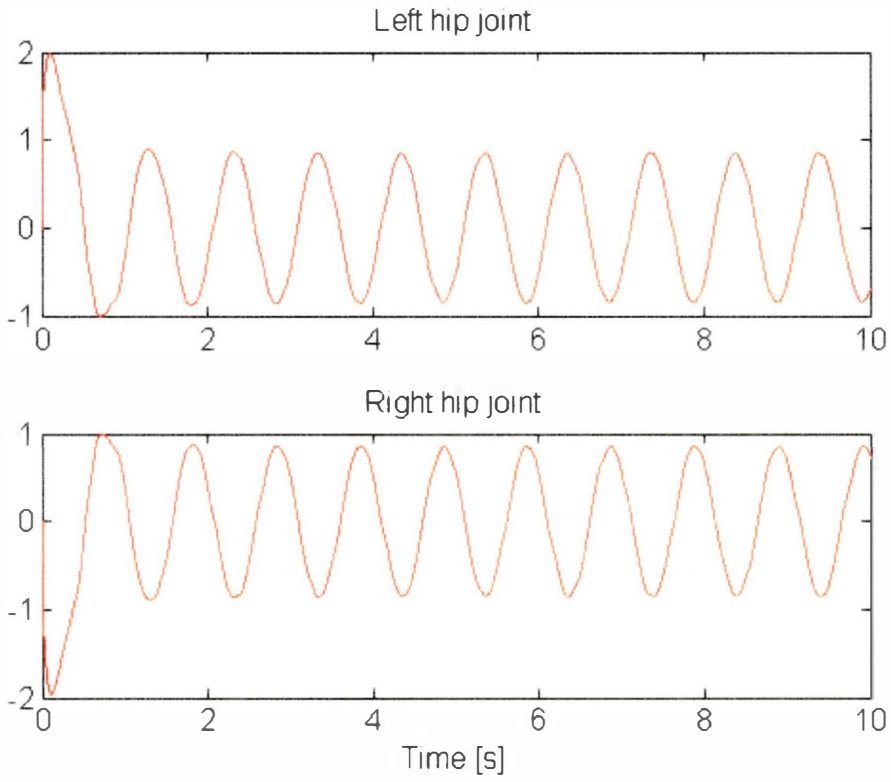

Fig.3.3. 14 Anti-phase output of neural oscillators with mutual inhibition

References

[1] Kiyotoshi Matsuoka, "Sustained Oscillations Generated by Mutually Inhibiting Neurons with Adaptation," *Biological Cybernetics,* vol.52,pp.367-376,1985.

[2] Kiyotoshi Matsuoka, "Mechanisms of Frequency and Pattern Control in the Neural Rhythm Generators," *Biological Cybernetics,* vol.56,pp.345-353,1987.

[3] Tomofumi Kasuga, Minoru Hashimoto, "Human-Robot Handshaking using Neural Oscillators," *IEEE Int. Conf. on Robotics and Automation,* Barcelona, pp.3813-3818, April 2005.

[4] Gentaro Taga, "A model of the neuro-musulo-skeletal system for human location I. Emergence of basic gait," *Biological Cybernetics,* 73,pp.97-111,1995.

[5] Matthew M.Williamson, "Neural control of rhythmic arm movement," *Neural Networks 11*,pp.1379-1394.

[6] Tomofumi Kasuga, Minoru Hashimoto, "Human—Robot Handshaking using Neural Oscillators," IEEE Int. Conf. on Robotics and Automation, Barcelona, pp3813-3818, April 2005.

Chapter 4

Synchronization-based motion assist and power assist

Chapter 4 Synchronization-based motion assist and power assist

It can be considered that there are two kinds of synchronization-based assist using the neural oscillator, one is synchronization-based motion assist and the other is synchronization-based power assist. Using the output of neural oscillator as the desired joint angle is called motion assist, and as the joint torque is called power assist. In order to get the human move intension with the premise that no sensor needs to be put on the human body, we proposed using the mutual joint torque and human joint torque as control input to the neural oscillator. Consequently, there are conceivably four patterns of input-output of the controller: they are 1) mutual joint torque-desired joint angle; 2) mutual joint torque-robot joint torque; 3) human joint torque-desired joint torque; 4) human joint torque-robot joint torque.

The mutual joint torque is the interaction torques acting upon both human and robot with reverse directions, and it will be generated once there is any difference arises between the user's motion and the robot's motion, and its direction changes depending on the relative positions of human to the robot. Here, we look at the mutual joint torque from the robot side.

For the mutual joint torque is effective in reflecting the human move intension, using the mutual joint torque as the input to neural oscillator and the output as the desired joint angle of robot can be considered as an operative way to realize synchronization. On the other hand, using the human joint torque as the input to neural oscillator and the output as robot joint torque can be considered as a reasonable way to realize synchronization.

As for the other two patterns of input-output of the controller (mutual joint torque-robot joint torque, human joint torque-desired joint torque), it can be considered there are no corresponding relations between the input-output. Therefore, in this study, we didn't analyze the feasibility of these two kinds of design.

As specified above, the synchronization-based motion assist can be realized by using mutual joint torque between the user and the robot as input to the neural oscillator, and the output of neural oscillator as the desired joint angle of the robot. The synchronization-based power assist can be realized by using the human joint torque as input to the neural oscillator and the output of the neural oscillator as robot joint torque. We investigated the mechanism of the two kinds of synchronization-based assist methods using simulations and experiments [1]. Using the results, we compared the two kinds of control methods, and finally chose the synchronization-based motion assist method in further study for walking assist, for its simple system, which also helps the robot act synchronously and provide assist. In addition, in the case of synchronization-based

motion assist method, we found that the "attenuation model" (See section 3.3.3) occurred when the mutual joint torque and desired angle were in reverse directions. The attenuation makes the desired angle of the robot to be generated more reasonably for motion assist, and the assist action to be more compliant.

In simulations, we showed how the neural oscillator enabled a virtual one-degree of freedom (DOF) robot synchronize with a virtual one-DOF human arm using two kinds of synchronization-based assist methods respectively. Also, we controlled a real one-DOF robot using both kinds of methods respectively to interact with another one-DOF robot arm. In addition, experiments of the knee joint flexion-extension assist were conducted for investigation of the feasibility. The simulation model and methods are given in section 4.1. Experimental device and methods of robot-robot interaction are given in section 4.2. Experimental device and methods of human knee joint flexion-extension assist are given in section 4.3. The results of synchronization-based motion assist are given in section 4.4, and the results of synchronization-based power assist are given in section 4.5. Discussions on the two assist methods and the difference between our technique and other technique are given in section 4.6.

4.1 Simulation model and methods

A virtual one-DOF robot interacts with a virtual one-DOF human arm. The assisting robot moves its joint via the neural oscillator which enables the robot synchronize with the human. Figure 4.1.1 shows the simulated model, and both of the two arms are bundled together. The constraint can be depicted as a spring and damping mechanism in between.

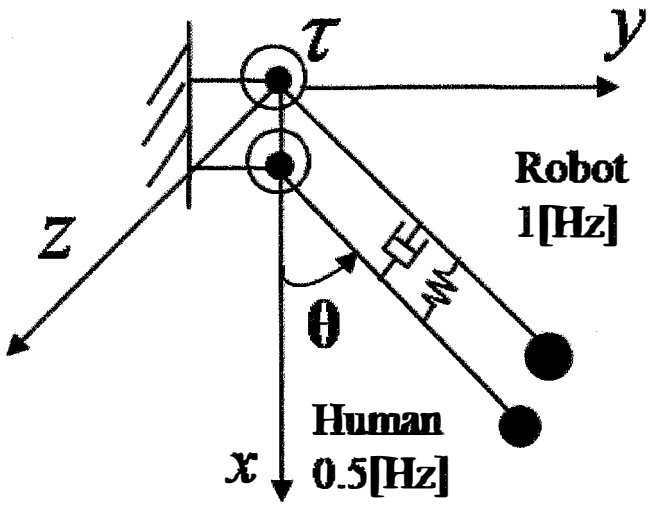

Fig.4.1. 1 Simulation model

Dynamic equation of this system is written by

$$\boldsymbol{\tau} = \begin{pmatrix} \tau_h \\ \tau_a \end{pmatrix} = \begin{pmatrix} J_h\ddot{\theta}_h + G_h + k_1(\theta_h - \theta_a) + k_2(\dot{\theta}_h - \dot{\theta}_a) \\ J_a\ddot{\theta}_a + G_a - k_1(\theta_h - \theta_a) - k_2(\dot{\theta}_h - \dot{\theta}_a) \end{pmatrix} \qquad (4.1)$$

J_h, J_a are the inertial moment, G_h, G_a are the gravity term, $k_1(\theta_h - \theta_a) + k_2(\dot{\theta}_h - \dot{\theta}_a)$ is the constraint force term between human and robot, k_1 is proportion coefficients and k_2 is viscous coefficients. By using the vectors, equation (4.1) can be represented as the Eq. (4.2)-Eq. (4.8).

$$\dot{\mathbf{x}} = A\mathbf{x} + B\boldsymbol{\tau} + C \qquad (4.2)$$

$$\mathbf{x} = \begin{pmatrix} \theta_h & \dot{\theta}_h & \theta_a & \dot{\theta}_a \end{pmatrix}^T \qquad (4.3)$$

$$A = \begin{bmatrix} 0 & 1 & 0 & 0 \\ -\frac{k_1}{J_h} & -\frac{k_2}{J_h} & \frac{k_1}{J_h} & \frac{k_2}{J_h} \\ 0 & 0 & 0 & 1 \\ \frac{k_1}{J_a} & \frac{k_2}{J_a} & -\frac{k_1}{J_a} & -\frac{k_2}{J_a} \end{bmatrix} \qquad (4.4)$$

$$B^T = \begin{bmatrix} 0 & \frac{1}{J_h} & 0 & 0 \\ 0 & 0 & 0 & \frac{1}{J_a} \end{bmatrix} \qquad (4.5)$$

$$C^T = \begin{bmatrix} 0 & -\frac{G_h}{J_h} & 0 & -\frac{G_a}{J_a} \end{bmatrix} \qquad (4.6)$$

$$G_h = m_h l_h \sin\theta_h \qquad (4.7)$$

$$G_a = m_a l_a \sin\theta_a \qquad (4.8)$$

The values of parameters of mutual joint torque term are listed in Table 4.1.1. The values of links' parameters used in this simulation are listed in Table 4.1.2.

Table4.1. 1 Parameters of mutual joint torque term

	k_1 [Nm/rad]	k_2 [Nm s/rad]
Values	1500	20

Table4.1. 2 Link parameters

	Human	Assist suit
Inertial moment [kg m^2]	1	0.25
Mass[kg]	4	1
Length[m]	0.5	0.5

Table4.1. 3 Parameters of mutual torque term and PD control

	k_p (Nm/rad)	k_d (Nm s/rad)
Values	1500	20

4.1.1 Motion-assist case

In simulations in the case of motion assist, the torque applied to the human arm is given by Eq. (4.9). The robot joint torque is determined by the PD feedback controller represented in Eq. (4.10).

$$\tau_h = A\sin(\omega_h t) \quad A = 5, \omega_h = 0.5 \qquad (4.9)$$

$$\tau_a = k_p(\theta_{da} - \theta_a) + k_d(\dot{\theta}_{da} - \dot{\theta}_a) \qquad (4.10)$$

Where, θ_{da} is output (desired angle) from the neural oscillator. The PD controller gain is shown in Table 4.1.3.

4.1.2 Power-assist case

In simulations in the case of power assist, the torque applied to the human arm is given by Eq. (4.11). The robot joint torque is given by Eq. (4.12).

$$\tau_h = A\sin(\omega_h t) \qquad A = 5, \omega_h = 0.5 \qquad (4.11)$$

$$\tau_a = K * output \qquad K = 10 \qquad (4.12)$$

Where, $output$ is output (robot joint torque) from the neural oscillator.

4.2 Robot-robot interaction

A real one-DOF robot interacts with another one-DOF robot arm. The assisting robot moves its joint via the neural oscillator which can respond to the input signals, and the input signals are mutual joint torque in the case of motion-assist and are the "human joint torque" in the case of

power-assist. Figure 4.2.1 shows the experimental devices, and both of the two arms are bundled together. The control system is depicted in detail in section 6.2 of Chapter 6.

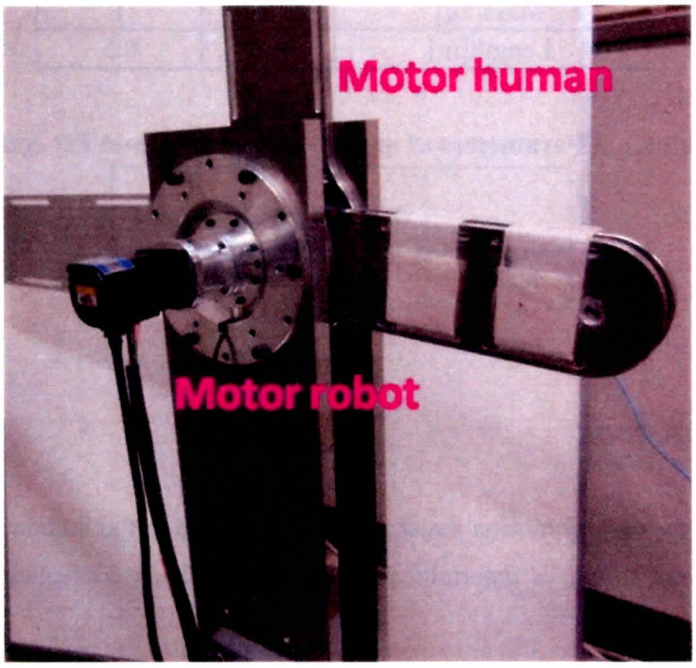

Fig.4.2. 1 Robot-robot interaction

4.2.1 Motion-assist case

In experiments in the case of motion assist, the torque applied to the "human arm" is given by Eq. (4.13). The robot joint torque is determined by the PID controller represented in Eq. (4.14).

$$\tau_h = A\sin(\omega_h t) \quad A = 1, \omega_h = 0.5 \qquad (4.13)$$

$$\tau_a = k_p(\theta_{da} - \theta_a) + k_d(\dot{\theta}_{da} - \dot{\theta}_a) + k_i(\theta_{da\ int} - \theta_{a\ int}) \qquad (4.14)$$

Where, θ_{da} is output (desired angle) from the neural oscillator. $\theta_{da\ int}$ is the integration of θ_{da} .The PID controller gains are listed in Table 6.2.5.

4.2.2 Power-assist case

In experiments in the case of power assist, the torque applied to the human arm is given by Eq. (4.15). The robot joint torque is given by Eq. (4.16).

$$\tau_h = A\sin(\omega_h t) \qquad A = 1, \omega_h = 0.5 \qquad (4.15)$$

$$\tau_a = K * output \qquad K = 1.2 \qquad (4.16)$$

Where, $output$ is output (robot joint torque) from the neural oscillator.

4.3 Knee flexion/extension motion assist

As can be seen in Fig. 4.3.1 the one-DOF robot, which is designed to assist the knee joint flexion-extension motion and consists of one link and one actuator FHA-14C-50-E200 provided by Harmonic Drive Systems Company. This actuator has a built-in joint torque sensor. The torque sensing technique utilizes a flexible harmonic drive gear, which not only allows joint torque sensing without reducing stiffness of robot but also compacts the structure of the joint [2]. ART-Linux is used for this control system. The control system is depicted in detail in section 6.2 of Chapter 6.

Fig.4.3. 1 Experimental scenarios of knee flexion-extension assist

The human knee joint torque is estimated using Eq. (4.17). The robot moves its joint using the output of the neural oscillator, represented in Eq. (4.18).

$$\tau_h = J_h\ddot{\theta} + D_h\dot{\theta} + m_h g l_h \sin\theta - \tau_{mutual} \qquad (4.17)$$

$$\tau_a = K * output, \qquad K = 1.2 \qquad (4.18)$$

Where, τ_{mutual} is mutual joint torque measured via the torque sensor. J_h is the inertial moment, D_h is the viscous coefficient, and $m_h g l_h$ is the gravitational torque. The values of parameters are defined referring to [3], and are listed in Table 4.3.1.

Table4.3. 1 Parameters of human impedance

Parameters	Value
J_h [kg m^2]	0.1225
D_h [Nm/(rad/sec)]	3.13
$m_h g l_h$ [Nm]	0.57

4.3.1 Motion-assist case

In experiments in the case of motion assist, the robot joint torque is given by Eq. (4.19).

$$\tau_a = k_p(\theta_{da} - \theta_a) + k_d(\dot{\theta}_{da} - \dot{\theta}_a) + k_i(\theta_{da\_\text{int}} - \theta_{a\_\text{int}}) \qquad (4.19)$$

Where, θ_{da} is output (desired angle) from the neural oscillator. θ_{da_int} is the integration of θ_{da} .The PID controller gains are listed in Table 6.2.5.

4.3.2 Power-assist case

In experiments in the case of power assist, the robot joint torque is given by Eq. (4.20).

$$\tau_a = K * output \qquad (4.20)$$

Where, $output$ is output from the neural oscillator, and $K = 1.2$.

4.4 Simulation and experimental results of synchronization-based motion assist method

Using the mutual joint torque as the external signal fed back, we can achieve synchronization of the robot with the human using the approach described as follows: firstly, use the mutual joint torque as the input signals to the neural oscillator, then use the synchronized output signals of the neural oscillator as the robot desired joint angle. Then by integrating Eq. (4.2) using the Runge-Kutta method, the robot joint angle can be calculated. Figure 4.4.1 shows the framework of the synchronization-based motion assist.

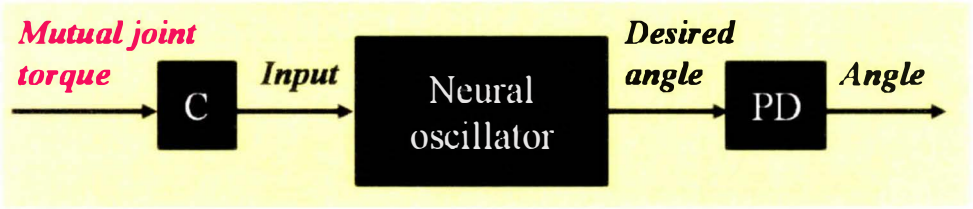

Fig.4.4. 1 Synchronization-based motion assist method

4.4.1 Simulation results

Using the simulation model and method described in section 4.1, we conducted extensive simulations.

Under free condition, the human moves the joint at a frequency of 0.5 [Hz] with amplitude of 0.73 [rad] by the torque given in Eq. (4.9), and the robot joint motion's frequency is about 1.0 [Hz]. The phase portrait of the natural motion of the human is shown in Fig. 4.4.2.

Under constraint condition, the robot which has a higher synchronization gain (C=0.003) synchronized its motion with that of the human arm. The frequency of the system became to 0.85 [Hz] with amplitude of 0.77 [rad]. That is, the frequency of the robot joint motion was entrained to get closer to that of the human, and the amplitude of the human joint angle increased compared to the natural amplitude 0.73 [rad]. The phase portrait of the motion of human under constraint condition is shown in Fig. 4.4.3.

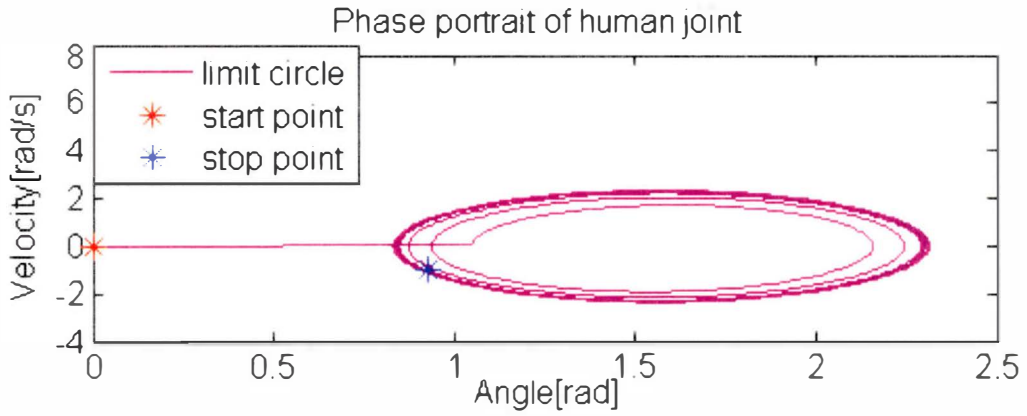

Fig.4.4. 2 Phase portrait of natural movement of human

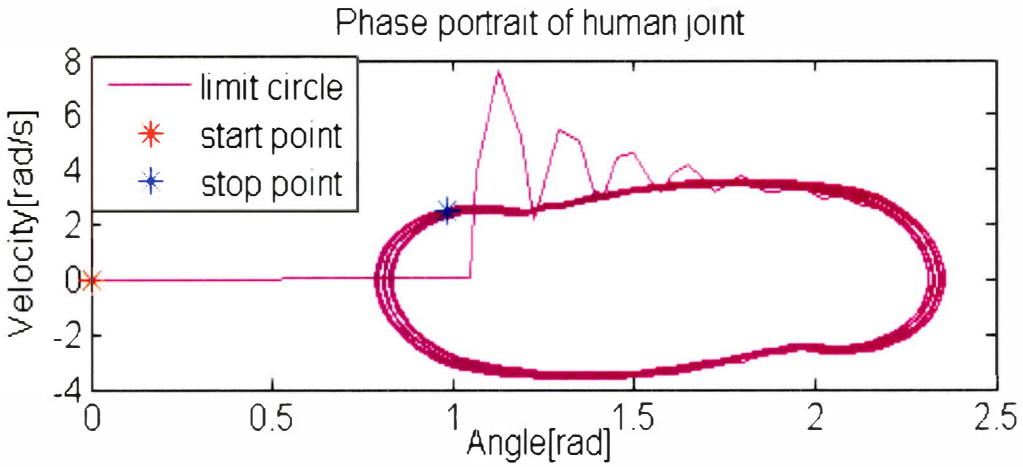

Fig.4.4. 3 Phase portrait of cooperative movement of human

By gradually increasing the synchronization gain from 0 to 0.003, we investigated the mutual joint torque between the human and robot, their joint torque, the amplitude and the frequency of the system's motion. Figure 4.4.4 shows the mutual joint torque, human joint torque and robot joint torque plotted against the synchronization gain. It can be found that the mutual joint torque, functioning as the external torque acting on the human, gets larger when C=0.001, but become smaller along with the further increase of the synchronization gain. The larger the mutual joint torque, the more significant the assist effect is, and vice versa. Figure 4.4.5 shows the amplitude of the system's motion. It can be found that the amplitudes get increased along with the increase of the synchronization gain. The increase of amplitude is due to the feature of the neural oscillator, which is explained in more detailed in section 3.3.1. Figure 4.4.6 shows the frequency of their motion, which is entrained to get closer to the natural frequency of the human. By increasing the synchronization gain larger than 0.003, the oscillation became unstable.

From the results shown in Fig. 4.4.4 to Fig. 4.4.6, we found that, the robot's joint toque became larger along with the increase the synchronization gain to counteract the increasing mutual joint torque, and the mutual joint torque assists the human to move with larger amplitude. However, the mutual joint torque has a limited value, which suggests that the synchronization-based motion assist method enables a limited assist effect.

We can conclude from the simulation results that , using the synchronization-based power assist method, the robot can synchronize with the frequency of the human's motion and assist human, an increase of 0.04 [rad] in amplitude from the simulation results. The robot's joint torque plays a part in counteracting the mutual joint torque which assists the human to move.

However, the synchronization-based motion assist method enables a limited assist effect.

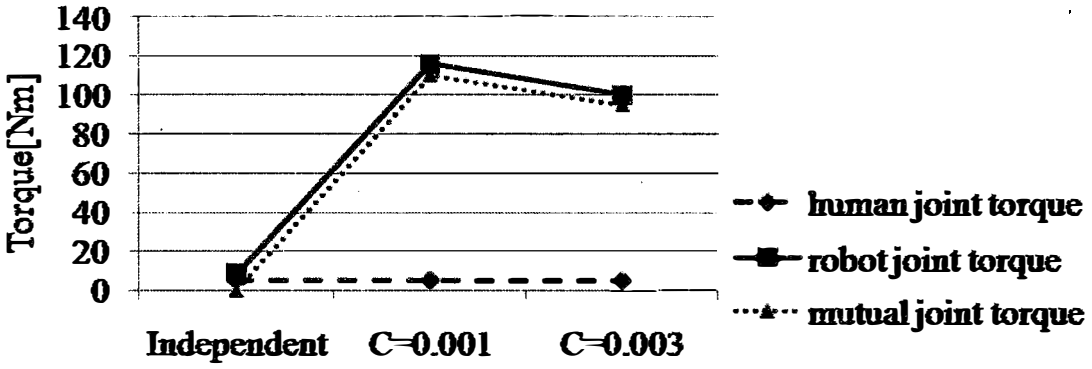

Fig.4.4. 4 Joint torque and mutual joint torque plotted against the synchronization gain

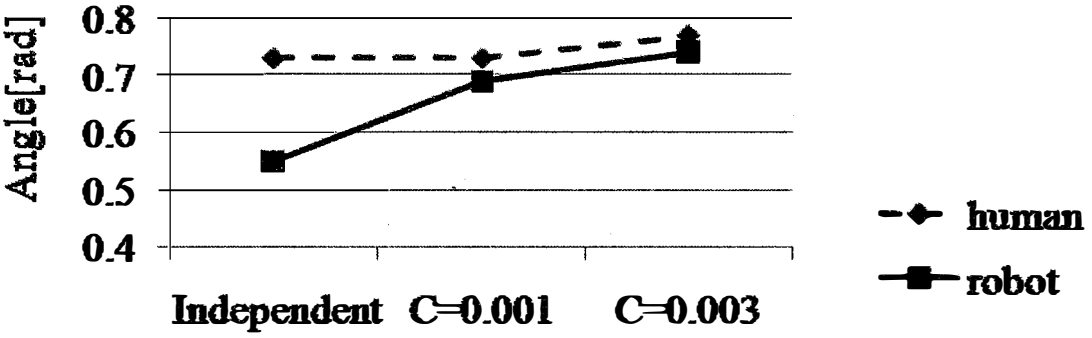

Fig.4.4. 5 Amplitude plotted against the synchronization gain

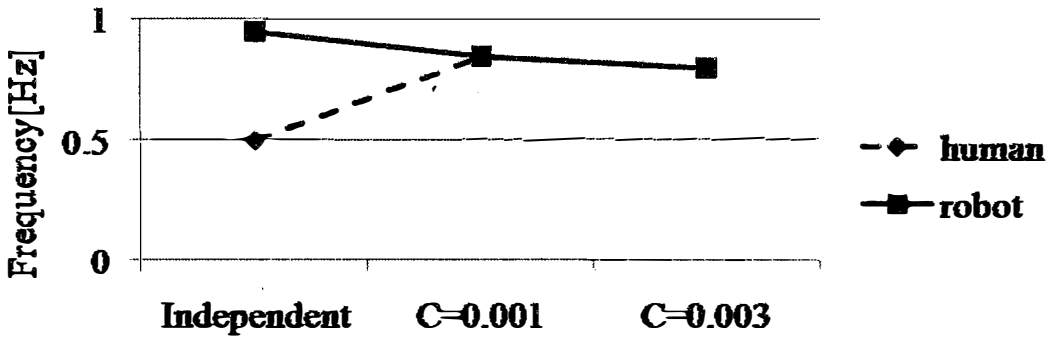

Fig.4.4. 6 Frequency plotted against the synchronization gain

In simulation where C=0.001, we stopped the human joint angle at the position of 90[deg] at

5 second, we found that the robot also stopped oscillating and attenuated to zero immediately. The result is shown in Fig. 4.4.7. We investigated the input-output of neural oscillator, that is, the mutual joint torque multiplied by C and the desired angle of the robot. Figure 4.4.8 shows the relationship between the mutual joint torque and the desired angle before-after 5 seconds. It can be found that before 5 seconds, the mutual joint torque and the desired angle are generally in co-directions, but are in reverse directions after 5 seconds. Due to the reverse directions between the mutual joint torque and the desired angle, that is, the reverse directions between the input-output of neural oscillator (Feature is depicted in detail in section 3.3.3), the desired angle turned to be attenuating. As a result, the robot stopped. To conclude, the robot stops immediately when human wants to make a stop in the case of motion assist.

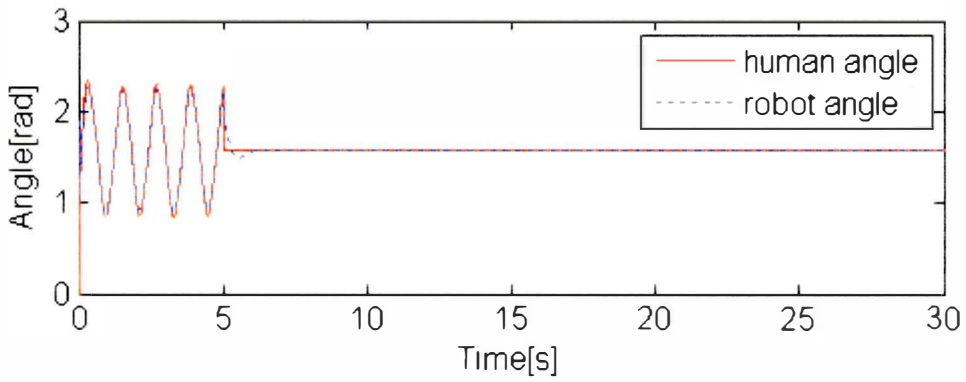

Fig.4.4. 7 Robot stops when human tries to stop

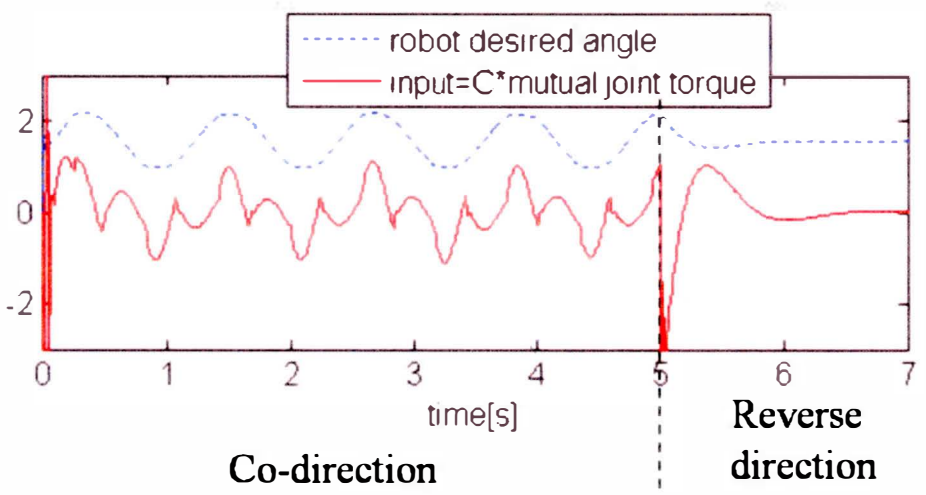

Fig.4.4. 8 Co-direction & reverse direction relationships between the input-output of neural oscillator

4.4.2 Experimental results of robot-robot interaction

Using the experimental devices described in section 4.2, we conducted experiments of the robot-robot interaction in the case of motion assist method.

By gradually increasing the synchronization gain from 0 to 0.7, we investigated the mutual joint torque between the human and robot, their joint torque, the amplitude and the frequency of the system's motion. Figure 4.4.9 shows the mutual joint torque, human joint torque and robot joint torque plotted against the synchronization gain. It can be found that the mutual joint torque, functioning as the external torque acting on the human, gets larger until C=0.3 but becomes smaller along with the further increase of the synchronization gain. The larger the mutual joint torque, the more significant the assist effect is, and vice versa. Figure 4.4.10 shows the amplitude of the system's motion. It can be found that the amplitudes get increased until C=0.3 but becomes smaller along with the further increase of the synchronization gain. The increase in amplitude when C=0.3 is due to the feature of the neural oscillator, which is explained in more detailed in section 3.3.1. Figure 4.4.11 shows the frequency of their motion, which is entrained to the natural frequency of the human. By increasing the synchronization gain larger than 0.7, the amplitude of oscillation became even larger.

From the results shown in Fig. 4.4.9 to Fig. 4.4.11, we found that, the robot's joint toque became larger along with the increase the synchronization gain to counteract the increasing mutual joint torque, and the mutual joint torque assists the human to move with larger amplitude. However, the mutual joint torque has a limited value, which suggests that the synchronization-based motion assist method enables a limited assist effect.

We investigated the input-output of neural oscillator to search for the reason why the mutual joint torque and angle of the robot became smaller with a larger synchronization gain. Interestingly, the mutual joint torque between human and robot and the desired angle of robot-i.e. the input-output of neural oscillator, were found to have two kinds of relationships. One is co-directions, the other is reverse directions, and the co-directions and reverse directions exist alternately through all the process of human-robot interaction. Figure 4.4.12 shows the input-output of neural oscillator in the case of C=0.7, and the gray region represents where the input-output are in reverse directions, the blank region co-direction. In the case of C=0.7, that is higher synchronization, the input-output (mutual joint torque-desired angle) appear to be in reverse directions every time when the desired angle is about to change its direction. Figure 4.4.13 shows the input-output of neural oscillator in the case of C=0.3. In the cased of C=0.3, that is lower synchronization, although input-output (mutual joint torque-desired angle) also

appear to be in reverse directions every time when the desired angle is about to change its direction, the time of the direction changing from reverse-direction to co-direction become greatly shorter compared to the case of C=0.7. Note that, once the input-output of neural oscillator are in reverse directions, the attenuation of output of neural oscillator is occurring, and the attenuation speed is proportionate to the amplitude of input which has opposite direction to the output (See section 3.3.3). We concluded that C=0.7 resulted in heavier attenuation, and the desired angle of the robot was generated more compliantly. Consequently, the mutual joint torque became smaller as a result.

We can conclude from the experimental results that, using the synchronization-based motion assist method, the robot can synchronize with the frequency of the human's motion and assist human, an increase of 0.61 [rad] in largest in amplitude from the experimental results. The robot's joint torque plays a part in counteracting the mutual joint torque which assists the human to move. However, as heavy attenuation tends to occur in higher synchronization level, the synchronization-based motion assist method enables a limited assist effect.

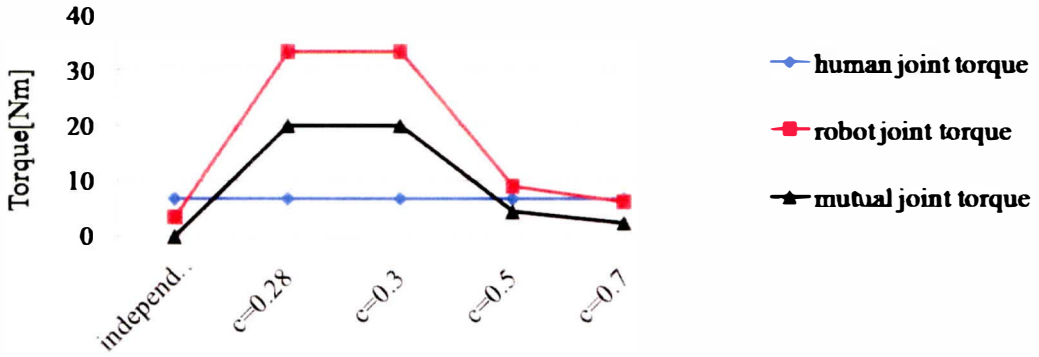

Fig.4.4. 9 Joint torque and mutual joint torque plotted against the synchronization gain

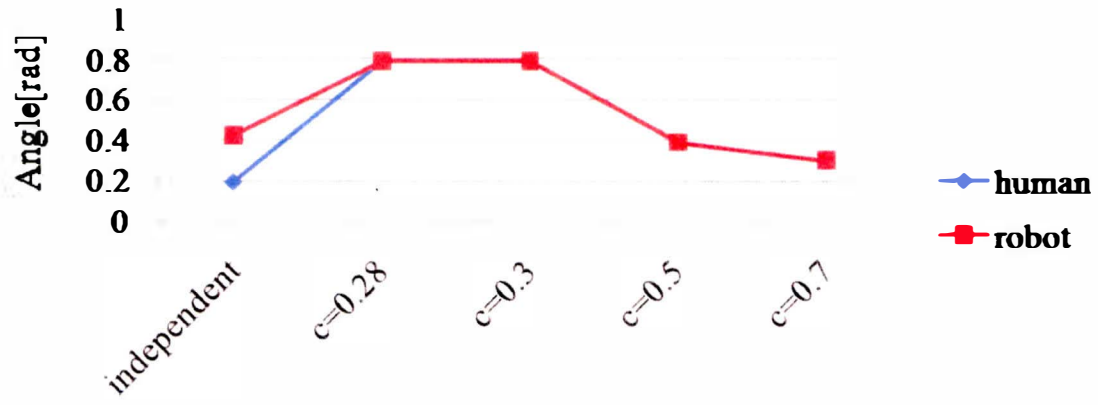

Fig.4.4. 10 Amplitude plotted against the synchronization gain

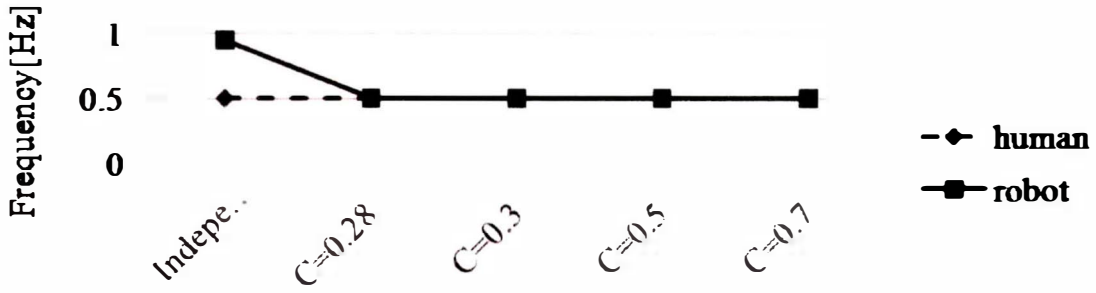

Fig.4.4. 11 Frequency plotted against the synchronization gain

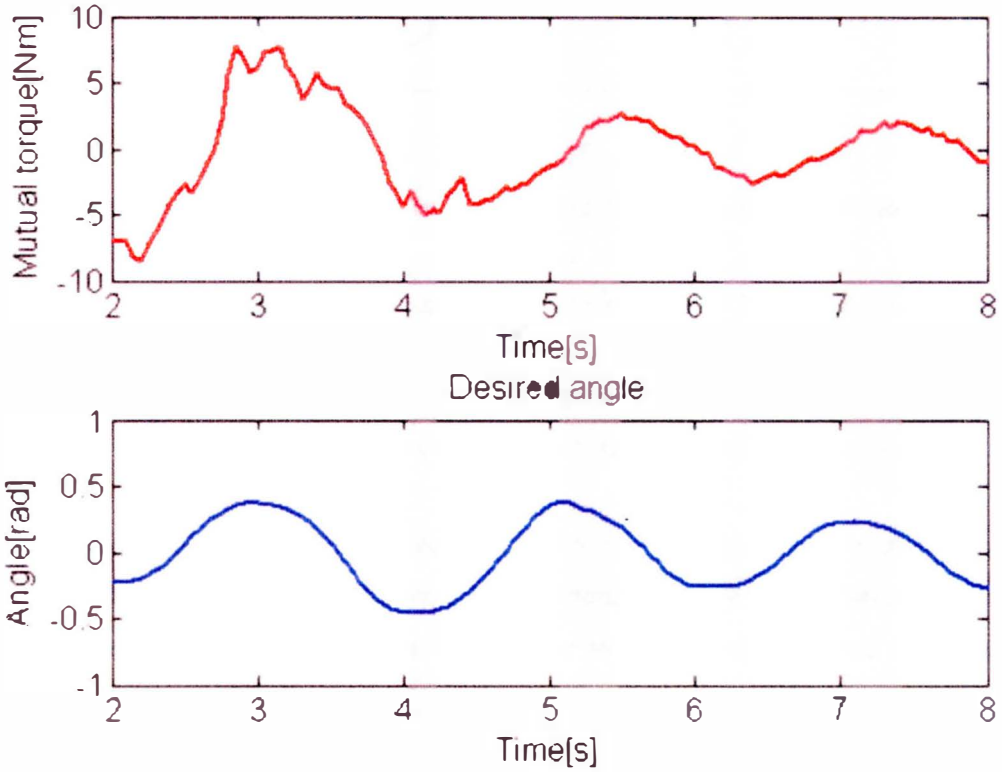

Fig.4.4. 12 Input-output (mutual joint torque-desired angle) of neural oscillator when C=0.7

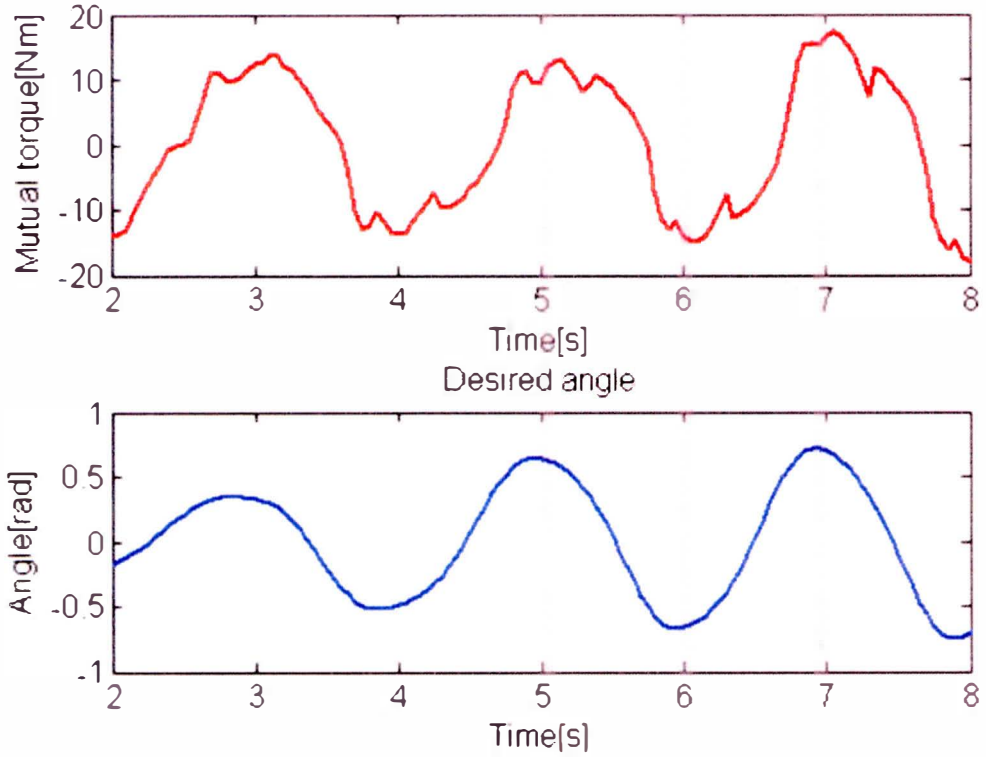

Fig.4.4. 13 Input-output (mutual joint torque-desired angle) of neural oscillator when C=0.3

4.4.3 Experimental results of human-robot interaction

Using the experimental devices described in section 4.3, we conducted experiments of the human-robot interaction in the case of motion assist method.

A series of experiments were conducted to examine the assist effect and synchronous behavior. In the experiment, the robotic suit was determined to move at a frequency of 1.0 Hz with the output signal from the neural oscillator. The natural motion of the subject, a university student, has a frequency of about 0.8 [Hz] with amplitude of about 0.35 [rad]. Where wearing the suit, she was asked to maintain the natural frequency by listening to a metronome. We investigated the cooperative motion, the user's muscle activity (using EMG-signal), mutual joint torque and robot joint torque under cooperative motion.

Under cooperative condition, the robot which had a higher synchronization gain (C=0.8) synchronized its motion's frequency with that of the user's motion. The frequency of the system became to 0.8 [Hz] with amplitude of about 24 [deg]. When the gain C=0.3, the frequency became to 0.9 [Hz] with amplitude of about 40 [deg]. That is, the frequency of the robot motion was entrained to get closer to that of the user. The cooperative motion of the system (C=0.3) and its power spectrum are shown in Fig. 4.4.14 and Fig. 4.4.15 respectively. Figure 4.4.16 shows

mutual joint torque and robot joint torque plotted against to the synchronization gain. The amplitude of the cooperative motion is shown in Fig.4.4.17. It can be found that the mutual joint torque, robot joint torque and amplitudes get increased until C=0.3 but become smaller along with the increase the synchronization gain. Figure 4.4.18 shows the frequency of their motion, which are synchronized to the natural frequency of the human.

We again investigated the input-output of neural oscillator to search for the reason why the mutual joint torque and angle of the robot became smaller with a larger synchronization gain. Figure 4.4.19 shows the input-output of neural oscillator in the case of C=0.8, and the gray region represents where the input-output are in reverse directions. In the case of C=0.8, that is higher synchronization, the input-output (mutual joint torque-desired angle) appear to be in reverse directions every time when the desired angle is about to change its direction. Figure 4.4.20 shows the input-output of neural oscillator in the case of C=0.3. In the cased of C=0.3, that is lower synchronization, although input-output (mutual joint torque-desired angle) also appear to be in reverse directions every time when the desired angle is about to change its direction, the time changing from reverse-direction to co-direction are short compared to the case of C=0.8. Note that, once the input-output of neural oscillator are in reverse direction, the attenuation of output of neural oscillator is occurring, and the attenuation speed is proportionate to the amplitude of input which has opposite direction to the output (See section 3.3.3). We concluded that C=0.8 resulted in heavier attenuation, and the desired angle of the robot was designed more compliantly, and the mutual joint torque became smaller as a result.

We used a personal-EMG to measure muscle activity (RMS signal) in three places in leg when human move independently and move together with assist suit. The three muscles are the Medial Vastus Muscle (MV), the Rectus Femoris Muscle (RF), and the Vastus Lateralis Muscle (VL). 100% MVC (Maximal Voluntary Contraction) method [4], which represents the ratio of muscle activity to the maximum muscle activity of each muscle, is used to show the physical power. Every maximum muscle activity of three muscles is measured beforehand by asking the subject to give out his largest force. Therefore, the higher the muscle activity ratio is, the bigger the physical power is consumed.

Figure 4.4.21 shows the muscle activity under both conditions of independent motion and cooperative motion (C=0.3). Average muscle activity reaches 8.5% when the user moves together with the robot as shown by pink block in Fig.4.4.21, but it reaches 16.4% when the user moves independently as shown by black block in Fig.4.4.21. The 7.9% deference, a decrease ratio of 48% in muscle activity to the original 16.4%, is the assist effect. Note that, the amplitude of human motion in both conditions of independent and assisted moving are almost the same. So herein, it can be considered the assist effect has been verified. The Rectus Femoris

Muscle which mostly relating to the flexion and extension of the knee joint was the most significantly assisted, and the muscle activity decreased approximately by 77%.

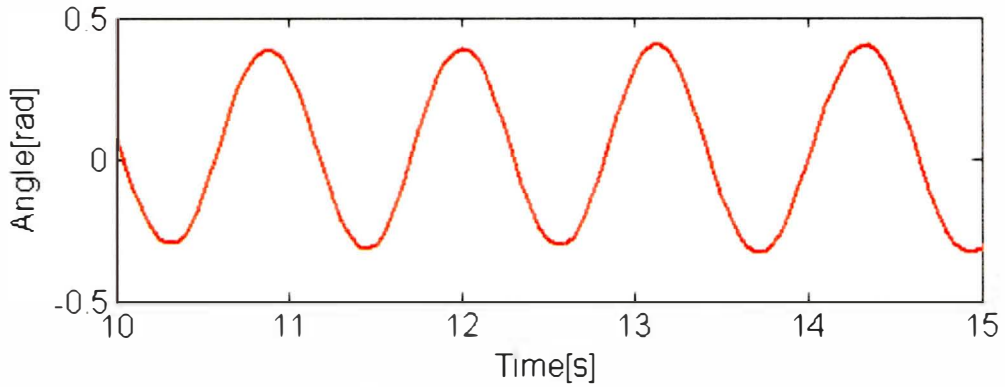

Fig.4.4. 14 Cooperative motion of the system

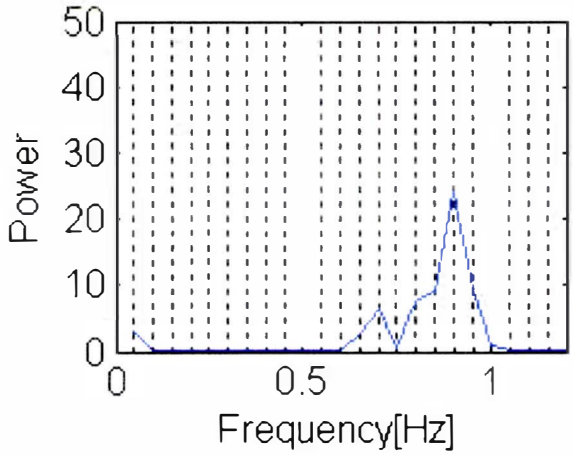

Fig.4.4. 15 Power spectrum of cooperative motion

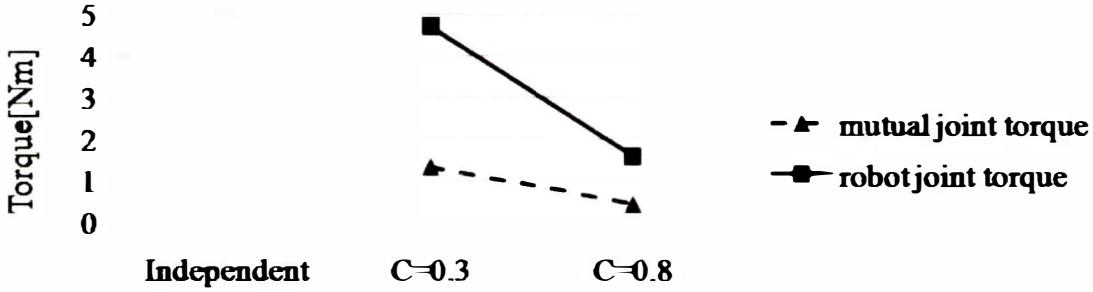

Fig.4.4. 16 Joint torque and mutual joint torque plotted against the synchronization gain

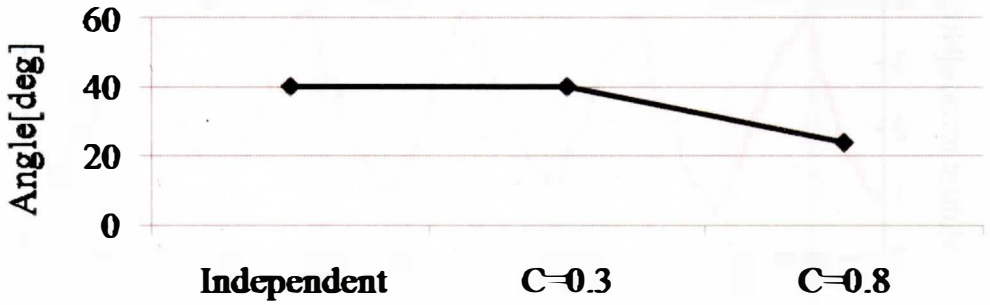

Fig.4.4. 17 Amplitude plotted against the synchronization gain

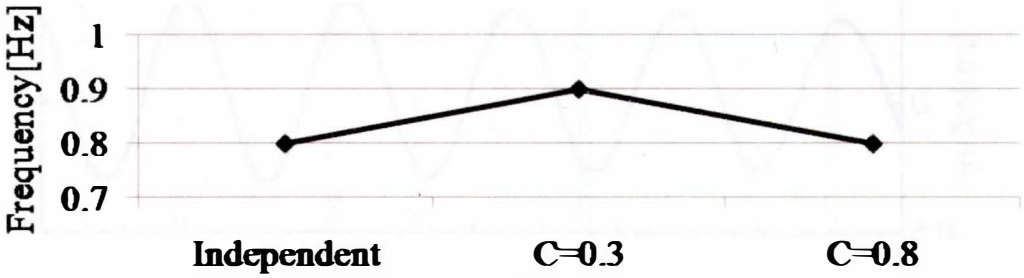

Fig.4.4. 18 Frequency plotted against the synchronization gain

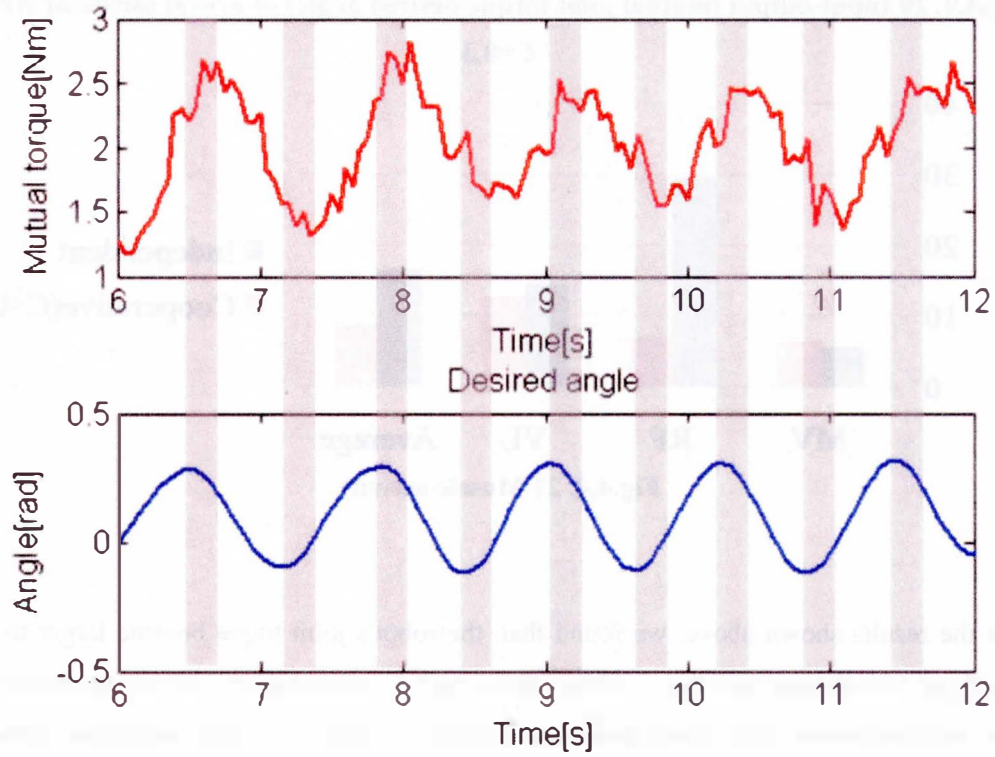

Fig.4.4. 19 Input-output (mutual joint torque/desired angle) of neural oscillator when C=0.8

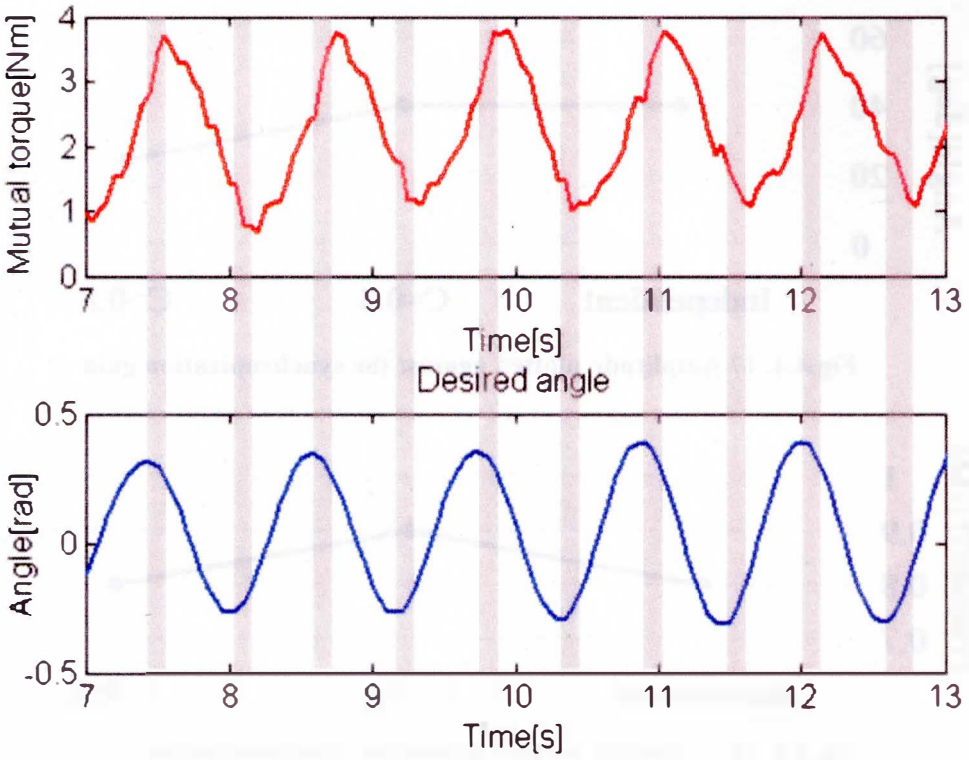

Fig.4.4. 20 Input-output (mutual joint torque/desired angle) of neural oscillator when C=0.3

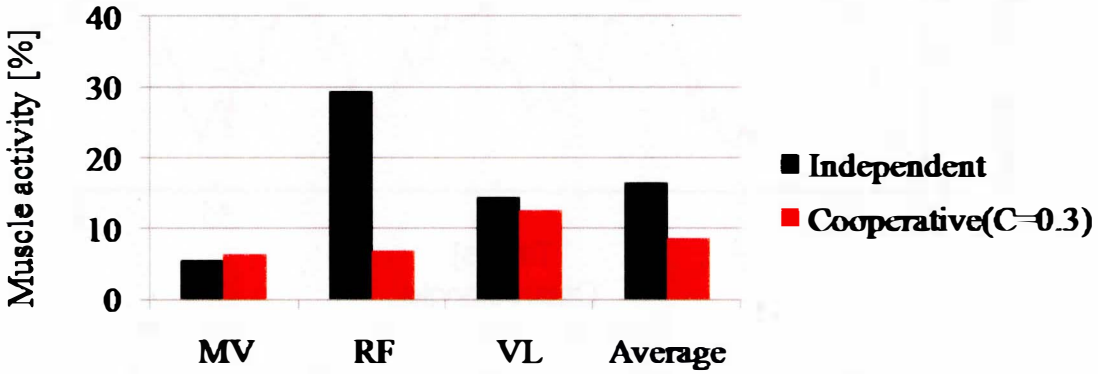

Fig.4.4. 21 Muscle activity

From the results shown above, we found that, the robot's joint toque became larger to some extent along with the increase the synchronization gain to counteract the increasing mutual joint torque, and the mutual joint torque assists the human to move with larger amplitude. However, the mutual joint torque has a limited value, which suggests that the synchronization-based motion assist method enables a limited assist effect.

We can conclude from the simulations and experimental results that , using the synchronization-based motion assist method, the robot can synchronize with the frequency of

the human's motion and assist human, an decrease ratio of 48% in muscle activity in largest from the experimental results. The robot's joint torque plays a part in counteracting the mutual joint torque and assisting the human to move. The "attenuation" in desired angle generation enables the robot provide friendlier and more compliant assist. However, the synchronization-based motion assist method enables a limited assist effect.

4.5 Simulation and experimental results of synchronization-based power assist method

Using the human joint torque as the external signal fed back, we can achieve synchronization of the robot with the human using the approach described as follows: firstly, use the human joint torque as the input signals to the neural oscillator, then use the synchronized output signals of the neural oscillator as the robot joint torque. Then by integrating Eq. (4.2) using the Runge-Kutta method, the robot joint angle can be calculated. Figure 4.5.1 shows the framework of the synchronization-based power assist.

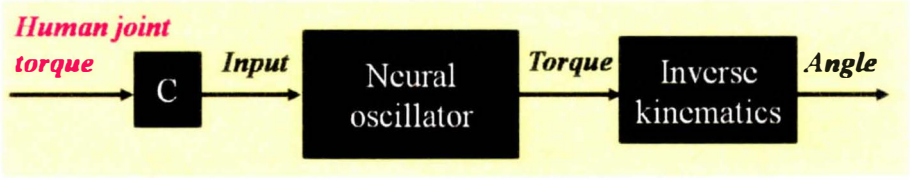

Fig.4.5. 1 Synchronization-based power assist

4.5.1 Simulation results

Using the simulation model and method described in section 4.1, we conducted extensive simulations.

Under free condition, the human moves the joint at a frequency of 0.5 [Hz] with amplitude of 0.73 [rad] by the torque given in Eq. (4.11), and the robot joint motion's frequency is about 1.0 [Hz]. The phase portrait of the natural motion of the human is shown in Fig. 4.5.2.

Under constraint condition, the robot which had a higher synchronization gain (C=0.2) synchronized its motion with that of the human arm. The frequency of the system became to 0.5 [Hz] with amplitude of 1.58 [rad]. That is, the frequency of the robot joint motion was completely entrained to that of the human, and the amplitude of the human joint's motion was greatly assisted and increased compared to the natural amplitude 0.73 [rad]. The phase portrait

of the cooperative motion of the human is shown in Fig. 4.5.3.

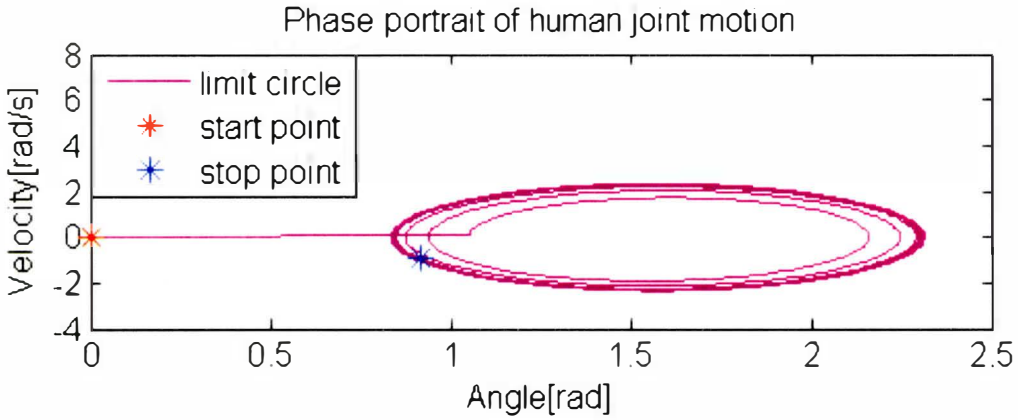

Fig.4.5. 2 Phase portrait of the natural motion of the human joint

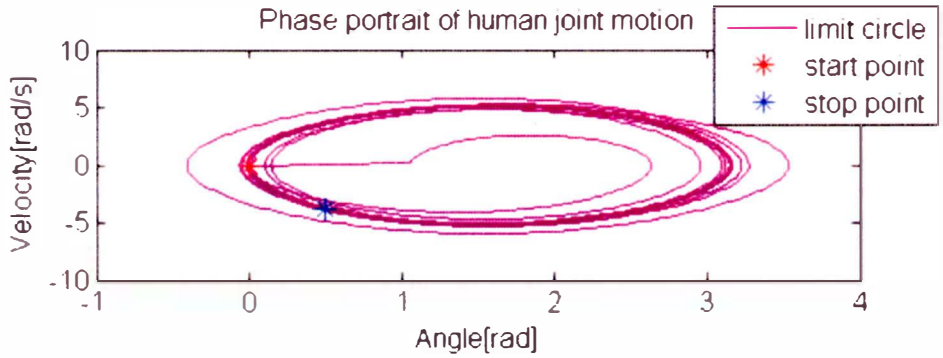

Fig.4.5. 3 Phase portrait of the cooperative motion of the human joint

By gradually increasing the synchronization gain from 0 to 0.2, we investigated the mutual joint torque between the human and robot, their joint torque, the amplitude and the frequency of the system's motion. Figure 4.5.4 shows the mutual joint torque, human joint torque and robot joint torque plotted against the synchronization gain. It can be found that the mutual joint torque, functioning as the external torque acting on the human, gets larger along with the increase of the synchronization gain. This result is due to the feature of the neural oscillator, which is explained in more detailed in section 3.3.1, and the larger the mutual joint torque, the more significant the assist effect, and vice versa. Figure 4.5.5 shows the amplitude of the system's motion. It can be found that the amplitudes get increased along with the increase of mutual joint torque. Figure 4.5.6 shows the frequency of their motion, which are entrained to the natural frequency of the human. By increasing the synchronization gain larger than 0.2, stable oscillation can also be

obtained with larger mutual joint torque, larger amplitude.

From the results shown in Fig. 4.5.4 to Fig. 4.5.6, we found that, the robot's joint toque became larger along with the increase the synchronization gain to counteract the increasing mutual joint torque, and the mutual joint torque assists the human to move with larger amplitude.

We can conclude from the simulation results that, using the synchronization-based power assist method, the robot can easily synchronize with the frequency of the human's motion and assist human significantly, an increase of 0.85 [rad] in amplitude from the simulation results. The robot's joint torque plays a part in counteracting the mutual joint torque which assists the human to move.

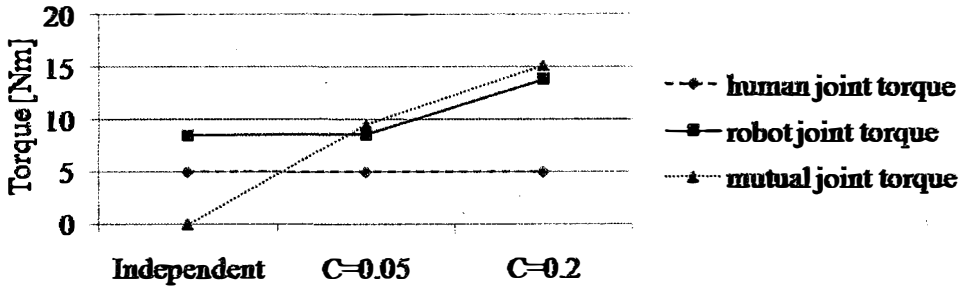

Fig.4.5. 4 Joint torque and mutual joint torque plotted against the synchronization gain

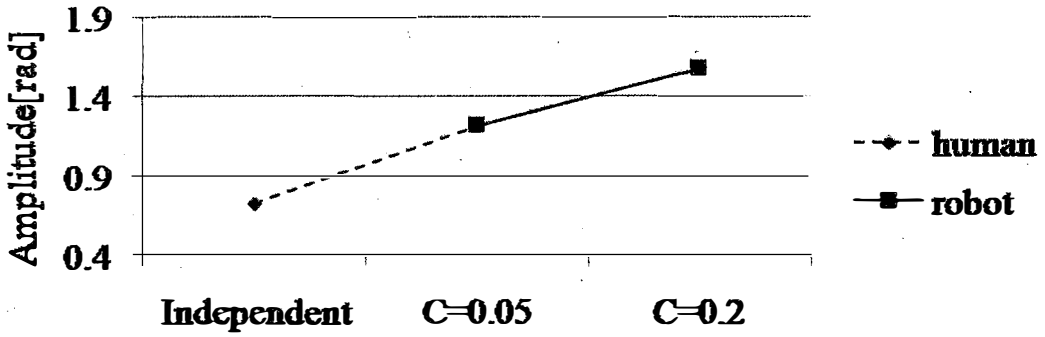

Fig.4.5. 5 Amplitude plotted against the synchronization gain. (The robot motion is not plotted out, because the robot motion is divergent under independent condition)

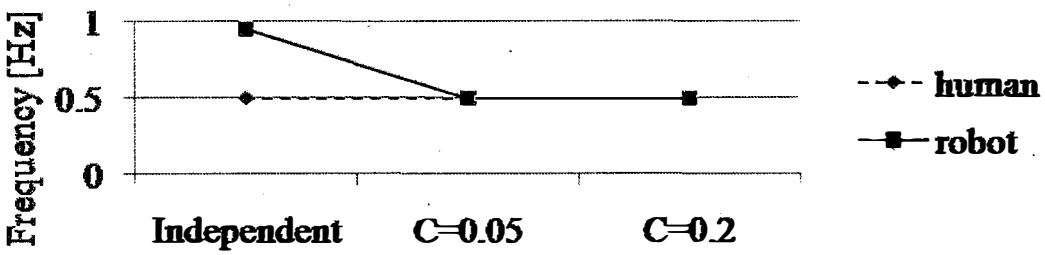

Fig.4.5. 6 Frequency plotted against the synchronization gain

In simulation where C=0.2, we assigned the human joint with 0 at 5 second, we found that the robot continued to oscillating. The result is shown in Fig. 4.5.7. We investigated the input-output of neural oscillator, that is, the human joint torque multiplied by C and the robot joint torque. Figure 4.5.8 shows the relationship between the human joint torque and the robot joint torque before-after 5 seconds. It can be found that before 5 seconds, the human joint torque and the robot joint torque were co-directions, but after 5 seconds the robot joint torque continued to oscillating regardless of the human joint torque becoming to zero. As a result, the robot continued to oscillating and took the human compulsively oscillate as well.

In conclusion, the robot never stops when human want to make a stop in the case of power assist.

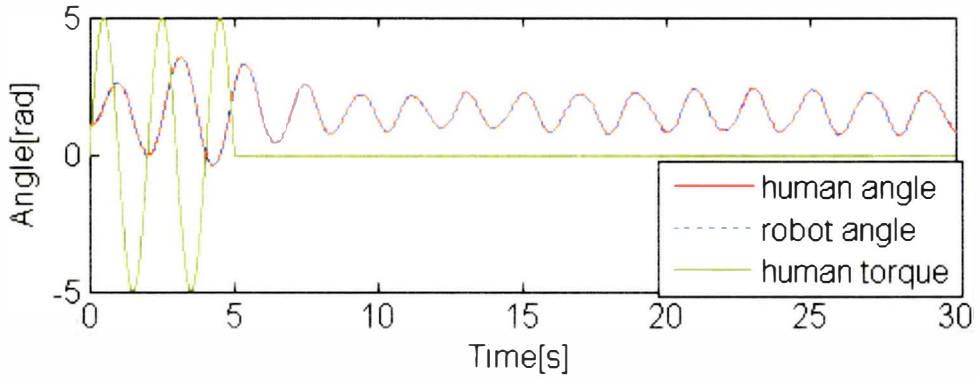

Fig.4.5. 7 Robot never stops when human try to stop

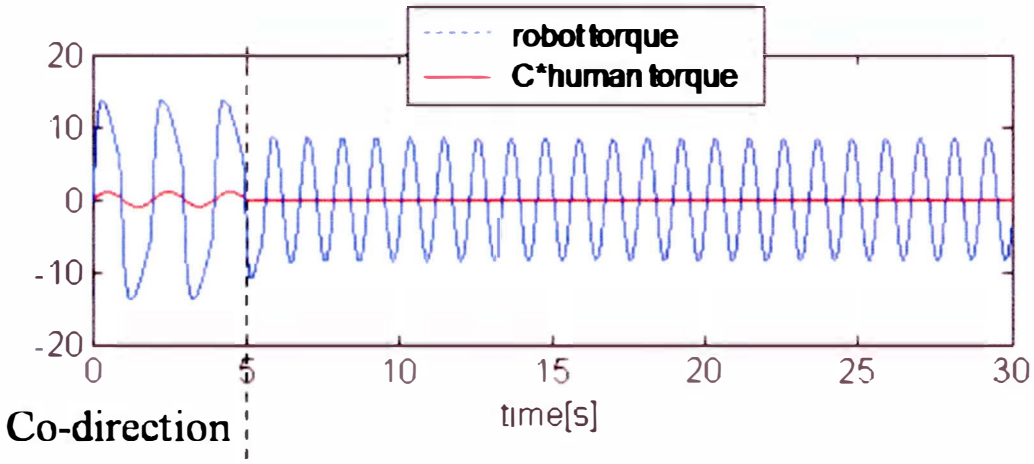

Fig.4.5. 8 Input-output of neural oscillator

4.5.2 Experimental results of robot-robot interaction

Using the experimental devices described in section 4.2, we conducted experiments of the robot-robot interaction model in the case of power-assist method.

By gradually increasing the synchronization gain from 0 to 2, we investigated the mutual joint torque between the human and robot, their joint torque, the amplitude and the frequency of the system's motion. Figure 4.5.9 shows the mutual joint torque, human joint torque and robot joint torque plotted against the synchronization gain. It can be found that the mutual joint torque, functioning as the external torque acting on the human, gets larger along with the increase of the synchronization gain. This result is due to the feature of the neural oscillator, which is explained in more detailed in section 3.3.1, and the larger the mutual joint torque, the more significant the assist effect. Figure 4.5.10 shows the amplitude of the system's motion. It can be found that the amplitudes get increased along with the increase of mutual joint torque. Figure 4.5.11 shows the frequency of their motion, which is entrained to the natural frequency of the human.

From the results shown in Fig. 4.5.9 to Fig. 4.5.11, we found that, the robot's joint toque became larger along with the increase the synchronization gain to counteract the increasing mutual joint torque, and the mutual joint torque assists the human to move with larger amplitude.

We can conclude from the simulation results that , using the synchronization-based power assist method, the robot can synchronize with the frequency of the human's motion and assist human, an increase of 0.6 [rad] in amplitude from the simulation results. The robot's joint torque plays a part in counteracting the mutual joint torque and assisting the human to move.

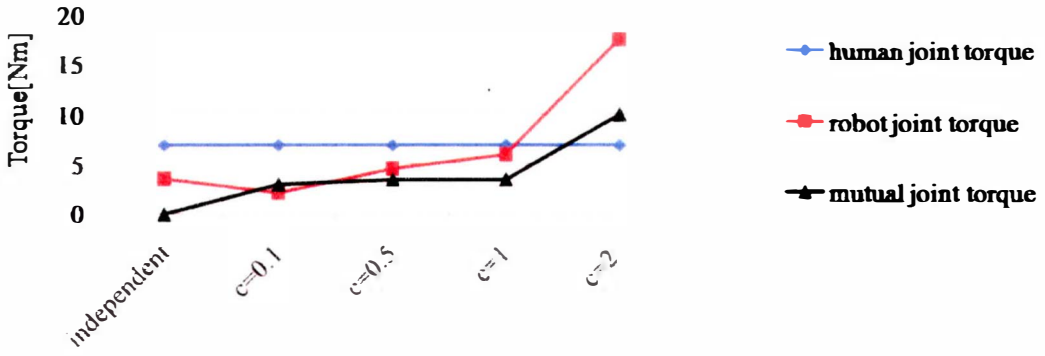

Fig.4.5. 9 Joint torque and mutual joint torque plotted against the synchronization gain

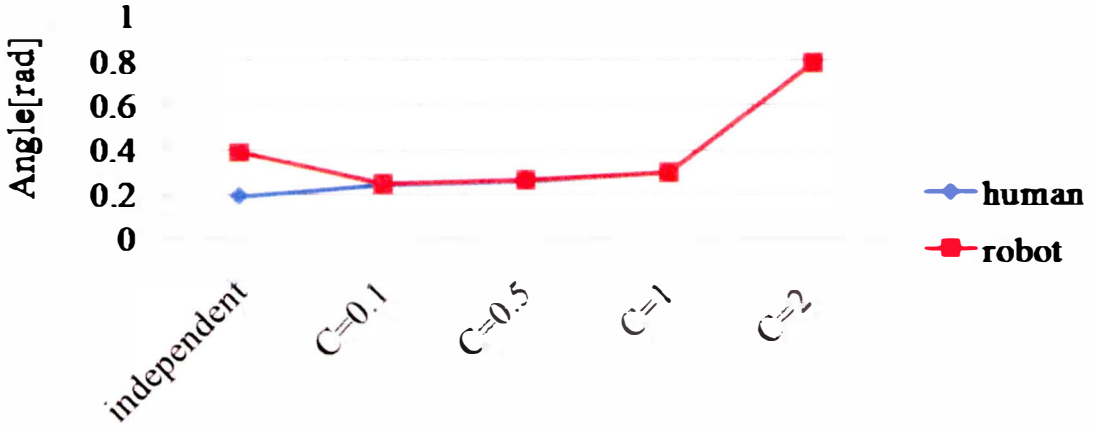

Fig.4.5. 10 Amplitude plotted against the synchronization gain.

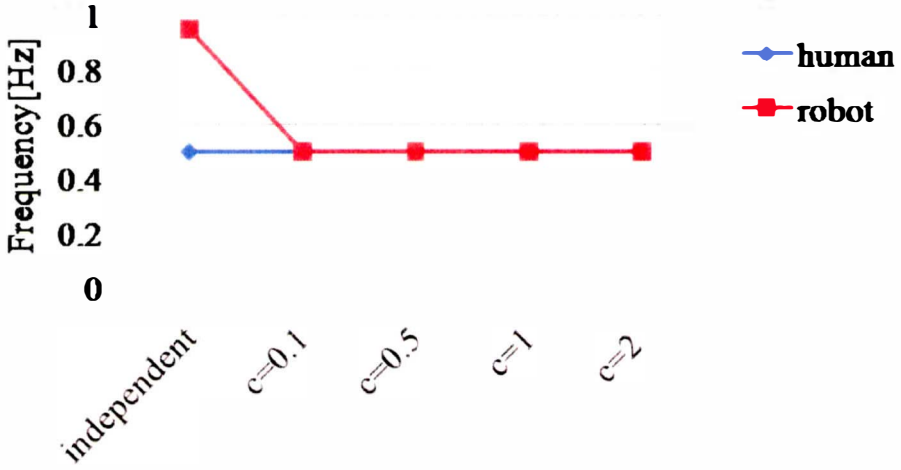

Fig.4.5. 11 Frequency plotted against the synchronization gain

4.5.3 Experimental results of human-robot interaction

Using the experimental devices described in section 4.3, we conducted experiments of the human-robot interaction model in the case of power assist method.

A series of experiments were conducted to examine the assist effect and synchronous behavior. In the experiment, the robotic suit was determined to move at a frequency of 1.0 Hz with the output signal from the neural oscillator. The natural motion of the subject, a university student, has a frequency of about 0.8 [Hz] with amplitude of about 0.35 [rad]. Where wearing the suit, she was asked to maintain the natural frequency by listening to a metronome. We investigated the cooperative motion, the user's muscle activity (using EMG-signal), mutual joint torque and robot joint torque under cooperative motion.

Under cooperative condition, the robot which had a higher synchronization gain (C=0.1) synchronized its motion's frequency with that of the user's motion. The frequency of the system became to 0.8 [Hz] with amplitude of about 0.57 [rad]. That is, the frequency of the robot

motion was entrained to that of the user, and the user was assisted to move with larger amplitude 0.57 [rad] compared to the natural amplitude 0.35 [rad]. The cooperative motion of the system and its power spectrum are shown in Fig. 4.5.12 and Fig. 4.5.13. Figure 4.5.14 shows mutual joint torque and robot joint torque plotted against to the synchronization gain. The amplitude of the cooperative motion is shown in Fig.4.5.15. It can be found that the mutual joint torque, robot joint torque and amplitudes get increased along increasing the synchronization gain. Figure 4.5.16 shows the frequency of their motion, which are synchronized to the natural frequency of the human.

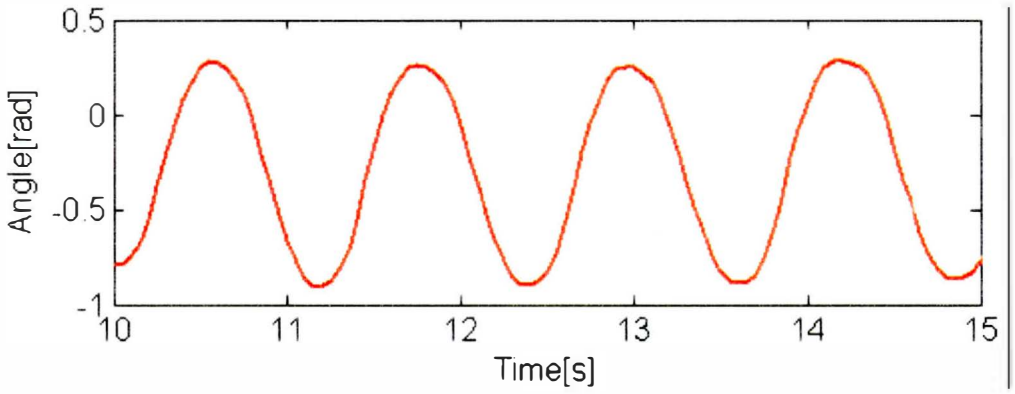

Fig.4.5. 12 Cooperative motion of the system

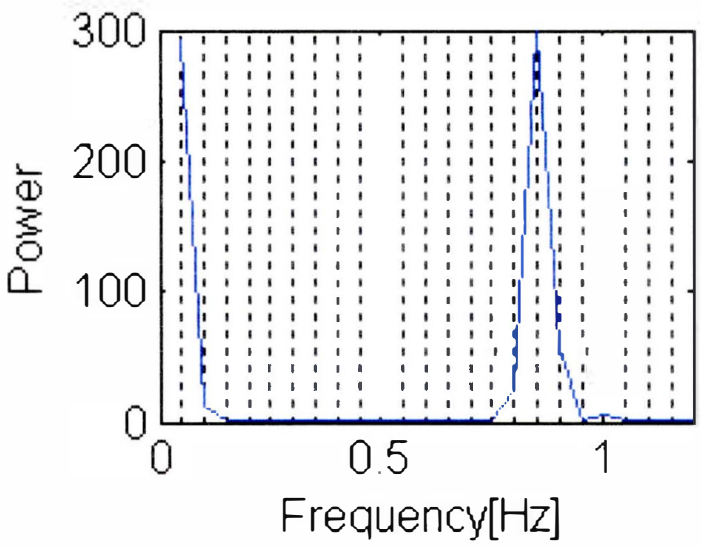

Fig.4.5. 13 Power spectrum of cooperative motion

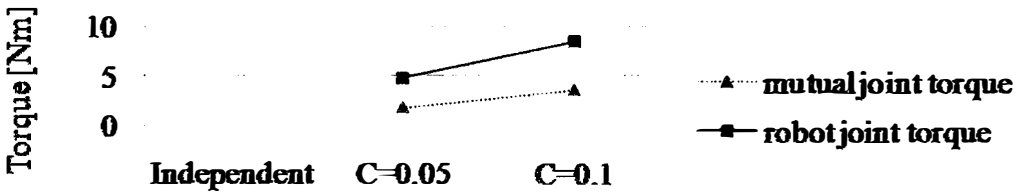

Fig.4.5. 14 Joint torque (real line) and mutual joint torque (dotted line) plotted against the synchronization gain

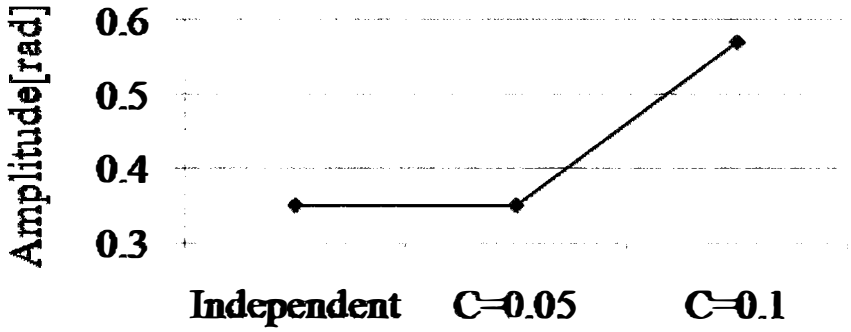

Fig.4.5. 15 Amplitude plotted against the synchronization gain

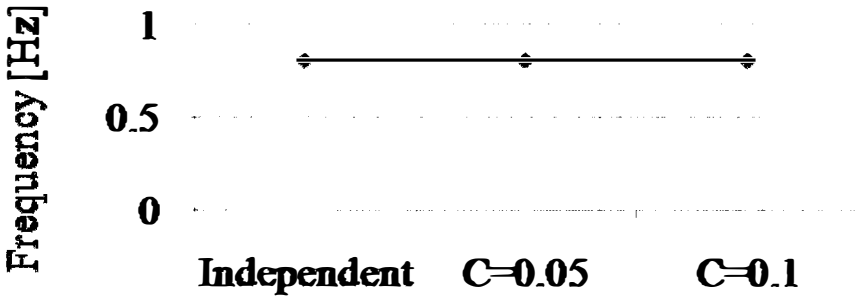

Fig.4.5. 16 Frequency plotted against the synchronization gain

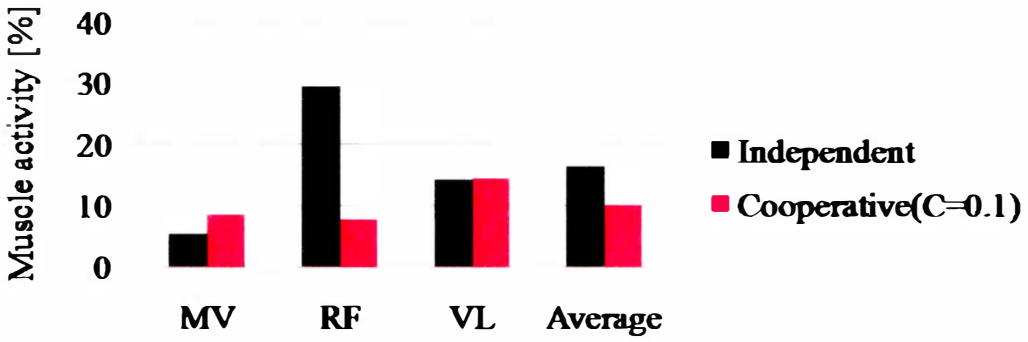

Fig.4.5. 17 Muscle activity

Figure 4.5.17 show the muscle activity under both conditions of independent motion and cooperative motion. Average muscle activity reaches 10.2% when the user moves together with the robot as shown by pink block in Fig. 4.5.17, but it reaches 16.4% when the user moves independently as shown by black block in Fig. 4.5.17. The 6.2% deference, a decrease ratio of 38% in muscle activity to the original 16.4%, is the assist effect. So herein, it can be considered the assist effect has been verified. The Rectus Femoris Muscle which mostly relating to the flexion and extension of the knee joint was the most significantly assisted, about 70% decrease.

4.6 Discussion

4.6.1 Comparison between power assist and motion assist

A. both synchronization-based power assist and synchronization-based motion assist are able to enable synchronization of the robot's movement with human movement.

B. In the case of synchronization-based motion assist method, the higher level the synchronization, the smaller the mutual joint torque is brought about. As mutual joint torque functions as the external torque acting on the user, smaller mutual joint torque means smaller assist effect. Therefore, synchronization-based motion control is effective in realizing synchronization, but it brings about limited assist effect. However, the "attenuation" phenomenon between the input-output (desired angle-mutual joint torque) make the desired angle to be generated more reasonably for walking assist. The attenuation in desired angle makes the robot to be more compliant to provide assistance. For example, the robot stops

immediately when human want to make a stop in the case of motion assist.

As the mutual joint torque can be measured by a torque sensor, and no other sensor attached on the human body, thus the control system is much simpler than any other previous one in the field of motion assist.

C, in the case of synchronization-based power assist method, the higher level the synchronization, the larger the mutual joint torque is brought about. As mutual joint torque functions as the external torque acting on the user, significant mutual joint torque means significant assist effect.

However, as the human torque is necessary for the control system, it needs to investigate the kinematics and dynamics of human, which will make the control system much complicated.

Furthermore, it would be inconvenient if the human user wants to stop, because the robot never stops in the case of power assist.

We want to realize the human-like assist of a robot with synchronization-based control which is as simple as possible and hopefully doesn't bring extra payload to the users. The synchronization-based motion assist method is a simple system, which also helps the robot obtain synchronous action and assist effect. In addition, the synchronization-based motion assist method makes the cooperative motion friendlier and facilitates easy stop. Therefore, we choose synchronization-based motion assist method in further study.

4.6.2 Comparison between other technique and our technique

Based on the discussion mentioned above, we hypothetically discussed the differences between our synchronization-based control system and the other system (Taking the HAL as the competitive technique), and summarized in Table 4.6.1.

Table4.6. 1 Comparison between other technique and our technique

	Competitive technique	Our technique
Operating principle	• The voluntary control system responds to signals originating in the brain, and the autonomous control system operates based on stored movement patterns and provides human movement sequences. • Adjusting the assisting torque by pushing the bottom on the suit.	• The movement is determined by the output of neural oscillator, and the output of neural oscillator is dependent on the its synchronization level, and how the suit interacting with its user. • Adjusting the assisting motion by adjusting the synchronization level.
Extra burden applied to its user	There is need to fix sensor on the skin surface to detect the bio-electrical signal, which would be an extra burden to the user.	There is no need to fix any sensor on the user's body, and thus no extra burden to the user.
Assisting target	• Normal people • The elderly • Some patients need rehabilitation	• Normal people • The elderly (especially those who walk with small steps) • Paralysis patients and those who have spasm of the lower limb

References

[1] Xia Zhang, Minoru Hashimoto, "A New Approach Using Neural Oscillator for Rhythmic Power Assist," *2011 IEEE Int. Conf. on Robotics and Biomimetics (IEEE ROBIO2011),* Phuket, Thailand, pp, 2896-2901, December, 2011.

[2] M.Hashimoto, Y.Kiyosawa, R.P.Paul, "Torque sensing technique for robots with harmonic drives," *IEEE Transaction on Robotics and Automation,* Vol. 9, No.1, pp.108-116, 1993.

[3] S. Lee, Y. Sankai, "Minimizing the Physical Stress by Virtual Impedance of Exoskeletal Robot in Swinging Motion with Power Assist System for Lower Limb ," *Transactions of the Japan Society of Mechanical Engineers,* Vol. 71, No. 705, pp.274-282.

[4] Tomohiro Kizuka, Tadashi Masuda, Tohru Kiryu and Tsugutake Sadoyama, 2006, *Biomechanism Library Practical Usage of Surface Electromyogram,* First Edition, Society of Biomechanisms, Japan, p.16(in Japanese).

Chapter 5

Preliminary experiments on knee joint movement assist

Chapter 5 Preliminary experiments on knee joint movement assist

In order to investigate the feasibility and validity of our proposal using neural oscillators for movement assist, we first conducted preliminary experiments on the knee joint movement assist. We examined the proposed method from three points of view. The first is whether synchronization of action between human and motion assist suit can be realized. The second is whether the assist effect can be obtained, and the third is whether the proposed method is comfortable for the user. We explored these three points of view by conducting computer simulations on a human-motion assist system and experiments with a joint torque sensing assist suit [1][2].

5.1. Simulations

Here, we assume that the human user also generates periodic motion patterns by neural oscillators, which is also the different feature from the model used in Chapter 4. Figure 5.1.1 shows our model of human-motion assist system, assuming that there are two joints at the knees, one is the human knee joint and the other is assist suit knee joint. Both knee joints are controlled by the neural oscillators, and the human leg and assist suit are bundled together.

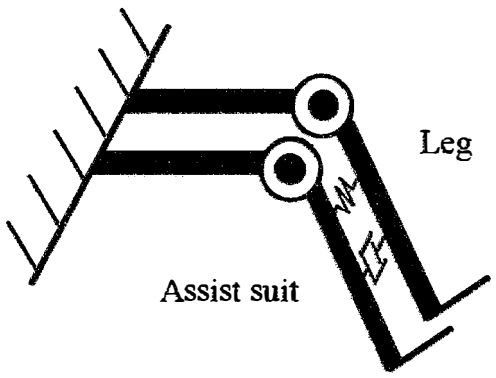

Fig.5.1. 1 Simplified human-robot system

5.1.1 Simulation method

Figure 5.1.2 shows the entire image of the control method used in the simulation. This specific approach can be described as follows: firstly, mutual joint torque generated by interaction will be used as input signals for the neural oscillators, and the synchronized output signals of the neural oscillators will be used as the desired angle of each joint. Then PD feedback control is used to control the each joint following the desired joint angle. Therefore new locomotion is generated, and again mutual joint torque is used as the input signal of the neural oscillator, and these flows described above are repeated again and again to achieve a series of entrained and synchronized motions between the human user and the assist suit.

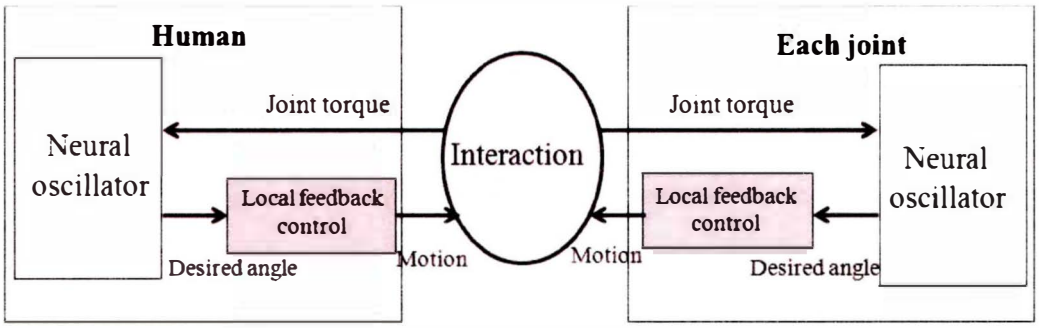

Fig.5.1. 2 Simulation method

5.1. 2 Dynamic Equations of System

Dynamic equation of this system is written by

$$\boldsymbol{\tau} = \begin{pmatrix} \tau_h \\ \tau_a \end{pmatrix} = \begin{pmatrix} J_h\ddot{\theta}_h + G_h + k_1(\theta_h - \theta_a) + k_2(\dot{\theta}_h - \dot{\theta}_a) \\ J_a\ddot{\theta}_a + G_a - k_1(\theta_h - \theta_a) - k_2(\dot{\theta}_h - \dot{\theta}_a) \end{pmatrix} \quad (5.1)$$

J_h, J_a are the inertial moment, G_h, G_a are the gravity term, $k_1(\theta_h - \theta_a) + k_2(\dot{\theta}_h - \dot{\theta}_a)$ is the constraint force term between human and assist suit, k_1 is proportion coefficients and k_2 is viscous coefficients. By using the vectors, equation (5.1) can be represented as the following equation.

$$\dot{\mathbf{x}} = A\mathbf{x} + B\boldsymbol{\tau} + C \tag{5.2}$$

$$\mathbf{x} = \begin{pmatrix} \theta_h & \dot{\theta}_h & \theta_a & \dot{\theta}_a \end{pmatrix}^{\mathrm{T}} \tag{5.3}$$

$$A = \begin{bmatrix} 0 & 1 & 0 & 0 \\ -\frac{k_1}{J_h} & -\frac{k_2}{J_h} & \frac{k_1}{J_h} & \frac{k_2}{J_h} \\ 0 & 0 & 0 & 1 \\ \frac{k_1}{J_a} & \frac{k_2}{J_a} & -\frac{k_1}{J_a} & -\frac{k_2}{J_a} \end{bmatrix} \tag{5.4}$$

$$B^T = \begin{bmatrix} 0 & \frac{1}{J_h} & 0 & 0 \\ 0 & 0 & 0 & \frac{1}{J_a} \end{bmatrix} \tag{5.5}$$

$$C^T = \begin{bmatrix} 0 & -\frac{G_h}{J_h} & 0 & -\frac{G_a}{J_a} \end{bmatrix} \tag{5.6}$$

$$G_h = m_h l_h \cos\theta_h \tag{5.7}$$

$$G_a = m_a l_a \cos\theta_a \tag{5.8}$$

$$\boldsymbol{\tau} = \begin{pmatrix} \tau_h \\ \tau_a \end{pmatrix} = \begin{pmatrix} k_p(\theta_{dh} - \theta_h) + k_d(\dot{\theta}_{dh} - \dot{\theta}_h) \\ k_p(\theta_{da} - \theta_a) + k_d(\dot{\theta}_{da} - \dot{\theta}_a) \end{pmatrix} \tag{5.9}$$

$\boldsymbol{\tau}$ is going to be defined by local feedback control as showed in equation (5.9). k_p is the proportional gain, k_d is the differential gain. In addition, θ_d is the desired angle output by the neural oscillator.

Equation (5.2) is integrated by the Runge-Kutta method. The values of links' parameters used in this simulation are listed in Table 4.1.2. The PD control gain and constraint force term are

listed in Table 4.1.1 and Table 4.1.3.

5.1.3 Simulation Results

Here we determine T_r by 0.12 and T_a by 0.6 for assist suit, T_r by 0.16 and T_a by 0.8 for human. Consequently, the basic frequencies of the human user and assist suit are determined to be 0.7 Hz and 1.0 Hz, respectively. Figure 5.1.3 shows an example of independent motion of the suit and the leg. The dotted line represents the human user's motion, and the solid line represents the assist suit's motion.

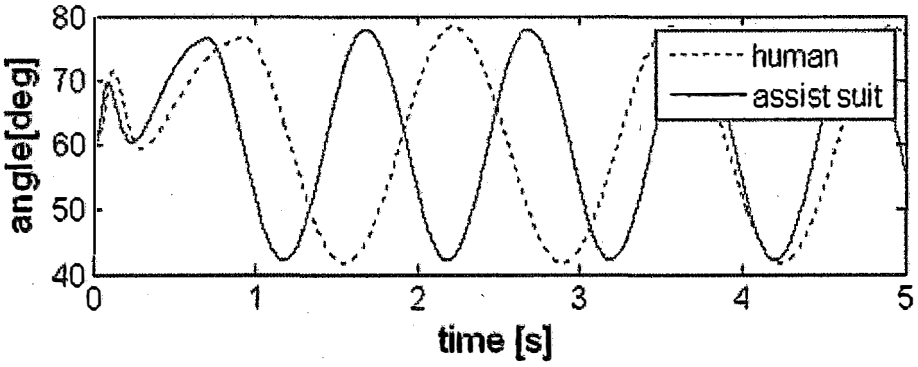

Fig.5.1. 3 Autonomous movement

We conducted a series of simulations on this human-assist suit system based on SBC. Next we will discuss the simulation results.

・Synchronization action

Figure 5.1.4 shows synchronized motions of assist suit and human leg in combination using SBC. Here, constraint force coefficients k_1 and k_2 are determined with a premises of binding the human leg and assist suit move together. Each synchronization gain of the human user and the assist suit is represented by C_h and C_a. Figure 5.1.4 (a) shows synchronized motions when C_h=0.0, and C_a=0.5, that is to say, the human user keeps his own frequency actively and assist suit's motion is entrained and synchronized with that of the human user. It can be seen from Fig. 5.1.4 (a) that the frequency of synchronized motion is 0.7 Hz as desired.

We investigated the changes of frequency brought about by the synchronization gain. Figure

5.1.4 (b) shows both real angles of the human user and the assist suit when C_h is determined by 0.5 and C_a is determined by 0.0. That is to say, the assist suit keeps its own frequency and amplitude actively and the user's motion is entrained and synchronized with that of the assist suit. We found that the frequency of the synchronized motion changes to 1.0 Hz. Figure 5.1.4 (c) shows both real angles of the user and the assist suit when C_h is determined to be 0.3and C_a is determined to be 0.3. Both assist suit and human are actively willing to inhibit their movement to a certain extent, as both of their motions are going to be entrained and synchronized. It is shown by Fig. 5.1.4 (c) that the frequency of synchronized motion changes to 0.85 Hz, which is in the middle of 0.7 Hz and 1.0Hz.

In addition, we conducted a simulation where we kept the human user's synchronization gain C_h at 0.0 but increased the assist suit's synchronization gain to 0.1, 0.3 and 0.5, then we make investigations on the change of mutual torque and frequency under each conditions. The results are shown in figure 5.1.5. As can be seen from figure 5.1.5, it is possible to achieve a variety of synchronization level and frequencies. But the trade-off is that the higher the level of synchronization, the smaller the assist effect. We conclude that it is important to properly determine the value of synchronization gain to get the most desirable outcome.

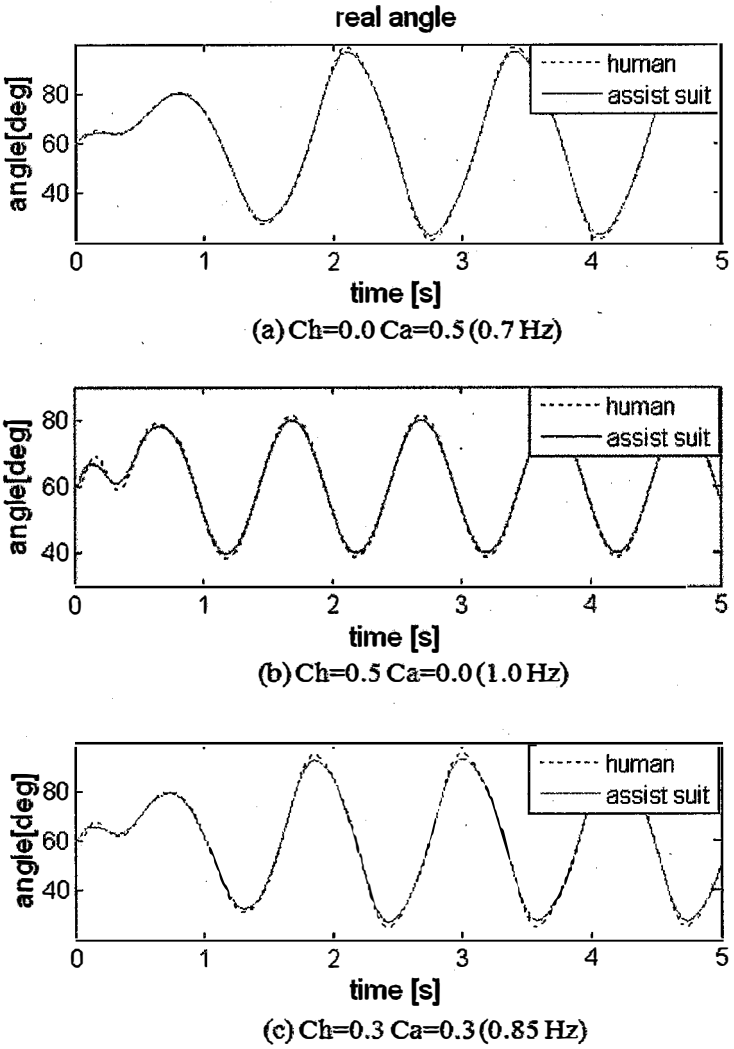

Fig.5.1. 4 Movement with SBC

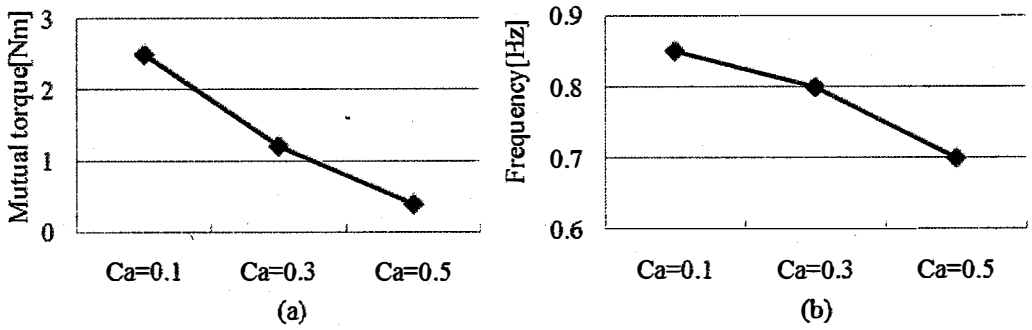

Fig.5.1. 5 (a) Relationship of mutual torque and synchronization gain, (b) Relationship of frequency and synchronization gain

· Assist Effect

We limit the human user who has a very small amount of force, not beyond 4.0±2.0 Nm to reproduce that this person himself cannot be expected to make any locomotion. In other words, he is willing yet unable to move his leg by his own torque of 4.0±2.0 Nm. Then we bind the human user's leg to the assist suit, and investigate their motion and the user's torque for the action. Here we set C_h and C_a to 0.0 and 0.5 respectively, their motion has been shown in Fig. 5.1.4 (a).

Figure 6.1.6 shows the torque of the human user with movement independently and together with assist suit respectively. To realizing the same movement (Fig. 5.1.4 (a)), when a human user moves by himself, he need to put forth physical effort about 8.0 Nm (absolute value relative to centricity of 4.0 Nm), shown by the dotted line in Fig. 5.1.6, but when combined with the assist suit, he can make such a locomotion with physical effort about 2.0 Nm (absolute value relative to centricity of 4.0 Nm) with the help of the assist suit which is shown by the solid line in Fig. 5.1.6. This shows how the human user's physical power has been assisted by the assist suit.

From simulation results, it can be concluded that not only assist effect can be obtained from the assist suit, but also three kinds of synchronization motion (active, passive, as well as between active and passive) can be realized with SBC using neural oscillators.

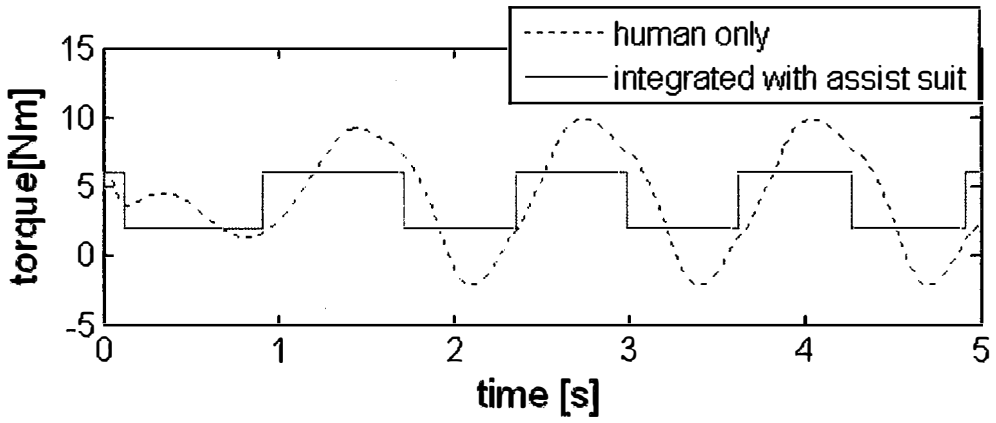

Fig.5.1. 6 Torques of human

5.2. Experiments

The proposed framework is examined by experiments of a human knee joint assisted movement with an assist suit. In this section we will describe experimentations including experimental devices and evaluation of experiment results.

5.2. 1 Experimental Equipment and Control System

As can be seen in Fig. 5.2.1 this single-DOF system, which is designed for knee joint and consists of one links and one actuator FHA-17C-50-E250 provided by Harmonic Drive Systems Company. This actuator has a built-in joint torque sensor. Once an external force is applied, the mutual joint torque will be measured. ART-Linux is used for this control system. Its control system is depicted in detail in section 6.2.

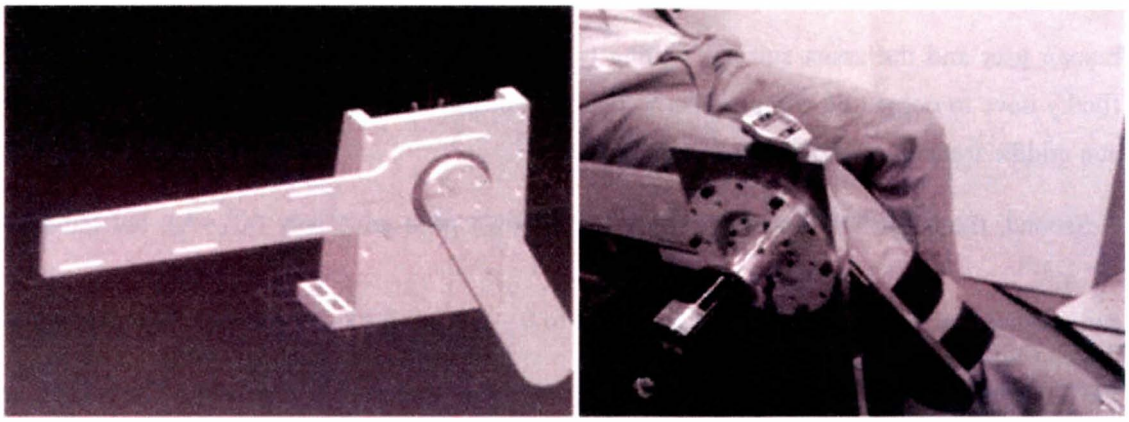

Fig.5.2. 1 Experiment device and experiment scenarios

5.2.2 Experimental Results

A series of experiments has been conducted to verify the results from the simulation. In the experiment, the assist suit is also determined to move at a frequency of 1.0 Hz and at an amplitude of 20.0 deg. We use a band to bind the user's leg and the assist suit tightly together as shown in Fig.5.2.1. The subject, a university student, was asked to keep a basic frequency of about 0.8 Hz by listening to a metronome.

In the experiment, we know it is difficult to determine the synchronization level of human by assigning a fixed value, nonetheless we defined human synchronization as follows: no synchronization, little synchronization and high synchronization are represented by A, B, C respectively.

· Synchronization action

First, we investigated the motion patterns when each synchronization gain changes. The result is shown in Fig. 5.2.2. In the case of C_h=A, C_a=0.28 (Fig. 5.2.2 (a)), human moves actively but assist suit moves passively, consequently the motion of whole system changes to the human user's basic frequency of 0.8 Hz. On the other hand, Figure 5.2.2 (b) shows the result of C_h=C, C_a=0.0, where the human user is very passive and adapts himself to the motion of the assist suit. We further investigated in the case of C_h=B, C_a=0.14 shown in Fig. 5.2.2 (c), both the human user and the assist suit are willing to keep their intentions active to some extent, but finally have to come to a compromise so that both of their motions are synchronized and move at a middle frequency of 0.85 Hz.

Second, the subject was asked to move at his own pace arbitrarily (C_h=A), but the assist suit's synchronization gain C_a was increased to 0.14, 0.28, 0.43 respectively. We investigated the changes of mutual torque, frequency and amplitude under each condition. The results are shown in Fig.5.2.3. We found that the results of the experiment matched those of the simulation.

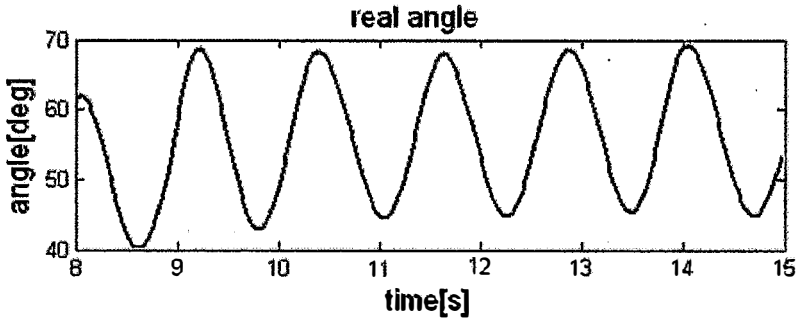

(a) Ch=A Ca=0.28 (0.8 Hz)

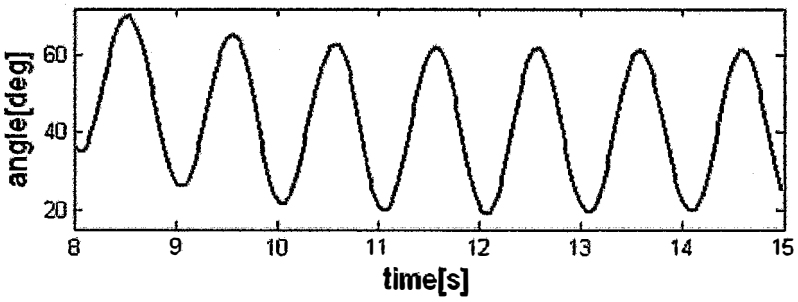

(b) Ch=C Ca=0.0 (1.0 Hz)

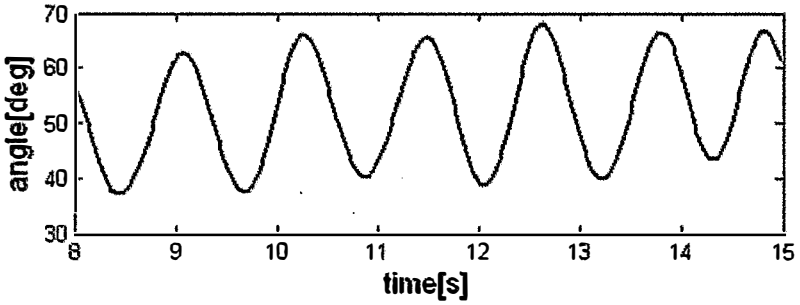

(c) Ch=B Ca=0.14 (0.85 Hz)

Fig.5.2. 2 Angles of human and assist suit

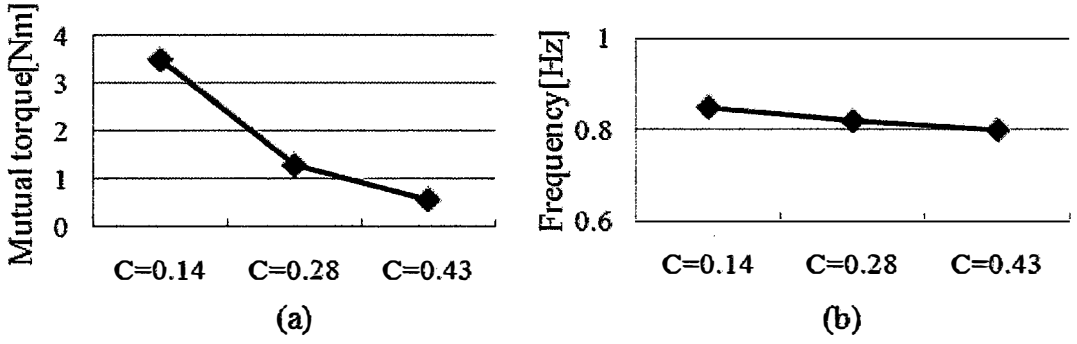

Fig.5.2. 3 (a) Relationship of mutual torque and synchronization gain, (b) Relationship of frequency and synchronization gain

· Assist effect

We used a personal-EMG to measure muscle activity (RMS signal) in five places in leg when human move independently and move together with assist suit.

When human moves together with assist suit, the assist suit's synchronization gain is determined to be 0.14, which means a middle synchronization level. These results are shown in Fig.5.2.4. Muscle activity reaches 6.5% when the user moves together with the assist suit as shown by solid line in Fig. 5.2.4, but it reaches 9.0% when the user moves by himself as shown by dotted line in Fig. 5.2.4. The 2.5% deference between these two is the assist effect. So herein, it can be considered the assist effect has been verified.

From the experimental results described above, we conclude that the human user's physical strength has been augmented but also passive and active motion assist styles can be realized by adjusting the value of synchronization gain.

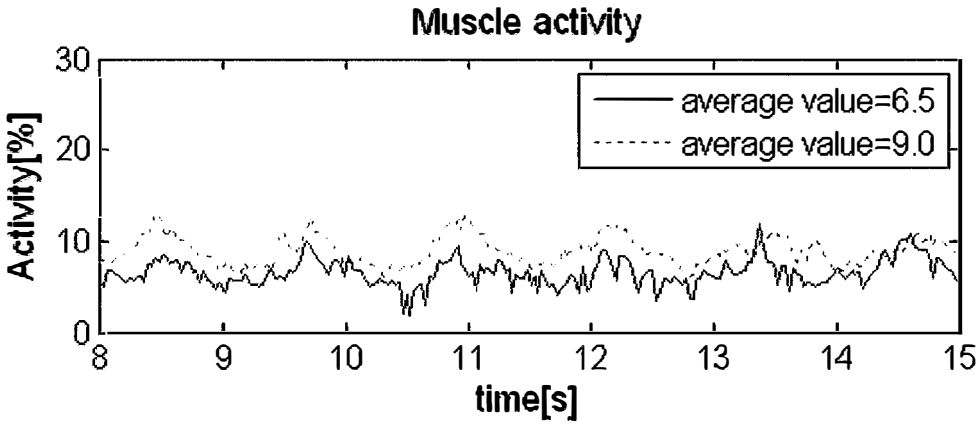

Fig.5.2. 4 Muscle activity

5.3 Evaluation experiments

We also conducted an experiment of comparing SBC with impedance control by using a paired comparison method proposed by Bradley [3]. Four samples are utilized. Samples (a) and (b) use the proposed control method with C_a = 0.28 and C_a = 0.14 respectively. Samples (c) and (d) use impedance control in order to compare with the proposed method. The desired impedance control is represented by equation (5.10) [4].

$$\tau(k) = Kf(q_d(k) - q_e(k)) + Dd(\dot{q}_d(k) - \dot{q}_e(k)) \qquad (5.10)$$

k represents the iteration time, $\tau(k)$ is the mutual joint torque sensed by torque sensor, and $q_d(k)$ is defined by $20\sin(2\pi k)$. Thus as can be seen from equation (10), we can determine the servo-desired angle, $q_e(k)$ using mutual joint torque. Then we use PID control to determine the real angle of assist suit. We changed the value of proportion gain, Kf to be larger to increase stiffness, also we set a small value to decrease the stiffness. The values of parameters of Sample (c) and (d) are listed in table 5.3.1.The frequency and amplitude of the desired trajectories is common to all samples.

We make six pairs of Samples (a) to (d) for the paired comparison. We asked the subjects to move together with the assist suit with pairs of different samples, and then answer which is better in terms of "coordination", "assist effect" and "flexibility". The total number of the subjects was 10. The results of the comparison in terms of "coordination", "assist effect" and "flexibility" are listed in Table 5.3.2, 5.3.3 and 5.3.4 respectively. The table shows number of subjects who answer that the sample listed on the left row is better than that on the top line. From these results we can find that many subjects select Samples (a) and (b) of the proposed control methods. In terms of "flexibility" the same results with in terms of "coordination" are obtained. (a) was the most highly rated, except for assist effect. From this we can conclude that the assist effect with a middle synchronization level is preferable than that with a high synchronization level. Table 5.3.5 lists the judging scale values and χ_0^2 . For all questions, the following inequality is satisfied $\chi_0^2 > \chi^2(3,0.05) = 7.82$. Then the statistical test using χ^2 distribution function shows that there are differences in rank among four samples. Consequently, we get to know the proposed method is preferable than conventional impedance control in motion assist.

Table5.3. 1 Parameters of impedance control

Parameters	c	d
Kf (Nm/deg)	0.1	1.0
Dd (Nm s/deg)	1.2	1.2

Table5.3. 2 Coordination

	a	b	c	d	total
a	–	8	10	10	28
b	2	–	10	9	21
c	0	0	–	10	10
d	0	1	0	–	1

Table5.3. 3 Assist effect

	a	b	c	d	total
a	–	3	8	8	19
b	7	–	6	8	21
c	2	4	–	9	15
d	2	2	1	–	5

Table5.3. 4 Flexibility

	a	b	c	d	total
a	–	8	10	10	28
b	2	–	10	9	21
c	0	0	–	10	10
d	0	1	0	–	1

Table5.3. 5 Interval scale and χ_0^2

	π_a	π_b	π_c	π_d	χ_0^2
Coordination	0.8062	0.1783	0.0141	0.0014	59.4988
Assist effect	0.3245	0.4109	0.2058	0.0587	16.6764
Flexibility	0.8062	0.1783	0.0141	0.0014	59.4988

5.4 Summaries

We examined the validity and feasibility of proposed method by conducting computer simulations on a human-assist system and experiments with a built-in joint torque sensor assist suit. From the results, we can conclude the following: by using SBC, firstly, the synchronization motion can be realized; secondly, the motion assist effect has been obtained; finally, this approach has a good usability. From above, it can be concluded SBC, which is inspired by human interaction effect is a useful control method for motion assist.

References

[1] X. Zhang, M. Hashimoto, "SBC for Motion Assist Using Neural Oscillator," *IEEE Int. Conf. on Robotics and Automation,* Kobe, Japan, pp.659-664, May 2009.

[2] Xia Zhang, Minoru Hashimoto, "Interaction Approach for Movement-Assist Control Using Neural Oscillators," *International Journal of Automation Technology*, Vol.3 No.6,741-749,2009

[3] R. A. Bradley and M.E. Terry: "Rank analysis of incomplete block designs I, The method of paired comparisons," *Biometric*, vol.39, pp.324-345, 1952.

[4] Haruhiko Asada and Jean-Jacques E. Slotine, "Robot analysis and control," *A Wiley Interscience publication*, ISBN 0-471-83029-1, 1986

Chapter 6

Prototype of the four-DOF wearable robotic suit

Chapter 6 Prototype of the four-DOF wearable robotic suit

The wearable robotic suit is designed to assist a user to walk and it is designed transferring its weight to the ground (not to the user). The robotic suit has three new features [1]. First, a new control architecture was developed to enable the robotic suit synchronize with a user, and this is explained in detail in former Chapters. Second, utilizing Harmonic Drive Gear and its built-in torque sensor, a compact structure of the robotic suit with relative high power is realized. Third, the synchronization-based control was developed that controls the robotic suit through measurements of the mutual joint torque, thus there is no need to apply any sensor to a user body to get the user's move intension. This eliminated problematic extra burden placed to the user. The following give an overview of the design of this architecture.

6.1 Overview of the robotic suit

The exoskeleton architecture with similar size to a human lower limb was chosen for the robotic suit. Thus, the exoskeleton has ankle, knee, and hip joints similar to human legs. The robotic suit attaches to the user at the feet via mountain boots and at the torso through a vest. Other connections between a user and device were allowed at thigh and lower thigh. The connection at the torso is made using a custom vest which allows some gap between human and exoskeleton, thereby preventing abrasion. The vest includes rigid plates on their backs for connection to the exoskeleton low back.

6.1.1 Degrees of freedom

Each leg of the exoskeleton has two degrees of freedom at the hip, one degree of freedom at the knee, and two degrees of freedom at the ankle. The flexion-extension degree of freedom at the hip joint and knee joint is actuated. The abduction-adduction degree of freedom at the hip joint is a passive joint equipped with a hinge. There are two passive ankle joints which connect the lower thigh links to a pair of shoes, so the total weight of the suit is transmitted to the ground which makes the human user feel little extra payload as long as at stance phase or single-stance phase. Additionally, as the hinge parts and the partial lower links is made of elastic

steel, certain degrees of rotation are allowed at hip joints and ankle joints. In total, each leg of the exoskeleton has two powered degrees of freedom: hip joint and knee joint in sagittal plane. This study concerns with the assistive movement in the sagittal plane.

The cables are hung up to the ceiling so that the user could not be pulled and impeded by the cables during walking. See Fig. 6.1.2 (a).

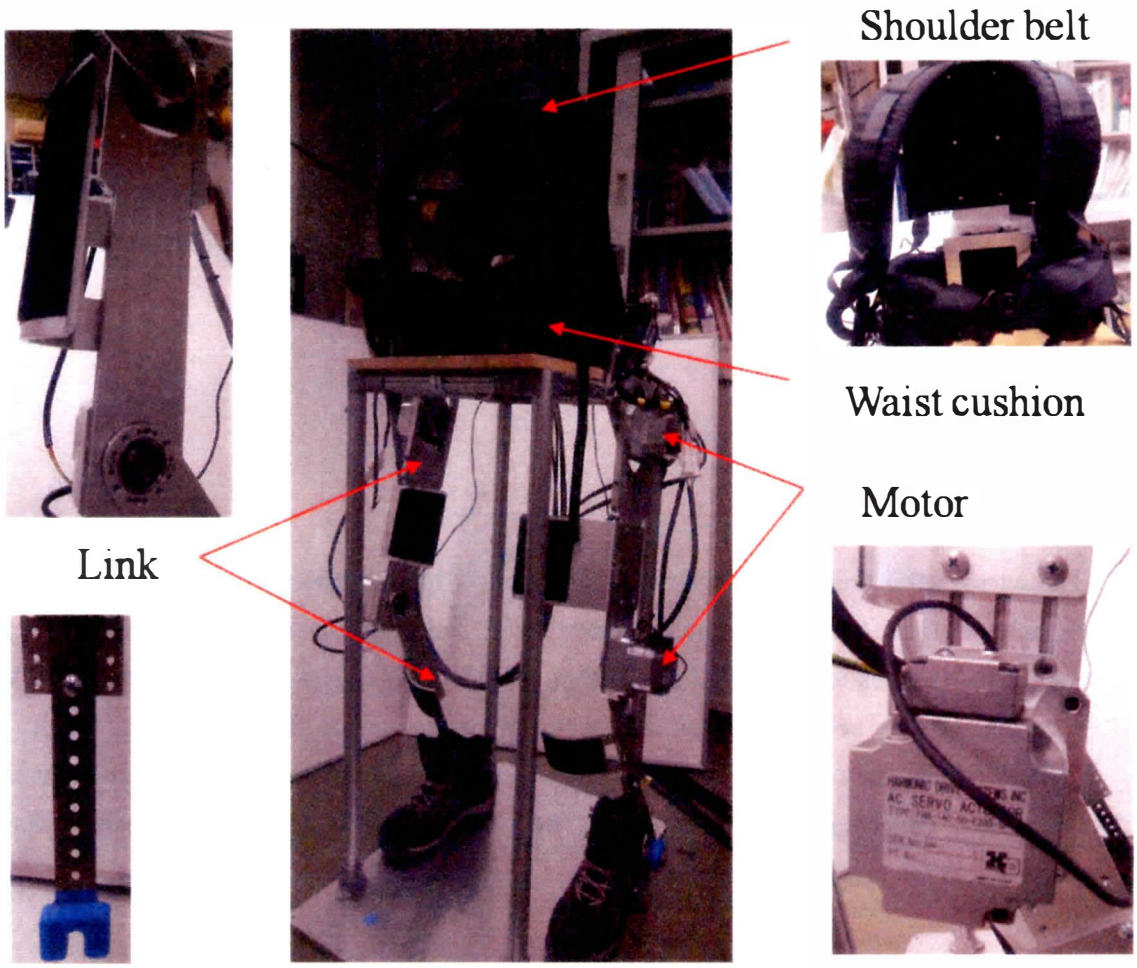

Fig.6.1. 1 Overview of the robotic suit

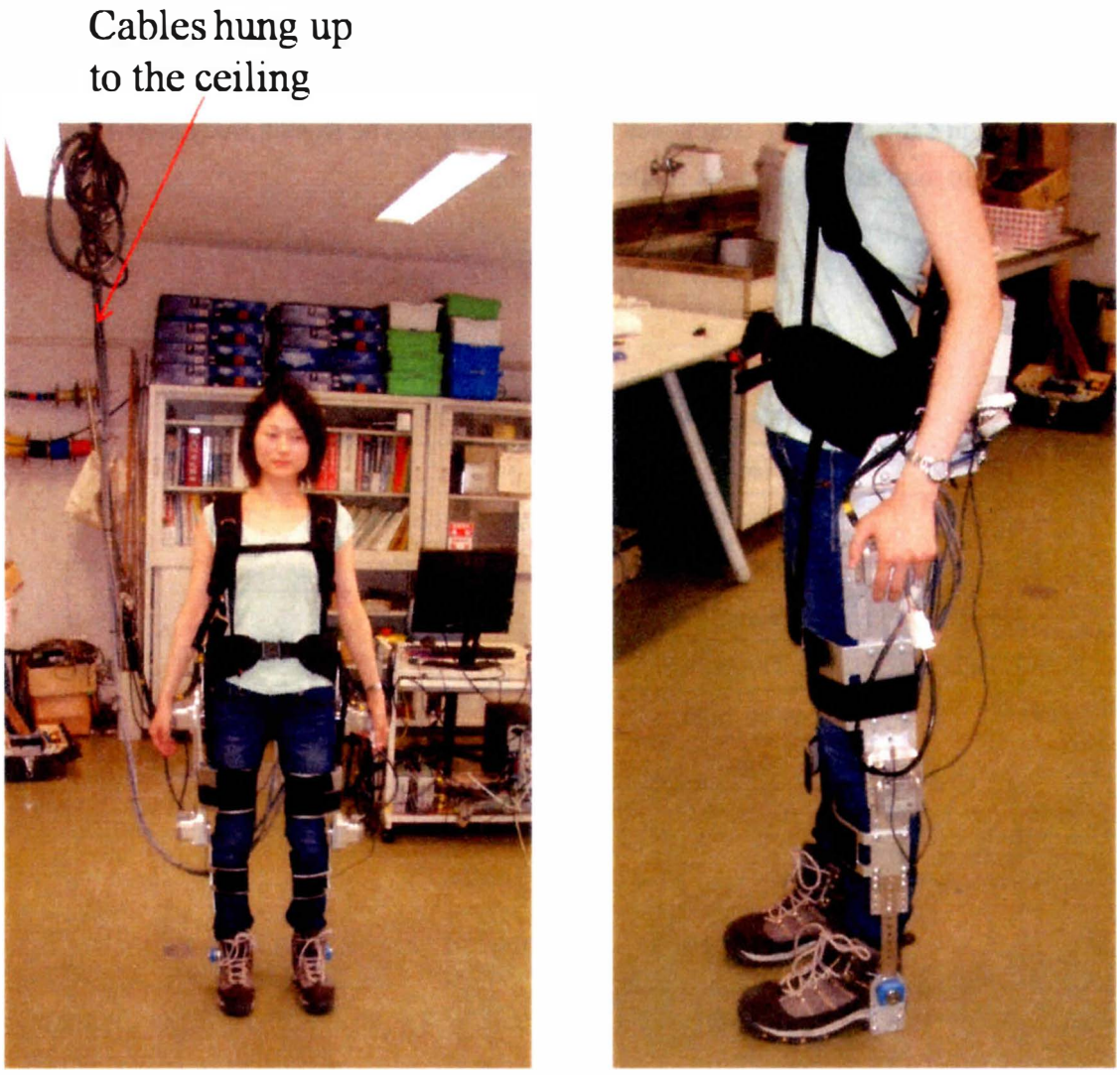

Fig.6.1. 2 Scenarios of wearing the robotic suit

6.1.2 Size of the robotic suit

Since we intended to design an anthropomorphic exoskeleton with similar lower-limb size and structure to a human, and the size of the robotic suit was designed to be adjustable. Allowing the exoskeleton to be fitted for users with 1550~1750mm tall, we designed the length of the thigh to be 370~455mm, and the lower thigh 270~430mm. The width of the waist was 600~850mm. The specific size of each part of the robotic suit is shown in Fig.6.1.3, and the

number 1,…,4 represents the number of each actuator. The length of the limb was determined referring to the average height of the elderly who are male Japanese and are older than 65, then we calculated the length of each segment by multiplying the height by the percentage of human body shown in Table 6.1.1 [2]. (Reference book [Anatomy of The Human Body page 113]). The average height used in this design is 1640mm referring to [3].

Table6.1. 1 Percentage of human body

Segments	Percentage
Head	13.7%
Neck	5.1%
Chest	12.6%
Abdomen	7.4%
Waist	7.4%
Thigh	24.3%
Lower thigh	24.3%
Foot	5.2%

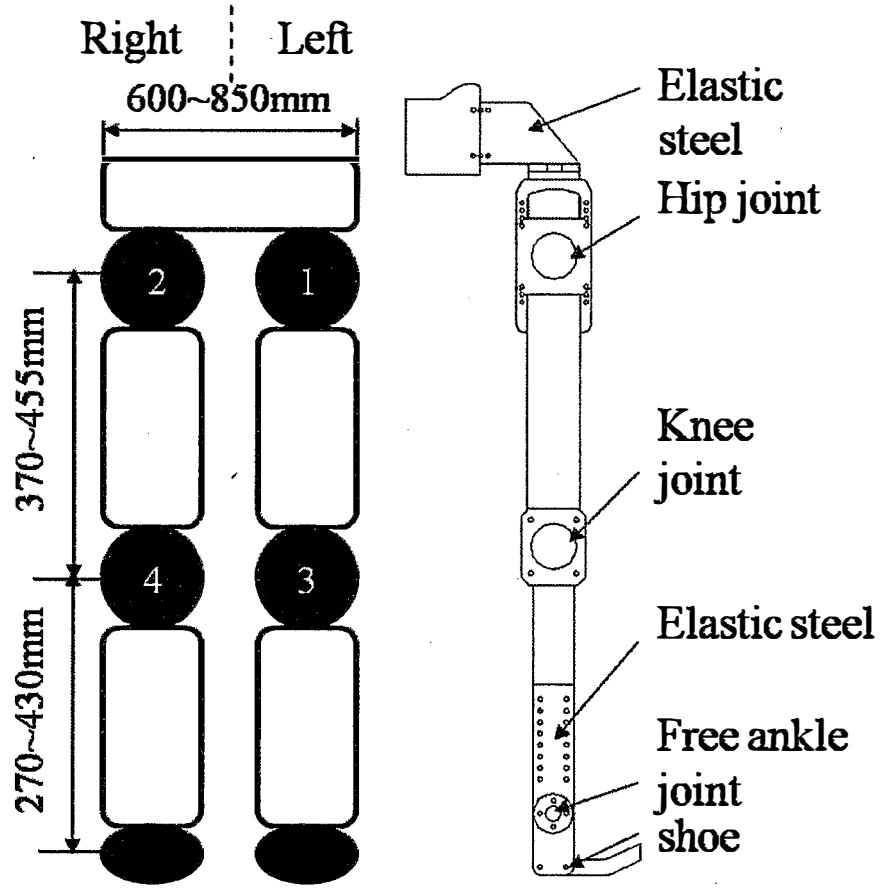

Fig.6.1. 3 Size of the robotic suit

6.1.3Actuator selection

Assuming the elderly who are male and older than 65 years old as the assist object, we investigated the average mass and the center of mass of each segment of the lower limb, and calculated the necessary torque of the hip and knee joint in the case of the normal walking. In the saggital plane, the hip joint torque was able to be calculated using equation (6.1), and knee joint torque using equation (6.2). The model is illustrated in Fig. 6.1.4

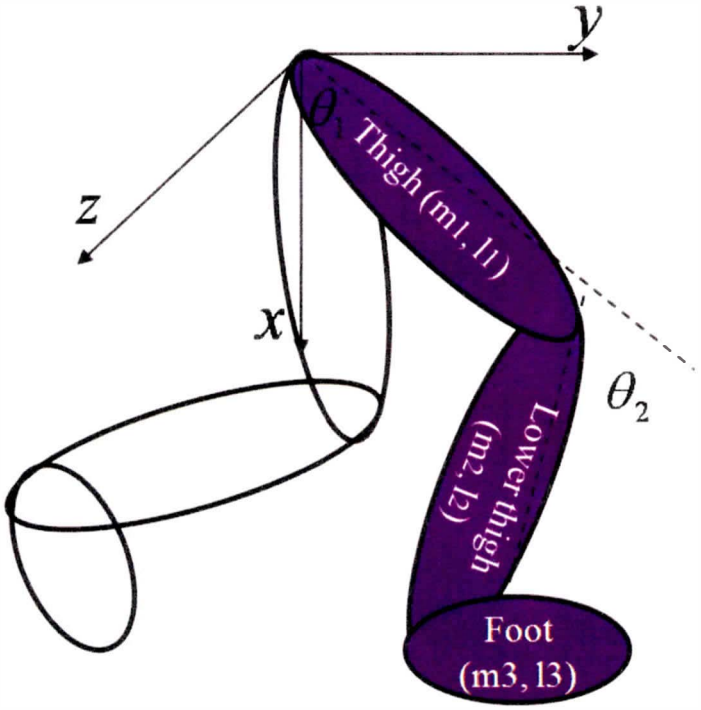

Fig.6.1. 4 simplified structure for calculating the gravity term

$$\tau_1 = m_1 g l_1 \sin\theta_1 + (m_2 g l_2 + m_3 g l_3)\sin(\theta_1 + \theta_2) \qquad (6.1)$$

$$\tau_2 = (m_2 g l_2 + m_3 g l_3)\sin(\theta_1 + \theta_2) \qquad (6.2)$$

Where, τ_1 is the joint torque of the hip joint due to gravity term, and τ_2 is that of the knee joint. $m_1 g l_1$ represents the gravity term of the thigh segment, and $m_2 g l_2$ represents that of the lower thigh, and $m_3 g l_3$ represents that of the foot . θ_1 represents the hip joint angle, and θ_2 represents the knee joint angle. The value of the mass and the center of mass of each segment are shown in Table 6.1.2. We calculated the mass of each segment by multiplying the average weight by the mass ratio of each segment shown in Table 6.1.2. (Reference matial [study/資料/人間特性解析/u-cog.pdf]). The average weight used in this design is 63.4kg referring to [3].

Table6.1. 2 Parameters of lower limb of the elderly

Segments	Mass m_i (kg)	Mass ratio	Center of mass l_i (m)
Thigh	5.8 (63.4*0.092)	0.092	0.481
Lower thigh	3.0 (63.4*0.047)	0.047	0.423
Foot	1.1 (63.4*0.017)	0.017	0.581

Since the exoskeleton is designed for assistive purpose, the required joint torques and power for the exoskeleton is chosen as an assistive torque. Determining the assistive torque as about 10Nm, we selected the harmonic drive gear (FHA-14C-50-E200, Harmonic Drive Systems Co., Japan) for both the hip and knee joint, and its specifications are shown in Table 6.1.3.

Table6.1. 3 Specifications of actuator

Items	Type : FHA-14C-50-E200
Maximum torque (Nm)	18
Torque constant (Nm/A)	7.2
Maximum currency (A)	3.2
Reduction ratio	50
Resolution	400000
Mass (kg)	1.2

6.1.4 Hardware specification

Hardware utilized in the system is depicted as following:

- Interface board

The interface board, Ritech Interface Board RIF－171－1(PCI bus type), has sixteen channels of AD transformer, sixteen channels of DA transformer and sixteen channels of PWM generator and sixteen channels of up-down Counter.

- Motor driver

HA-655 is made by Harmonic Drive Systems Co., Japan

- Actuator

FHA-14C-50-E200 is made by Harmonic Drive Systems Co., Japan

The reduction gear consists of three parts including wave generator, flexspline and circular spline. The wave generator acts as input shaft, and the circular spline acts as output shaft and serves as a fix part. The structure of harmonic drive gear is compact for the one shaft structure, and the gear is also light and has high reduction ratio. The structure of harmonic drive gear is shown in Fig. 6.1.5.

The actuator has a built-in torque sensor, which consists of 6 strain gauges cemented on the flexspline of the harmonic drive gear [4] [5]. The flexspline is a flexible structure made from steel. The elasticity of the flexspline is used to sense the joint torque. The basic principle of the torque sensing technique is discussed in [5]. Once there is a difference between the movements of the user and suit, a mutual joint torque is generated and measured by the torque sensor.

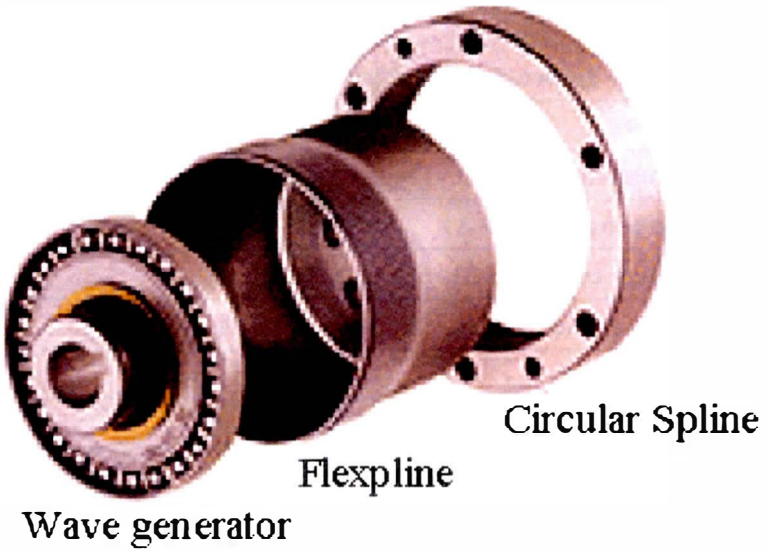

Fig.6.1. 5 Structure of a harmonic driver

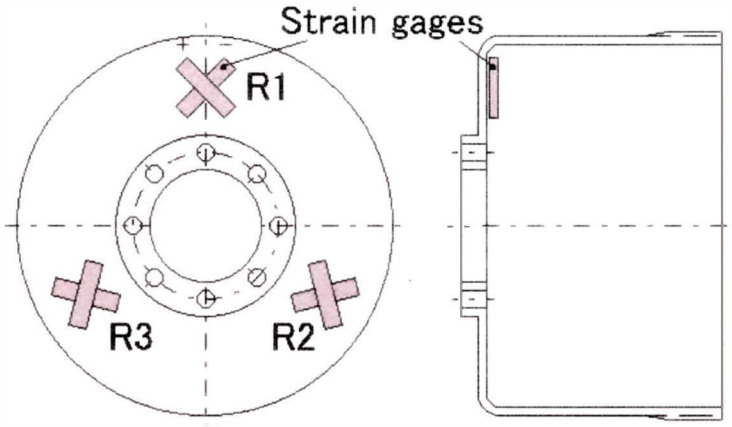

Fig.6.1. 6 Strain gauges on flexspline

6.2 Control system

ART-Linux is used as the Operation System. The AD converter, DA converter and Counter of the Interface board are used in the control system. The mutual joint torque generated from the difference of the user and suit's movement is measured by the built-in torque sensor, and is input into the computer by AD converter. Simultaneously the joint angle of the robotic suit is measured by an encoder and is input into the computer by the Counter. The block diagram of control system for one actuator is shown in Fig. 6.2.1.

6.2.1 Synchronization-based motion assist

In the case of synchronization-based motion assist, mutual joint torque is used as the oscillator input signal and synchronized neural oscillator output signals are used as the desired suit joint angle. A proportional integral differential (PID) feedback controller generates a control signal (voltage) for each joint of the robotic suit to follow the desired joint movement. The control signal (voltage) determined by PID controller is exported by the DA converter to the motor driver, and then the voltage is transferred to currency and is sent to the actuator by the motor driver. These flows are repeated to achieve a series of entrained and synchronized movements between a user and the robotic suit. Therefore, new locomotion is thus generated and again mutual joint torque used as the input signal of the neural oscillator. These processes are repeated every 1ms to achieve a series of entrained and synchronized movements between a user and the suit. The PID control gains have been decided to make the joint angle follow the desired angle accurately and quickly, and their gains are shown in Table 6.2.5.

6.2.2 Synchronization-based power assist

In the case of synchronization-based power assist, the human joint torque, presumed using the dynamics and kinematics and angle detected via the encoder, is used as the oscillator input signal and synchronized neural oscillator output signals are used as the suit joint torque. The joint torque is a control signal (voltage), and the control signal (voltage) is exported by the DA converter to the motor driver, and then the voltage is transferred to currency and is sent to the actuator by the motor driver. These flows are repeated to achieve synchronization-based power assist. These processes are repeated every 1ms.

6.2.3 Layout of I/O port

The layout of I/O port for each actuator is shown in Table 6.2.1-Table 6.2.4. The system arrangement is shown in Fig. 6.2.2, and the torque sensor amplifier layout is shown in Fig. 6.2.3.

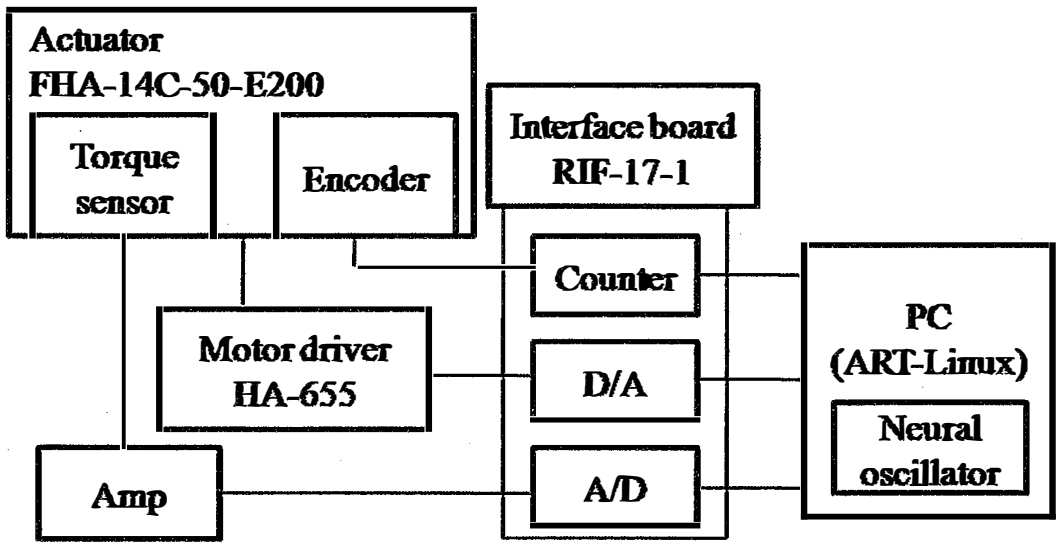

Fig.6.2. 1 Block diagram of control system for one actuator

Table6.2. 1 I/O Port layout for motor NO.1

Interface board I/O Port	Actuator side
AD1	Amp (CN1_5)
DA1	HA-655 (CN2_31)
APha1	HA-655 (CN2_44)
BPha1	HA-655 (CN2_46)
ZPha1	HA-655 (CN2_48)

Table6.2. 2 I/O Port layout for motor NO.2

Interface board I/O Port	Actuator side
AD2	Amp (CN1_5)
DA2	HA-655 (CN2_31)
APha2	HA-655 (CN2_44)
BPha2	HA-655 (CN2_46)
ZPha2	HA-655 (CN2_48)

Table6.2. 3 I/O Port layout for motor NO.3

Interface board I/O Port	Actuator side
AD3	Amp (CN1_5)
DA3	HA-655 (CN2_31)
APha3	HA-655 (CN2_44)
BPha3	HA-655 (CN2_46)
ZPha3	HA-655 (CN2_48)

Table6.2. 4 I/O Port layout for motor NO.4

Interface board I/O Port	Actuator side
AD4	Amp (CN1_5)
DA4	HA-655 (CN2_31)
APha4	HA-655 (CN2_44)
BPha4	HA-655 (CN2_46)
ZPha4	HA-655 (CN2_48)

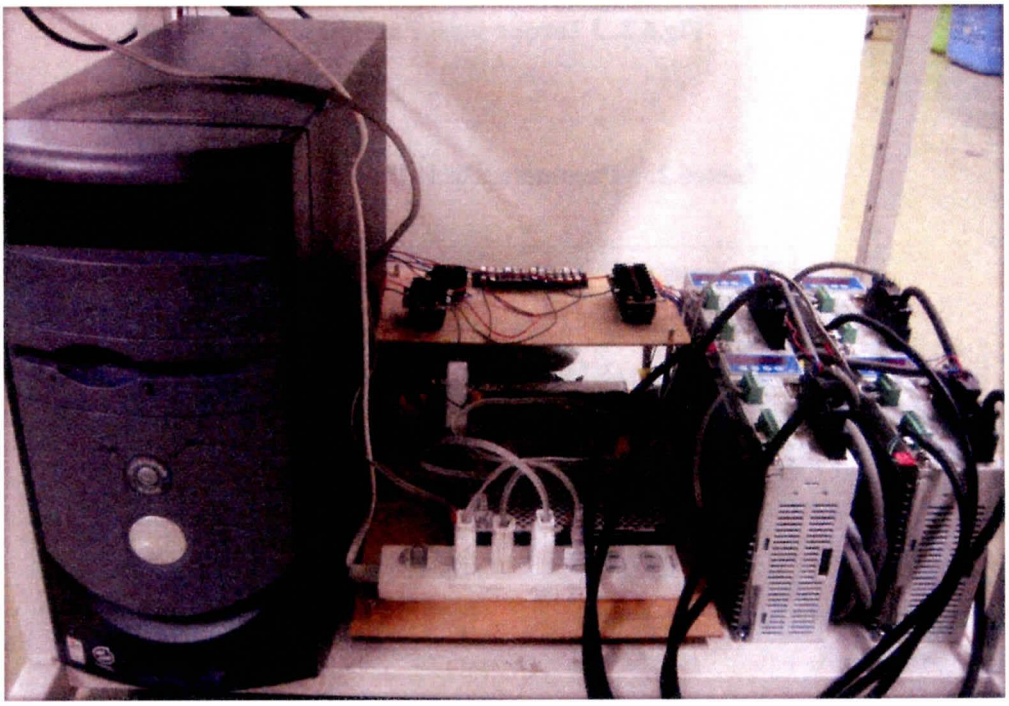

Fig.6.2. 2 Control systems

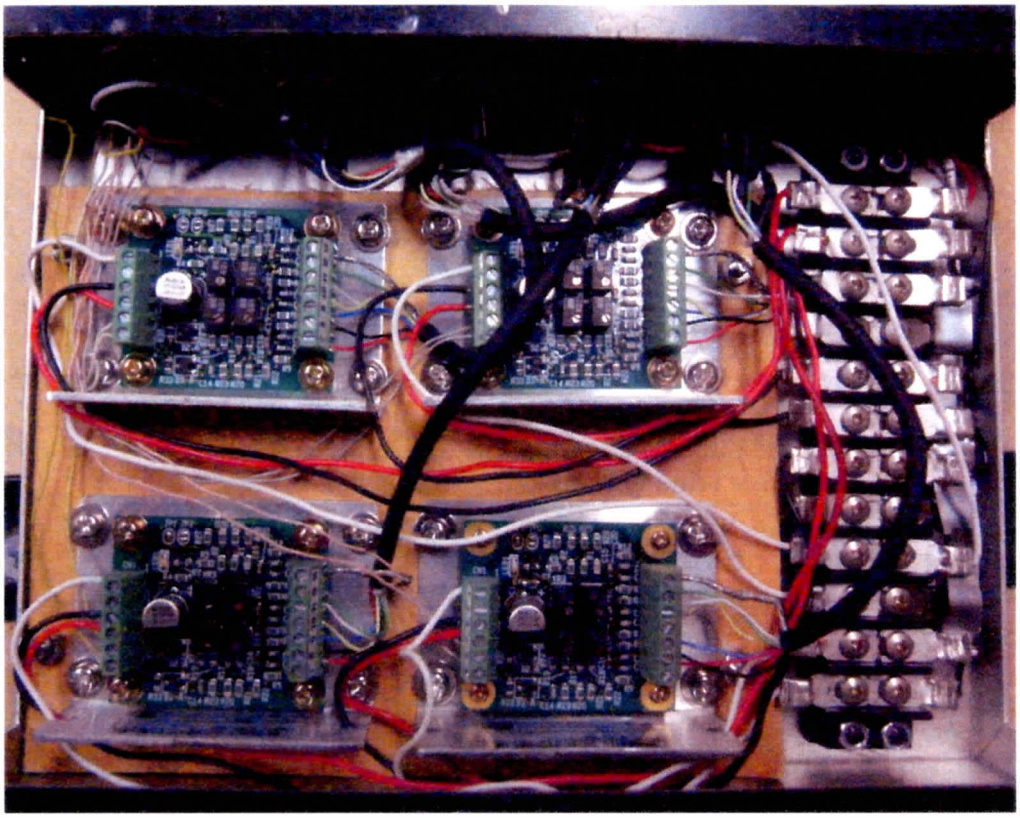

Fig.6.2. 3 Torque sensor amplifier

Table6.2. 5 Parameters of PID control gain

Parameter	value
Proportional gain (V/deg)	6.0
Integral gain (V*s/deg)	1.5
Differential gain (V/deg)	0.2

6.3 Sensitivity of torque sensor

In this section, we conducted experiment to investigate the sensitivity of the torque sensor built-in each motor. The sensitivity represents how quickly a torque sensor responds to the applied force/torque. In the calibration experiments, a 1kg weight was used as the load and was stick to the terminal of the link connected to the motor's output. The link was controlled rotating slowly 360 degrees in clockwise direction within 20 seconds, and then it was controlled

returning back to the original place in anti-clockwise direction within the same 20 seconds from the desired place. Since the speed is slow, the inertial moment and the centrifugal force can be ignored. The load torque due to the gravity of the weight was measured by the torque sensor and was recorded throughout the rotation. Theoretically, the load torque can also be calculated using the equation $Torque = mgl\sin(2\pi\theta/360)$. Where, m is the mass of the object, l is the length of the link, θ is the joint angle of the link, and its unit is [deg]. The experimental method is shown in Fig. 6.3.1.

The torque measured by the torque sensor is plotted against the joint angle of the link in clockwise and anti-clockwise directions and is shown in Fig. 6.3.2 and Fig. 6.3.4 respectively. The calculated torque against the measured voltage in clockwise and anti-clockwise directions is shown in Fig. 6.3.3 and Fig.6.3.5.

The calibration result shows that the sensitivity of the torque sensor is about 7.2[Nm/V]. The error of the torque sensor is about 4%.

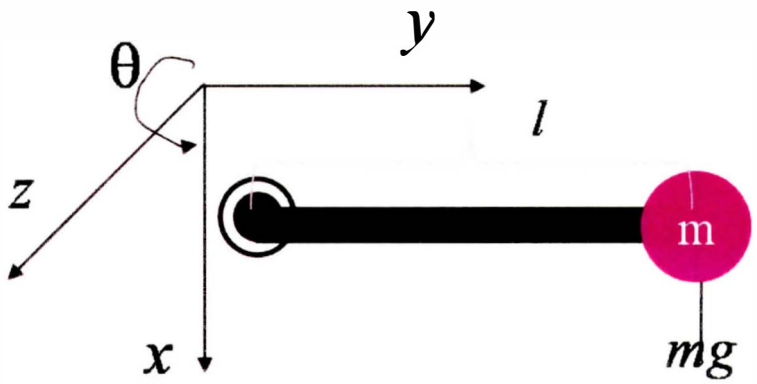

Fig.6.3. 1 Experimental method of torque sensor calibration

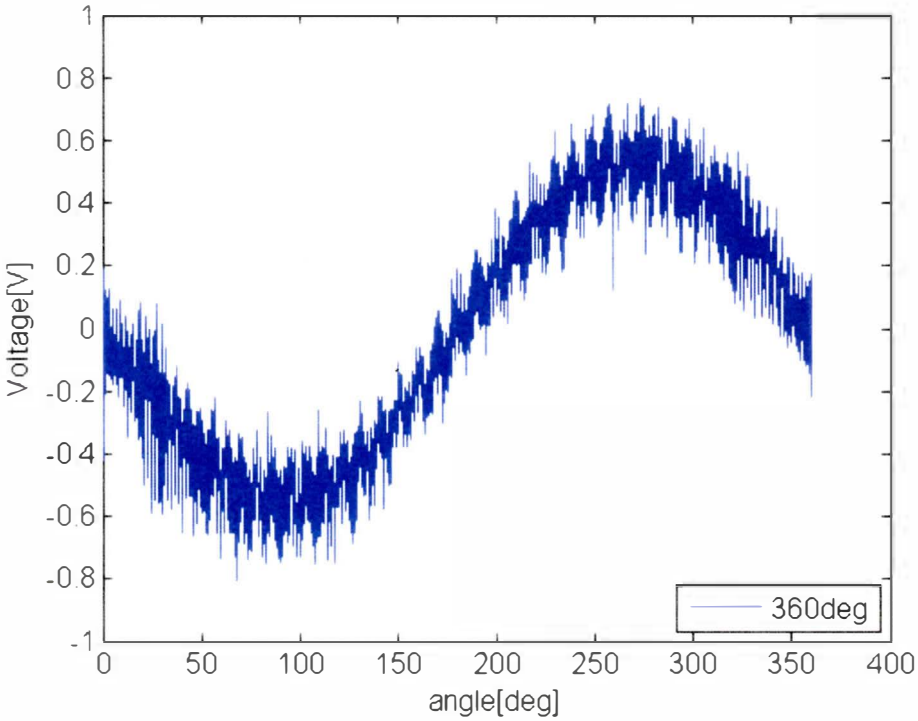

Fig.6.3. 2 Output of torque sensor in clockwise rotation

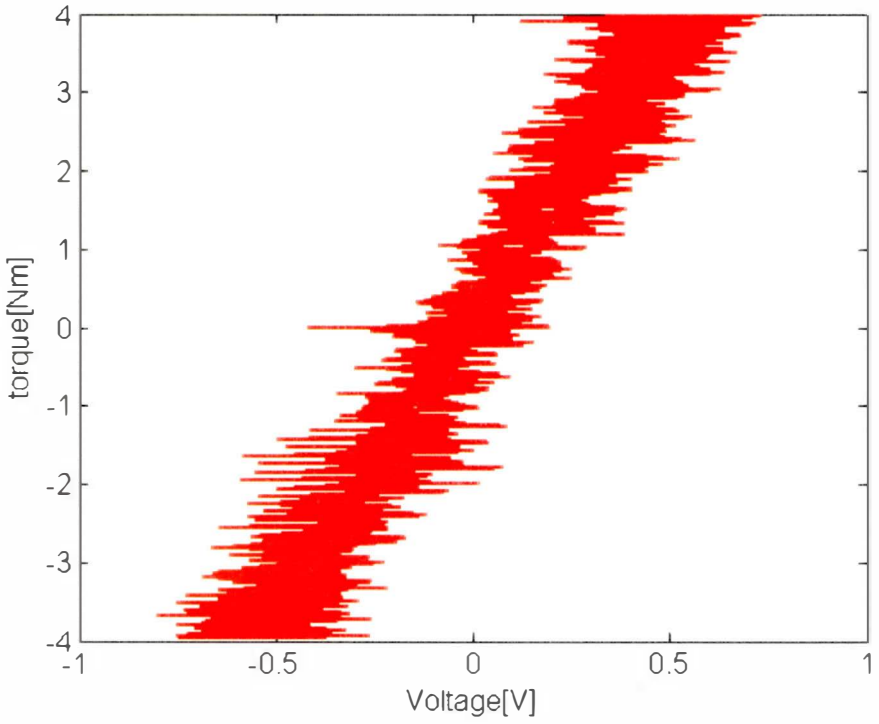

Fig.6.3. 3 Relationship of voltage and torque in clockwise rotation

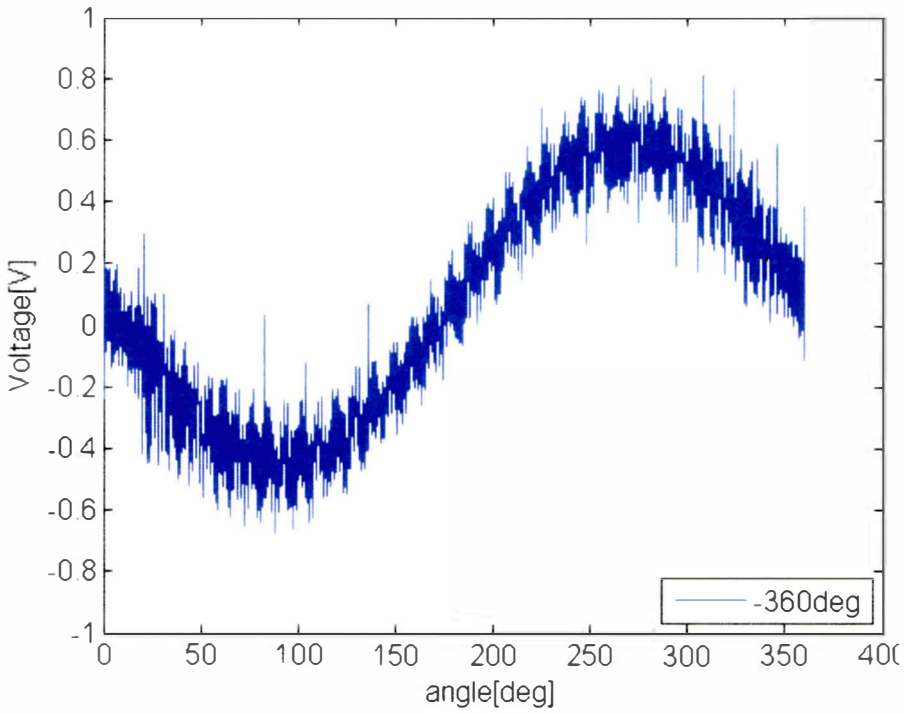

Fig.6.3. 4 Output of torque sensor in anticlockwise rotation

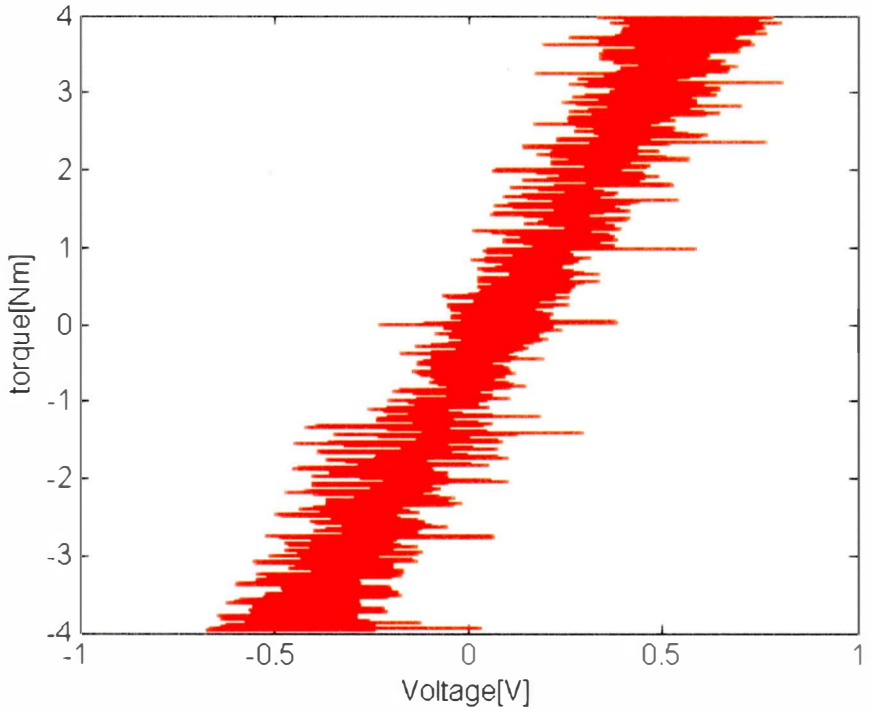

Fig.6.3. 5 Relationship of voltage and torque in anticlockwise rotation

6.4 Cancellation of gravity term

For correct measurement of mutual joint torque between human and suit, it is necessary to cancel joint torque caused by the suit's dynamics, i.e. the gravity term, the inertial moment, the Centrifugal force and the Coriolis force.

We think that it is the gravity term, which largely affects the joint torque even when external force is zero. We deal with the parameters related to gravity term using identification experiment. The simplified two-dimensional model of one side of the robotic suit is shown in Fig.6.4.1.

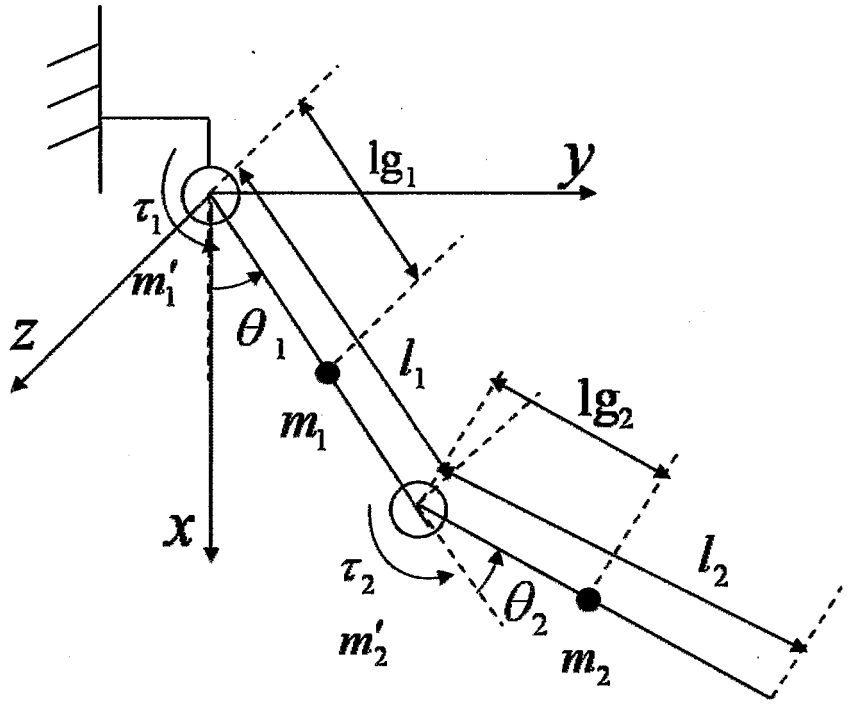

Fig.6.4. 1 Simplified model of one leg of the robotic suit

The dynamic equation of the robotic suit is written in equation (6.3).

$$\boldsymbol{\tau} = \mathbf{g}(\boldsymbol{\theta}) \qquad (6.3)$$

Where, $\boldsymbol{\tau}$ is the joint torque due to gravity term and is detected by torque sensor, $\mathbf{g}(\boldsymbol{\theta})$ is the gravity term written by the Lagrange method [6], as following,

$$g_1 = (m_1 g l_{g1} + m_2' g l_1 + m_2 g l_1)\sin(\theta_1) + m_2 g l_{g2} \sin(\theta_1 + \theta_2) \qquad (6.4)$$

$$g_2 = m_2 g l_{g2} \sin(\theta_1 + \theta_2) \qquad (6.5)$$

Where, g is the gravitational acceleration, m_j is the mass of link j, m'_j is the mass of motor j, lg_j is the position of the mass center of link j, l_j is the length of link j.

We conduct the identification experiment. The joint angle and the joint torque are measured under a static condition so that the effects of velocity and acceleration on the joint torque are ignored. The desired angle of the joint is assigned to be 30, 45, 60, and 90 degrees, and we then use PID control to determine the joint angle θ. τ is measured by the built-in torque sensor of the motor. We can measure the mass of the link and thus use four combinations of θ and τ to calculate the average value of the mass center lg_j. The values of parameters computed with Eq. (6.4) are listed in Table 6.4.1. The calibration results of the left-right legs are shown in Fig. 6.4.2 and Fig. 6.4.3.

Table6.4. 1 Leg parameters

	Left leg	Right leg
m_1(kg)	0.31	0.35
m_2(kg)	0.17	0.17
m'_2 (kg)	1.20	1.20
l_1(m)	0.35	0.35
l_2(m)	0.30	0.30
lg_1(m)	0.01	0.01
lg_2(m)	0.15	0.15

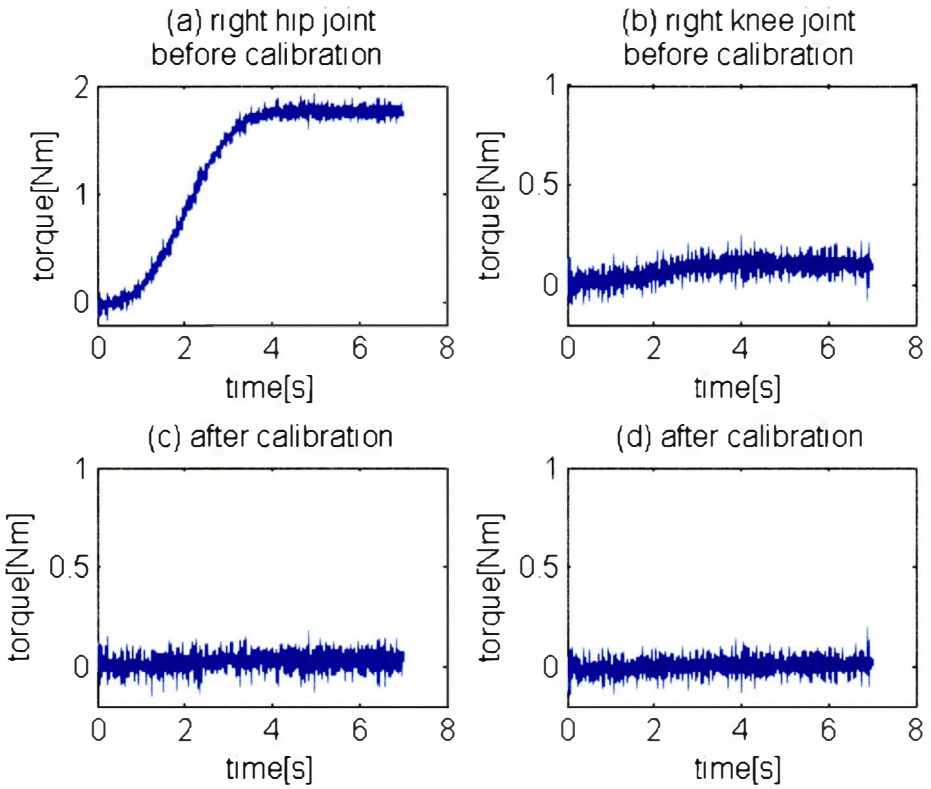

Fig.6.4. 2 Calibration results of the right leg

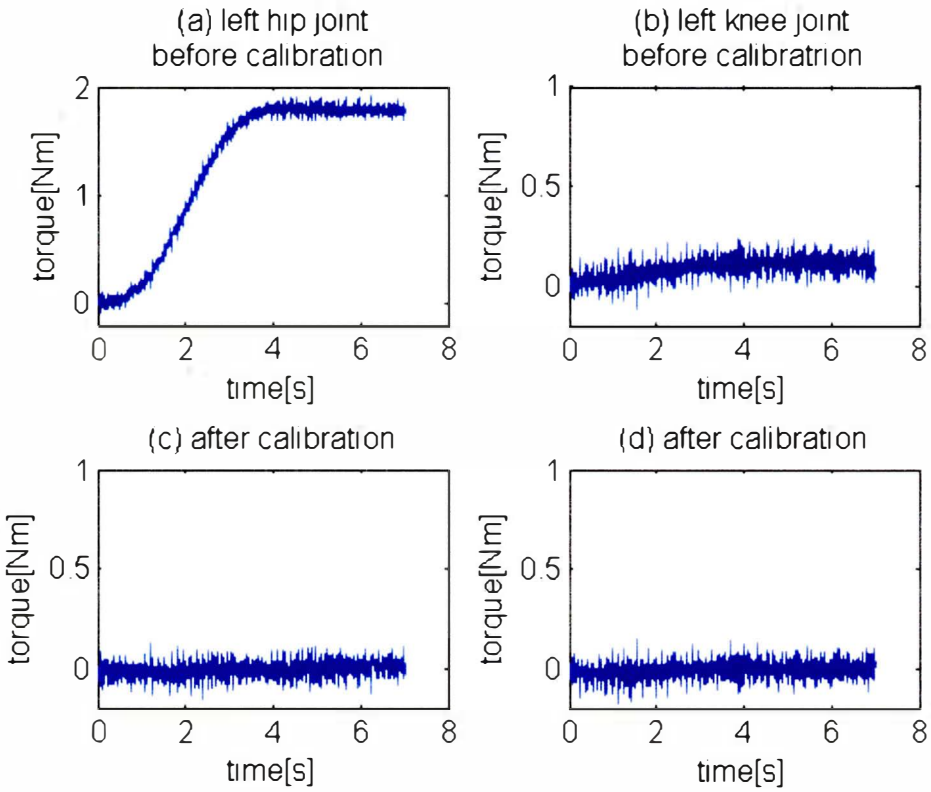

Fig.6.4. 3 Calibration results of the left leg

6.5 Affects of the inertial moment and the interaction torques

Besides the mutual joint torque generated by human-robot interaction, the dynamic equations of the robotic suit shown in Fig. 6.4.1 are actually characterized by an inertia, gravity torques, and interaction torques by the accelerations of the other joints and the existence of centrifugal and Coriolis effect [7][8]. In order to investigate the affects of the moment of inertia and interaction torques of the robotic suit on the mutual joint torque generated from human-robot interaction, we need to calculate the interaction torques and inertial moment of the robotic suit in normal walking, and compare those to the mutual joint torque.

Referring to Fig.6.4.1, the dynamic equations of one side of the robotics suit are written in equation (6.6) and (6.7).

$$\tau_1 = NET_1 + INT_1 + G_1 + \tau_{mutual1} \tag{6.6}$$

$$\tau_2 = NET_2 + INT_2 + G_2 + \tau_{mutual2} \tag{6.7}$$

$$NET_1 = M_{11}\ddot{\theta}_1 \tag{6.8}$$

$$INT_1 = M_{12}\ddot{\theta}_2 + h_{122}\dot{\theta}_2^{\,2} + 2h_{112}\dot{\theta}_1\dot{\theta}_2 \tag{6.9}$$

$$G_1 = (m_1 g l_{g1} + m_2' g l_1 + m_2 g l_1)\sin(\theta_1) + m_2 g l_{g2}\sin(\theta_1 + \theta_2) \tag{6.10}$$

$$NET_2 = M_{22}\ddot{\theta}_2 \tag{6.11}$$

$$INT_2 = M_{21}\ddot{\theta}_1 + h_{211}\dot{\theta}_1^{\,2} \tag{6.12}$$

$$G_2 = m_2 g l_{g2}\sin(\theta_1 + \theta_2) \tag{6.13}$$

$$M_{11} = \tilde{I}_1' + \tilde{I}_1 + \tilde{I}_2' + \tilde{I}_2 + m_1 l_{g1}^{\,2} + m_2' l_1^{\,2} + m_2 l_1^{\,2} + m_2 l_{g2}^{\,2} + 2m_2 l_1 l_{g2}\cos(\theta_2) \tag{6.14}$$

$$M_{12} = M_{21} = m_2 l_{g2}^{\,2} + m_2 l_1 l_{g2}\cos(\theta_2) + \tilde{I}_2 \tag{6.15}$$

$$M_{22} = m_2 l_{g2}^{\,2} + \tilde{I}_2 \tag{6.16}$$

$$h_{112} = h_{122} = -h_{211} = -m_2 l_1 l_{g2}\sin(\theta_2) \tag{6.17}$$

$$\tilde{I}_1' = \frac{2}{5} m_1'(0.03)^2 \tag{6.18}$$

$$\tilde{I}_1 = \frac{1}{12} m_1 l_1^{\,2} \tag{6.19}$$

$$\tilde{I}_2' = \frac{2}{5} m_2'(0.03)^2 \tag{6.20}$$

$$\tilde{I}_2 = \frac{1}{12} m_2 l_2^{\,2} \tag{6.21}$$

Where, τ_1 , τ_2 is the joint torque of the hip joint and the knee joint due to the mutual joint torque, the inertia, the interaction torques and the gravity torques, and is detected by the built-in torque sensor. NET_1 , NET_2 represent the moment of inertia with respect to the hip joint and

the knee joint respectively when the other joint is immobilized. INT_1, INT_2 represent the reaction torque induced by the other link act upon the current link. G_1 , G_2 is the gravity term act upon the hip joint and the knee joint. $\tau_{mutual1}$, $\tau_{mutual2}$ are mutual joint torque of the hip joint and the knee joint calculated by taking away the gravity term from the measured joint torque. The gravity torque is calculated using Eq. (6.10) and Eq. (6.13).

$\widetilde{I}_j$ is the inertial moment term of link j, $\widetilde{I}'_j$ is the inertial moment term of motor j, g is the gravitational acceleration, m_j is the mass of link j, m'_j is the mass of motor j, lg_j is the position of the mass center of link j, l_j is the length of link j. The value of each parameter is shown in Table 6.4.1, and $m'_1 = 1.2kg$.

We asked a participant to wear the four-DOF robotic suit and walk normally, and the robotic suit was not under control. The joint torque was measured by the built-in torque sensor, and the mutual joint torque between the robotic suit and its user was calibrated by taking away the gravity term from the measured joint torque. The angle of the hip joints and knee joints were encoded by the encoders, and the joint angles were used to calculate the angular velocity and acceleration. Using the joint angle, angular velocity and acceleration, we calculated the gravity torques, the inertial moment, and the interaction torques between multi-joints.

The joint angles of the hip and knee joint of the left leg is shown in Fig. 6.5.1

The mutual joint torque, the inertia, the interaction torques, and the gravity torques of the hip joint are shown in Fig. 6.5.2, and their Fast Fourier Transform (FFT) results are shown in Fig. 6.5.3. The mutual joint torque, the inertia, the interaction torques, and the gravity torques of the knee joint are shown in Fig. 6.5.4, and their FFT results are shown in Fig. 6.5.5. We calculated the ratio of each term to the total torque, and shown the results in Table 6.5.1. From Table 6.5.1, it can be found that the moment of inertia and the interaction torques are small and could be negligible comparing to the mutual joint torque. In the hip joint, it is necessary to cancel the gravity term which largely affects the mutual joint torque. This result verified the relevancy of our methodology of gravity cancellation specified in section 6.4.

Table6.5. 1 Ratio of each term to the total torque

Ratio (%)	Hip joint	Knee joint
Mutual joint torques	0.0613*100/0.2592=23.6	0.0479*100/0.0493=97.1
Inertia	0.0122*100/0.2592=4.7	0.0000*100/0.0493=0.0
Interaction torques	0.0000*100/0.2592=0.0	0.0000*100/0.0493=0.0
Gravity	0.1917*100/0.2592=73.9	0.0007*100/0.0493=1.4

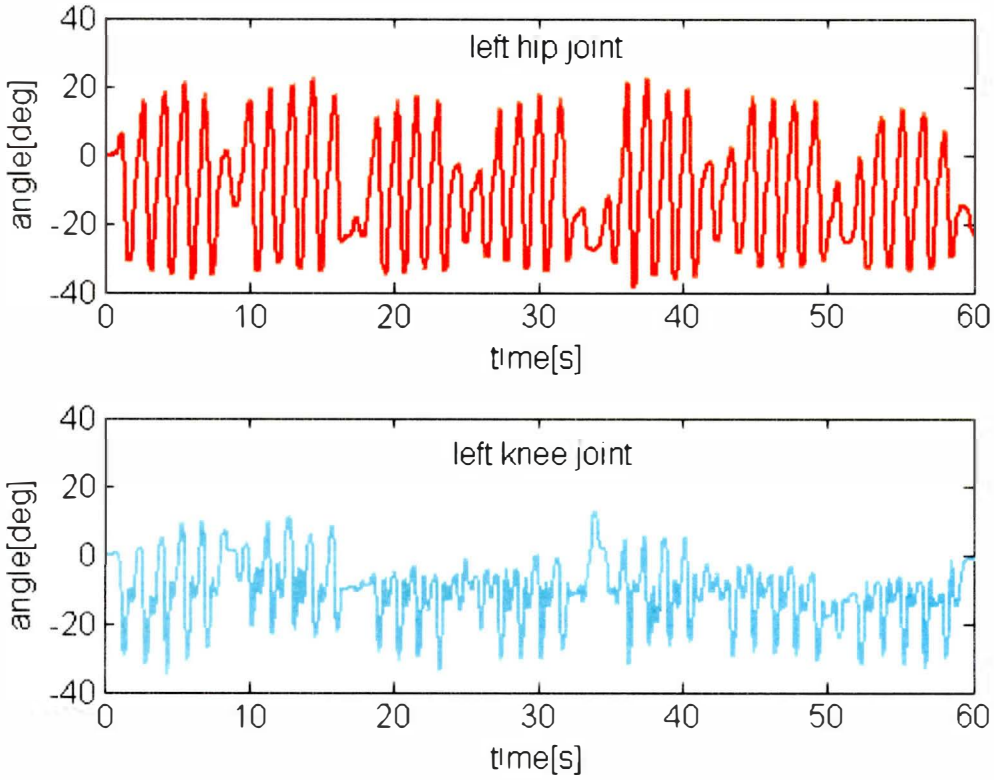

Fig.6.5. 1 Joint angles of the left leg in normal walk

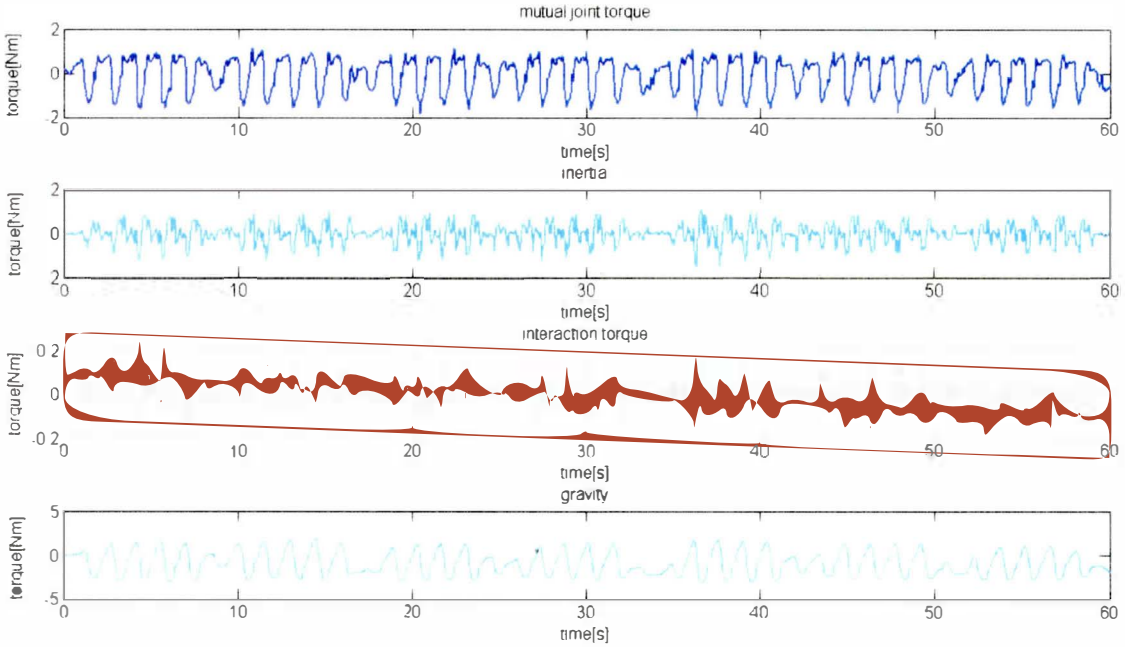

Fig.6.5. 2 Each term of joint torque of the hip joint in normal walk

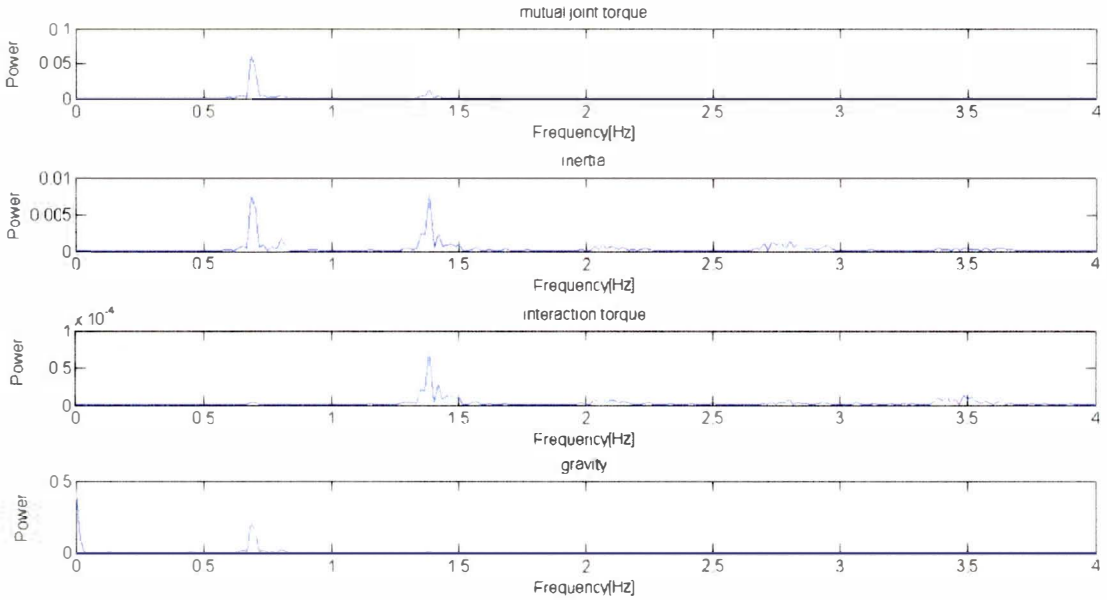

Fig.6.5. 3 Result of FFT for the hip joint

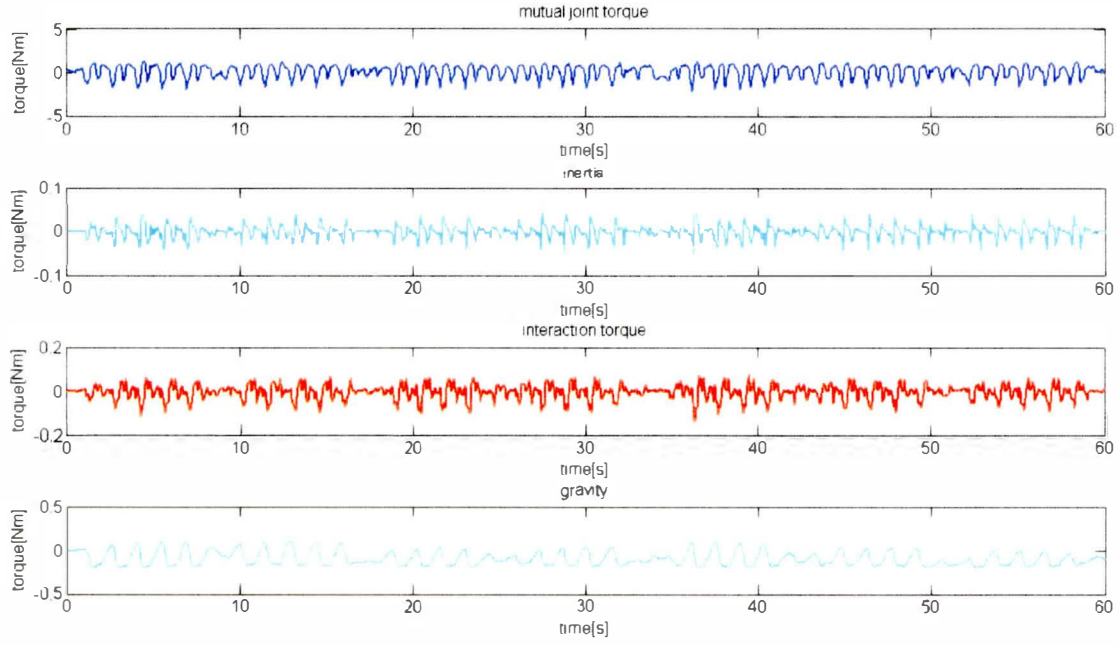

Fig.6.5. 4 Each term of joint torque of the knee joint in normal walk

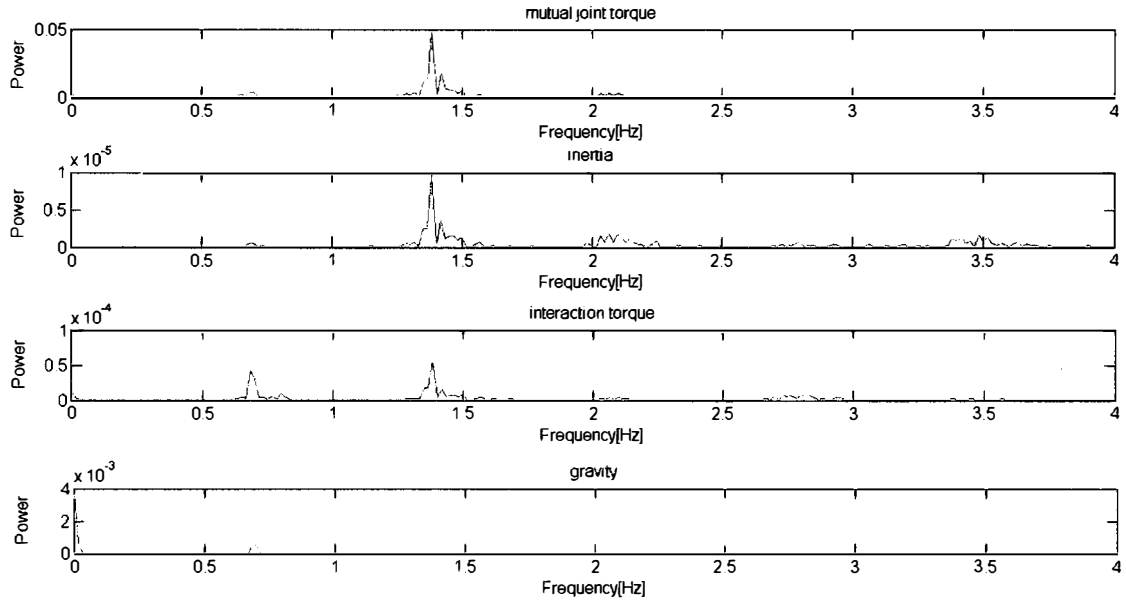

Fig.6.5. 5 Result of FFT for the knee joint

6.6 Safety measures

Safety measures are prepared for preventing any emergency occurring to hurt the user. Limiters of speed and angle are included in the program, and if the speed or angle exceeds the limiter, the program will suspend and give zero control command via DA to the actuator. In addition, an urgency stop switch is connected to the command output of the driver of the actuator, and the switch is set nearby the control computer. If any emergency occurs, the experiment implementer can immediately push the urgency stop switch at hand.

References

[1] Xia Zhang, Minoru Hashimoto, "Evaluation on Interaction Ability of a Walking Robotic Suit with Synchronization Based Control," *IEEE Int. Conf. on Robotics and Biomimetics (IEEE ROBIO2010),* Tianjin, China, pp. 265-270, December, 2010

[2] Iijima Takasi, Anatomy of The Human Body, *CGWORLD*, page 113

[3] http://www.kgef.ac.jp/ksjc/ronbun/031000s.htm (in Japanese)

[4] M.Hashimoto, Y.Kiyosawa, R.P.Paul, "Torque sensing technique for robots with harmonic drives," *IEEE Transaction on Robotics and Automation,* Vol. 9, No.1, pp.108-116, 1993.

[5] I. Godler, M. Horiuchi, M.Hashimoto, T. Ninomiya, "Accuracy Improvement of Built-In Torque Sensing for Harmonic Drives," *IEEE/ASME IEEE/ASME Transactions on Mechatronics*, 5(4), pp. 360-366, 2000.

[6] M.Hashimoto, T.Hattori, M.Horiuchi, T.Kamata: "Development of a Torque Sensing Robot Arm for Interactive Communication", in proc. Of the 11th IEEE International workshop on Robot and Human Interactive Communication, pp344-349, 2002.

[7] Haruhiko Asada, Jean-Jacques E.Slotine, "Robot analysis and control," *A Wiley Interscience publication,* 1985, pp100-103.

[8] Hiroshi Nagasaki, "Movement Coordination and the Interaction Torque in Multijoint Motion," Rigakuryoho Kagaku, Vol.21(1),pp.75-79,2006

Chapter 7

Walking experiments using two-DOF robotic suit

Chapter 7 Walking experiments using two-DOF robotic suit

To verify the validity of our proposal for walking assistance, we first conducted a series of walking experiments with a two-DOF robotic suit that assists by supporting hip joint movement and maintaining an anti-phase relationship in walking [1][2]. The two-DOF robotic suit is part of the four-DOF robotic suit by moving away the knee joint, and it has the same control system with that of the four-DOF robotic suit.

When addressing the problem of walking assistance, an important consideration is how to provide stability assistance. In this Chapter, incorporation of mutual inhibition between neural oscillators is proposed for the walking stability assistance of a robotic suit by maintaining anti-phase movement of the left and right hip joints. One neural oscillator is connected to each joint of the robotic suit to synchronize the suit's movement with the human user's movement. At the same time, mutual inhibition is incorporated between the neural oscillators on the left and right hip joints of the suit to maintain a human-gait-like anti-phase relationship. There may be an intuitive and simple solution to maintaining the anti-phase movement using only one neural oscillator and multiplying its output by –1. However, we cannot adopt this solution because not only do left and right hip joints of the robotic suit need to move in anti-phase but they also need to interact with the left and right hip joints of a user respectively. Otherwise, the user would lose at least one DOF when wearing the robotic suit. To properly assign the mutual inhibition weight between neural oscillators to enable both outer synchronization (synchronization of the suit's movement with the user's movement) and inner synchronization (maintenance of a human-gait-like anti-phase relationship), we conducted extensive simulations.

In section 7.1, the structure of the incorporation of mutual inhibition between neural oscillators for a robotic suit is proposed, and the assignment of an inhibitory weight is discussed. The structure of the robotic suit is introduced in section 7.2. Experiments are conducted in section 7.3. Finally, a conclusion to this chapter and a discussion of future work are given in section 7.4.

7.1 Mutual inhibition between neural oscillators

It is necessary for the robotic suit to confer stability in walking assistance. That is, there should be human-like cooperative motion between each joint of the robotic suit. To achieve this, we propose incorporating mutual inhibition between neural oscillators, which is discussed in detail in this section.

7 .1.1 Mutual inhibition

Mutual inhibition between neurons will activate the two neurons alternately. So far, mutual inhibition between neural oscillators has been applied to control biped robots to help maintain an anti-phase relationship between the robots' left and right legs. In our study, not only the mutual inhibition from the other neural oscillator but also the mutual joint torque from outside the human user is fed back to the current neural oscillator. Figure 7.1.1 shows the mutual-inhibition structure of two neural oscillators. The numbers of neurons are $i, j = 1, \cdots, 4$, and the number of neural oscillators is $k = 1,2$. $a_{12} = a_{34} = 1.2$. The synchronization gain C controls outer synchronization, and the inhibitory weights a_{13} and a_{24} control inner inhibition. Changing the value of the inhibitory weight affects the basic frequency of neural oscillators. We investigated the basic frequency when assigning $a_{13} = a_{24}$ as 0.0, 0.005, 0.015, 0.03, 0.06, 0.12, 0.36, 0.6, and 1.0 in simulations. The results are shown in Fig.7.1.2. When the inhibitory weight exceeds 0.36, the basic frequency decreases from 1.0 Hz.

It is predicted that once the pair of input signals for the left and right neural oscillators do not have the same frequency or are not in anti-phase, the pair of neural oscillators become confused between outer synchronization and inner inhibition, or even worse, their outputs become unstable (this statement will be verified in the next section). Therefore, it is important to determine the inhibitory weight properly.

The inhibitory weight should be properly assigned to meet the requirements that (1) synchronization should not be impeded and be able to be adjusted freely and (2) the basic frequency should not change too greatly. That is, for any mutual joint torque, the neural oscillator properly synchronizes with the input according to C, and the pair of neural oscillators reestablish an anti-phase relationship immediately with mutual inhibition once the mutual joint torque becomes negligible. This outer-synchronization and inner-inhibition mechanism is repeated throughout the assisting process to achieve stabilized assisted movement. The next section discusses how the inhibitory weight is assigned.

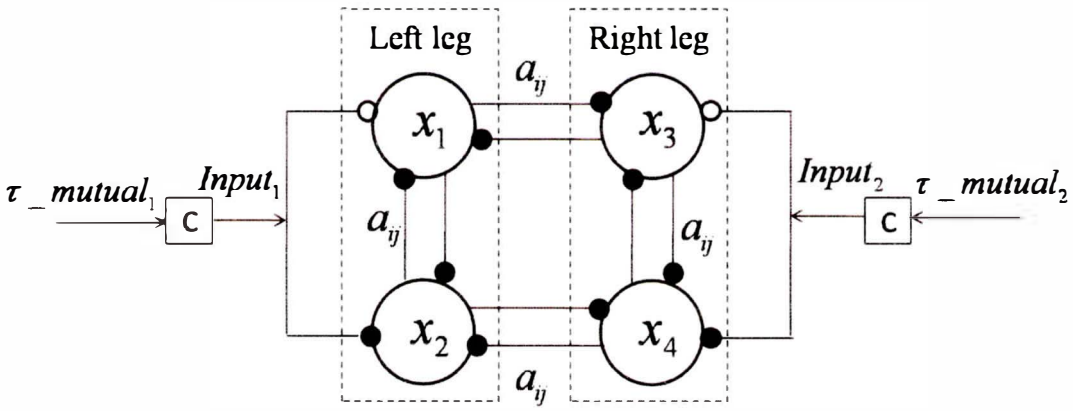

Fig.7.1. 1 Neural oscillators with mutual inhibitory functionality

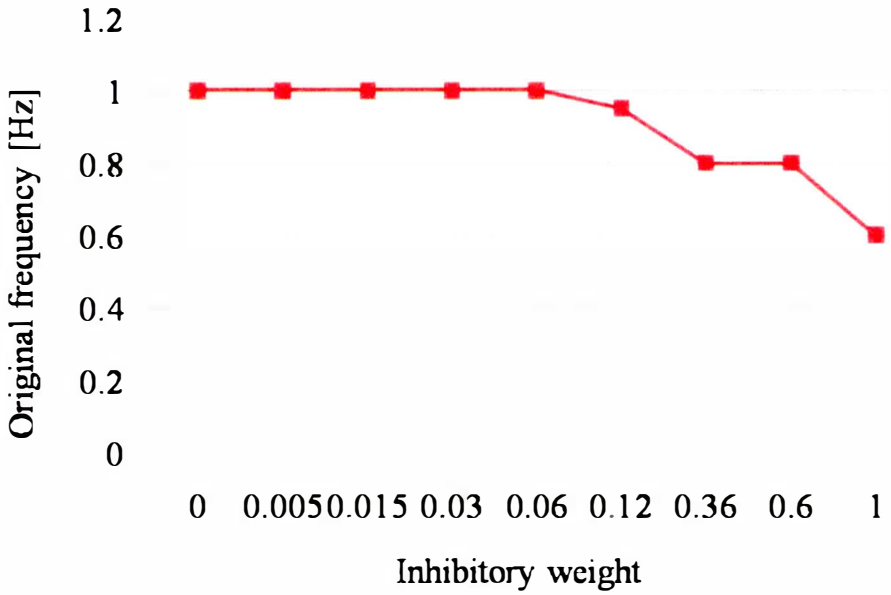

Fig.7.1. 2 Original frequency of the neural oscillator with different inhibitory weights

7.1.2 Assignment of the inhibitory weight $a_{13} = a_{24}$

It is assumed that a different inhibitory weight between neural oscillators will bring about a different outcome. To determine a proper inhibitory weight for our system, we analyzed the behavior of the paired neural oscillators with different inhibitory weights in a series of

simulations.

We used a pair of anti-phase sinusoidal curves (with frequency of 0.7 Hz) as the pair of inputs to the neural oscillators. We then observed the output of the neural oscillators, each time assigning $a_{13}=a_{24}$ as 0.0, 0.005, 0.015, 0.03, 0.06, 0.12, 0.36, and 0.6 with a gradual increase of the synchronization gain from 0 to 1. A valve value of the synchronization gain, found for each inhibitory weight, separates the output of neural oscillators into three groups: one group maintains the original anti-phase movement, a second group is synchronous with the input signals, and the third group implies transient oscillation changing from inner inhibition to outer synchronization (i.e., the frequency changes from the original frequency to that of the input). An example of different behaviors of neural oscillators with different synchronization gains in the case of $a_{13} = a_{24} = 0.12$ is presented in Figs. 7.1.3 and 7.1.4. Figure 7.1.3 shows the output of neural oscillators when the synchronization gain is zero. The dotted lines represent the input signal, and the solid lines represent the output signal. Input 1, defined by $\sin(1.4\pi t)*C$, is the input to the neural oscillator of the left hip joint. Input 2, defined by $\sin(-1.4\pi t)*C$, is the input to the neural oscillator of the right hip joint. In contrast to Fig. 7.1.3, Fig. 7.1.4(a) indicates that $C = 0.01$ leads to inner inhibition; Fig. 7.1.4(b) $C = 0.09$ leads to transient oscillations, where the value 0.3 is the so-called valve synchronization gain for an inhibitory weight of 0.12; and Fig. 7.1.4(c) $C = 0.64$ leads to outer synchronization. The different valve values for different inhibitory weights, found in simulations, are shown in Fig. 7.1.5. The figure shows that different inhibitory weights have different valve synchronization gains, and adjusting the synchronization gain leads to a different outcome: inner inhibition or outer synchronization. Note that the valve synchronization gain does not change until the inhibitory weight exceeds 0.12. By trying another pair of anti-phase sinusoidal curves (with frequency of 0.8 Hz), a series of similar results with smaller valve gains, which are shown in Fig. 7.1.6, were found. From these results, we conclude that the closer the basic frequency of the input signals to that of the neural oscillator, the smaller the valve values of the synchronization gain for each inhibitory weight. Again, the valve synchronization gain does not change until the inhibitory weight exceeds 0.12. Note that the original frequency of the pair of neural oscillators is 0.95 Hz (see Fig. 3). We conclude from Figs. 7.1.5 and 7.1.6 that synchronization takes place more easily when the input is closer in frequency.

With the premise of meeting the aforementioned requirements that (1) the synchronization behavior should not be impeded and be able to be adjusted freely and (2) the basic frequency should not change too greatly, we boldly choose 0.12 (with other small values perhaps satisfying the requirement) for the inhibitory weight $a_{13} = a_{24}$ and investigate whether this weight is

suitable for stability assistance.

The weight of mutual inhibition is assigned with symmetric values $a_{13} = a_{24} = 0.12$. If there is no input fed back, the behavior (output signal) of neural oscillators, computed as $\max(0, x_i) - \max(0, x_{i+1})$ $(i = 1,3)$, is anti-phase as well, which is shown by the blue dotted line in Fig. 7.1.7 (a). Compared with the output signals for no mutual inhibition, the output signals for mutual inhibition are a little slower. The output signals are used to calculate the desired joint-angle trajectories of the robotic suit.

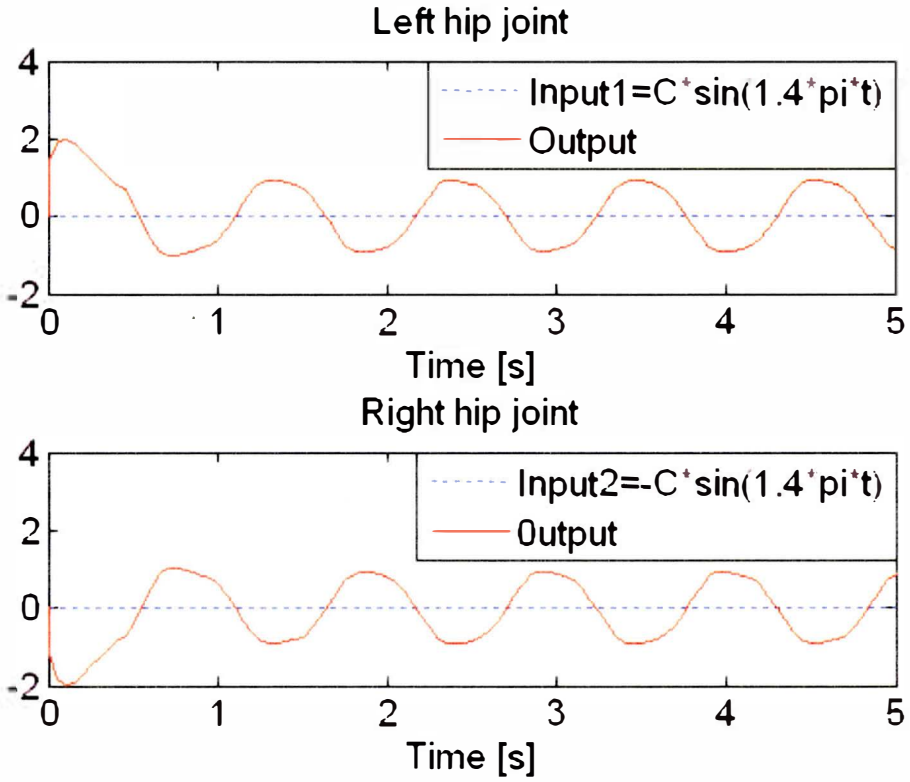

Fig.7.1. 3 Outputs of neural oscillators when the synchronization gain C = 0. The dotted lines represent the input signal, and the solid lines represent the output signal. Input 1 is the input to the neural oscillator of the left hip joint, and input 2 is the input to the neural oscillator of the right hip joint.

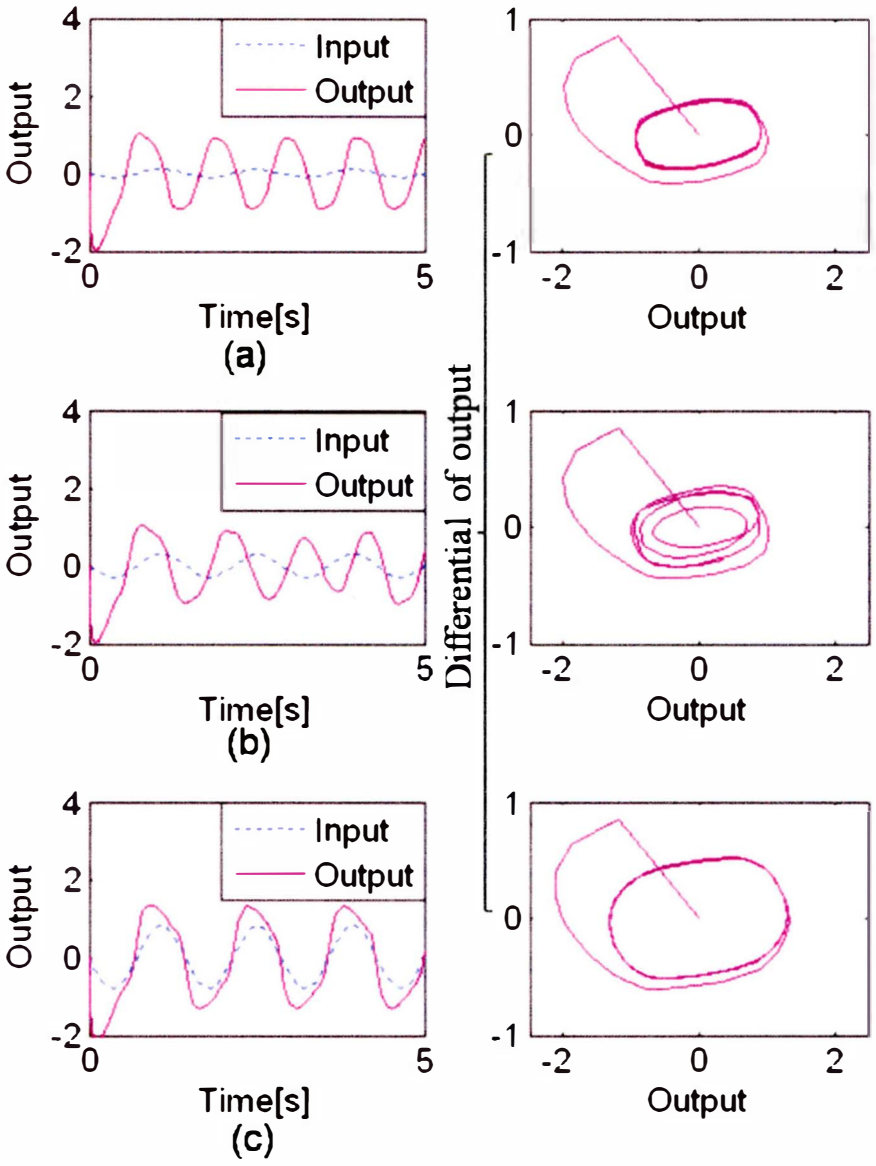

Fig.7.1. 4 Example of one neural oscillator (right hip joint) with different synchronization gains and with an inhibitory weight of 0.12: (a) C = 0.01 leads to inner mutual inhibition; (b) C = 0.09 leads to transient oscillations; (c) C = 0.64 leads to outer synchronization

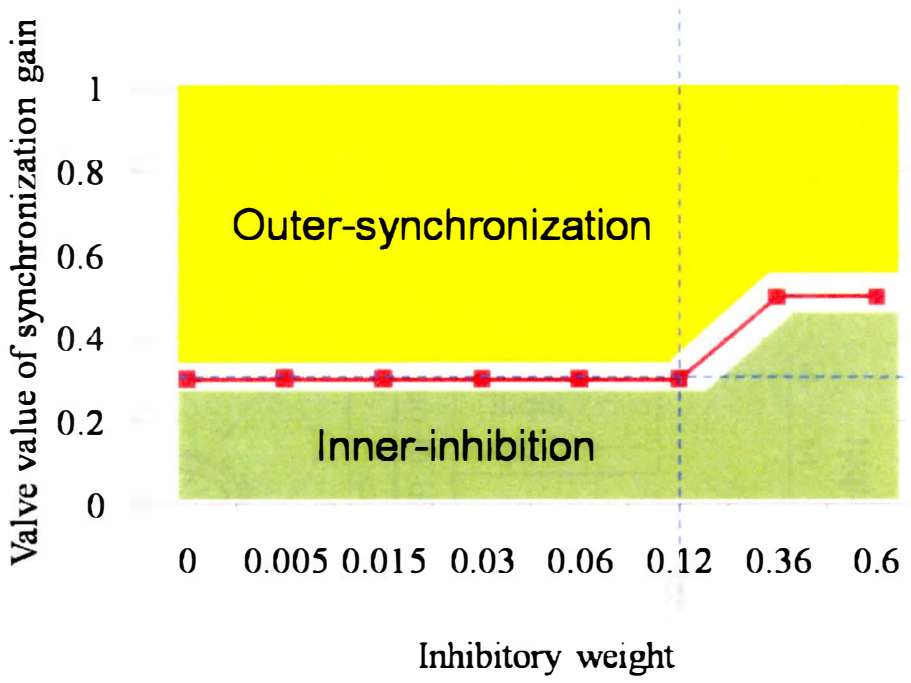

Fig.7.1. 5 Valve value of the synchronization gain for each inhibitory weight (based on the input signals with a frequency difference of 0.25 Hz relative to the original signal of the neural oscillator), separating the output of neural oscillators into three groups: one group maintains the original anti-phase movement, the second group is synchronous with input signals, and the third group is unstable oscillations that provide neither inner inhibition nor outer synchronization. If the synchronization gain is greater than the valve value for the current inhibitory weight then the trend is for outer synchronization; otherwise, the trend is for inner inhibition. The dotted lines illustrate the valve value for an inhibitory weight of 0.12.

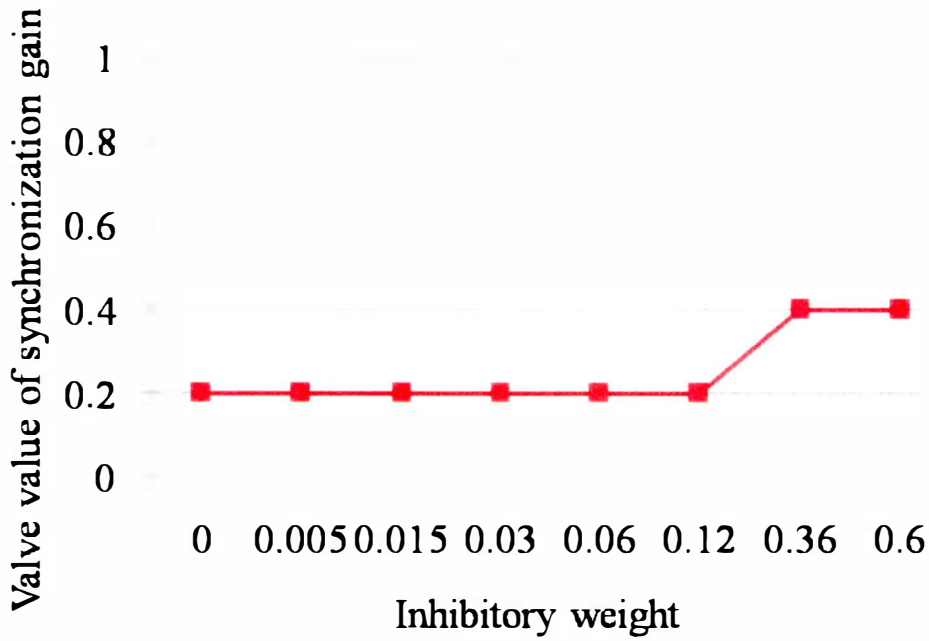

Fig.7.1. 6 The valve value of the synchronization gain for each inhibitory weight: based on the input signals with a frequency difference of 0.15 Hz relative to the original signal of the neural oscillator.

7.1.3 Maintaining anti-phase movement

We looked at the outputs of the pair of neural oscillators, with and without mutual inhibition, by giving a pair of different input signals (Input 1 represented by the red solid line in Fig. 7.1.7(b) is a normal sinusoidal curve and Input 2 represented by the dotted blue line is partly a sinusoidal curve and partly a constant of zero) and then letting them go to zero from 5 s. The light regions in Fig. 7.1.7(a) and Fig. 7.1.7(b) indicates C = 0 and the dark region in Fig. 7.1.7(b) indicates C = 1.

・Case without mutual inhibition

In the case without mutual inhibition, neural oscillators synchronize with different input signals respectively (outputs shown by the pink solid line in Fig. 7.1.7(b)), but after the different input signals become zero at 5 s, the original anti-phase relationships (outputs shown by the pink solid line in Fig. 7.1.7 (b)) become disordered and are not able to return to the original anti-phase relationship.

・Case with mutual inhibition

In the case with mutual inhibition, we found that the neural oscillators synchronize with input signals as well. What is important is that the behavior of neural oscillators, shown by the blue

dotted line in Fig. 7.1.7(b), returns to the original anti-phase relationship immediately once the input signals disappear. The autonomous anti-phase behavior of the robotic suit helps the user preside over the walking stability.

Figure 7.1.8 shows the assumed relationship of walking stability and the suit's synchronization gain under situations with and without inhibition. "Normal level of walk stability" in Fig. 7.1.8 means the usual walk stability of a user while maintaining anti-phase movement when not wearing the robotic suit. The normal level of walk stability can be low, moderate or high according to the physical condition of the user. The dotted line illustrates that the walking immediately becomes unstable without inhibition (because the anti-phase relationship becomes disordered after the pair of neural oscillators synchronizes with different input signals) but approaches the normal level of the user gradually with an increase in the synchronization gain. The solid line illustrates that stability is well maintained with inhibition (because the anti-phase movement is maintained well by the mutual inhibition even though the pair of neural oscillators synchronize with different input signals) but approaches the normal level of the user gradually with an increase in synchronization gain.

One important clarification is that, since the inhibitory weight assigned is small, it is not high enough to maintain the anti-phase relationship if outer synchronization takes place, but if the outer synchronization becomes negligible, the mutual inhibition helps the robotic suit maintain the anti-phase relationship.

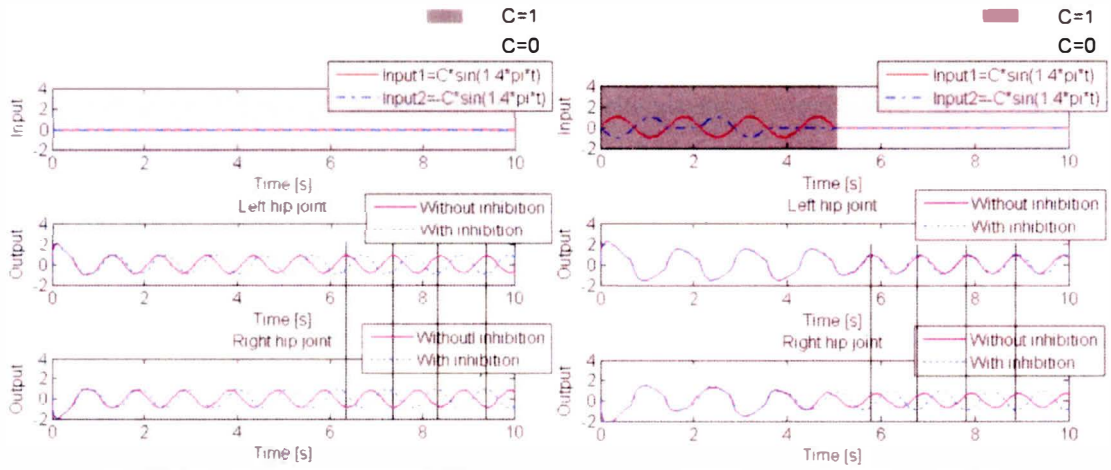

(a) Anti-phase outputs of neural oscillators when C=0 with and without mutual inhibition

(b) Outputs of neural oscillators when different inputs fed back with and without mutual inhibition

Fig.7.1. 7 Anti-phase behavior of neural oscillators with mutual inhibition. Input1 is the input to the neural oscillator of the left hip joint, and input2 is the input to the neural oscillator of the right hip joint. The light region indicates C = 0 and the dark region C= 1. Pink solid lines represent outputs of neural oscillators without mutual inhibition, and blue dotted lines represent those with mutual inhibition.

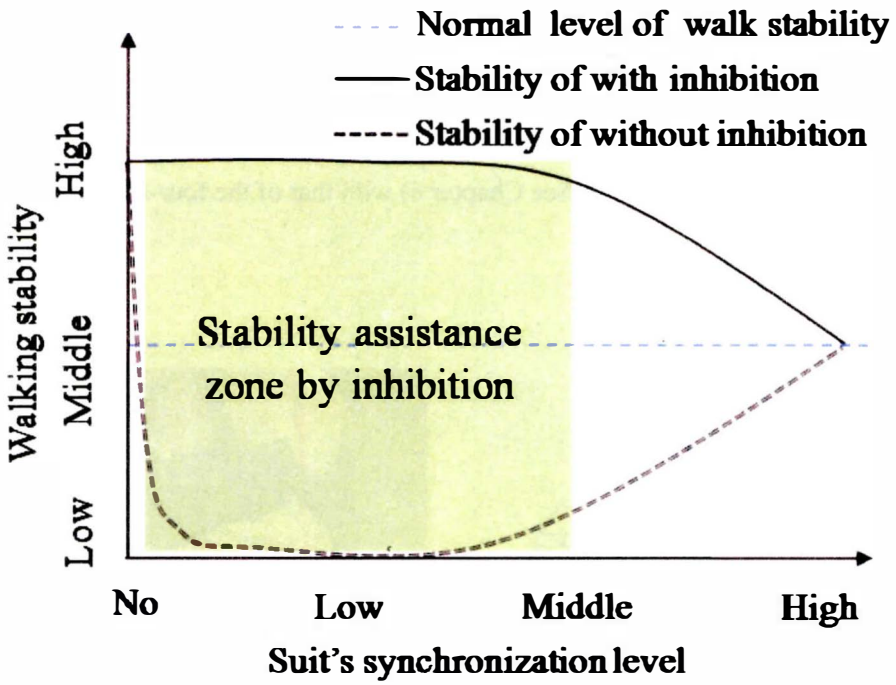

Fig.7.1.8 Stability assistance zone and the different stabilities for the cases with and without inhibition, "Normal level of walk stability" means the normal walk stability of the user when maintaining anti-phase movement while not wearing the robotic suit.

7.2 Robotic suit

Figure 7.2.1 shows the general design of the robotic suit for walking assist by supporting the hip joints movement in walk, which consists of two links and two actuators. The two-DOF robotic suit is part of the four-DOF robotic suit (See Chapter 6) by moving away the knee joint, and it has the same control system (See Chapter 6) with that of the four-DOF robotic suit.

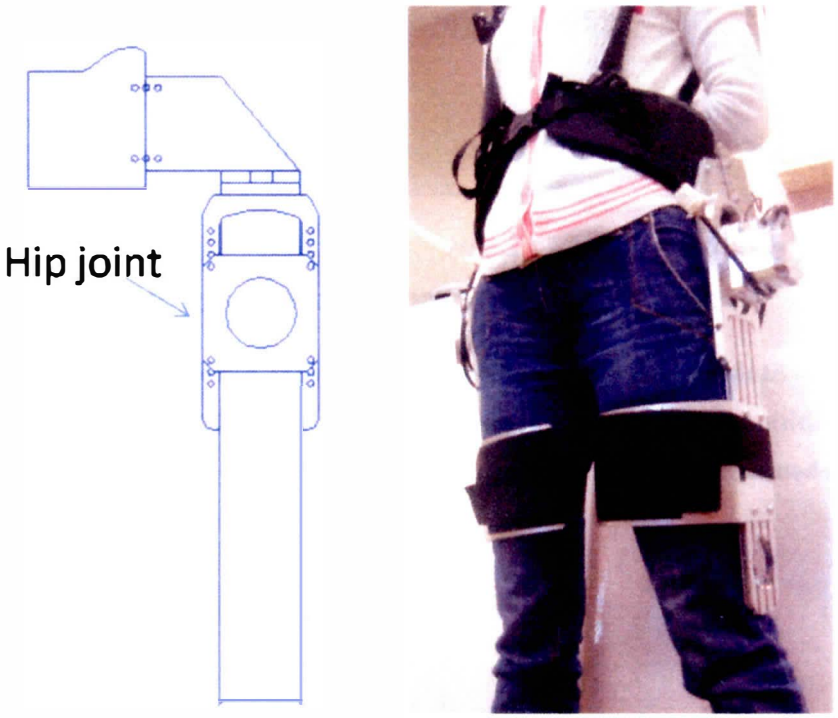

Fig.7.2. 1 Two-DOF robotic suit

7.3 Experiment

7.3.1 Cancellation of the gravity term

For correct measurement of the mutual joint torque between the human and suit, the joint torque due to the gravitational force has been cancelled using the method depicted in section 6.4.

7.3.2 Task and subjects

To demonstrate the ability of the robotic suit to provide synchronous and stable assistance with mutual inhibition between neural oscillators on the left and right hip joints, we conducted pairs of walking comparison experiments for three scenarios, one of which was normal walking without wearing the robotic suit, and the other two were cooperative walking (wearing the robotic suit) with and without mutual inhibition between left and right neural oscillators. Throughout all the experiments, a pseudo-gait disturbance was applied to subjects by attaching a load (2.0 kg) to the right ankle. The subjects were 10 fully able university students who were instructed to walk continuously in walking tests at their usual self-determined rate. They walked back and forth in a room for 1 min along a route with length of 5 m, and the steps and time when walking in a straight line were recorded to calculate the step length and speed. The floor was flat. Figure 7.3.1 illustrates the procedures of experiments.

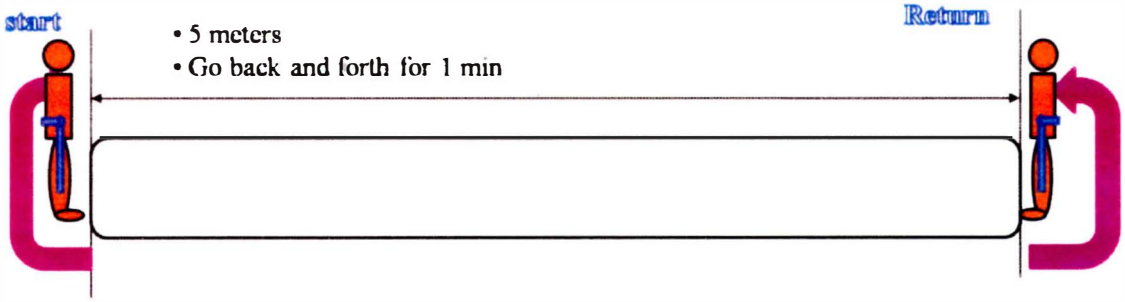

Fig.7.3. 1 Procedures of walk experiments

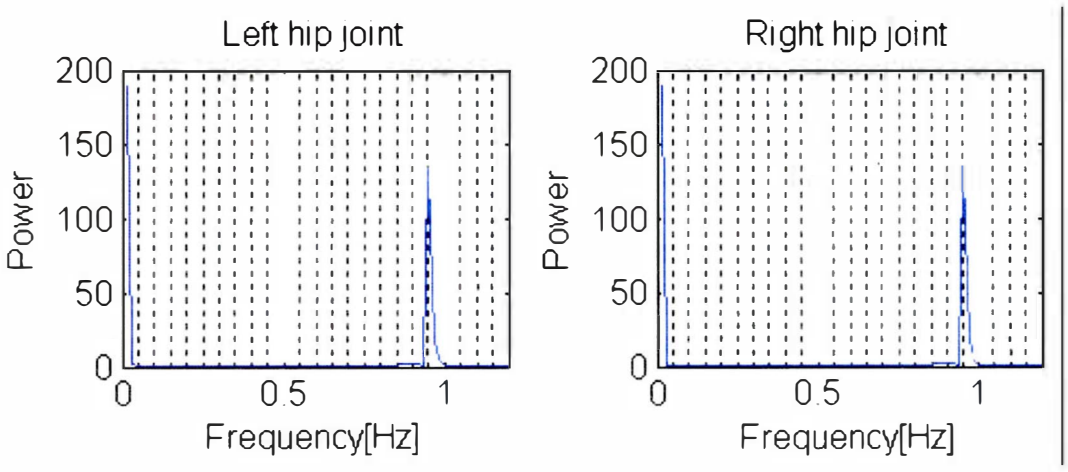

Fig.7.3. 2 Basic frequency of the robotic suit

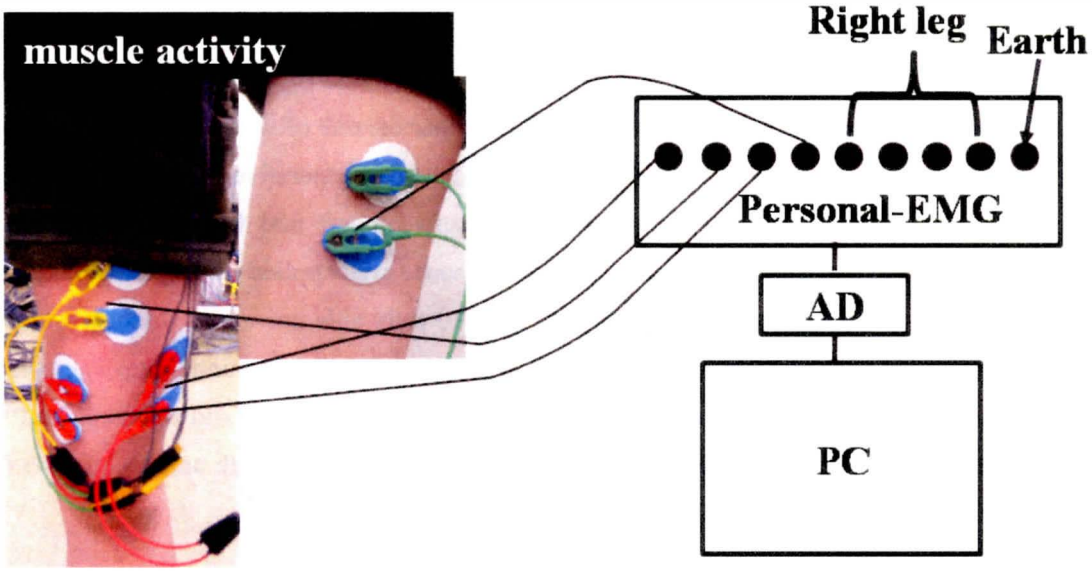

Fig.7.3. 3 Scene for the muscle activity measurement

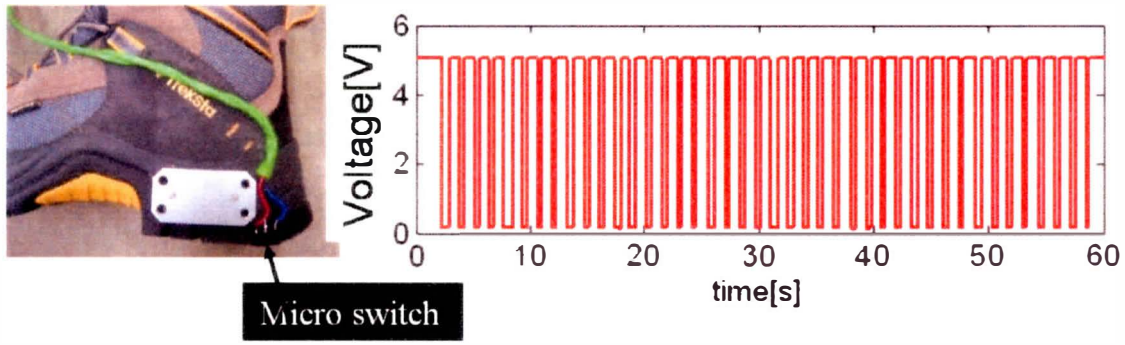

Fig.7.3. 4 Measurements of stride periods

Each subject wore the robotic suit and was asked to walk synchronously with the robotic suit along the same route that they had walked independently. The robotic suit moved at a frequency of 0.95 Hz, as shown in Fig. 7.3.2., and with amplitude of 15 ± 26.0 degrees. The desired angles of the hip joints, θ_d, were calculated with equation (7.1) using the outputs of neural oscillators.

$$\theta_d = \theta_p + K_a \mathbf{Output} \quad (7.1)$$

where $\theta_p = 15$ degrees is an offset for emulating the natural motion of the hip joint, **Output** [Nm] is the output from the neural oscillators , and $K_a = 28 \deg/Nm$ is a constant to convert the physical unit from torque to angle and to tune the amplitude.

There were a total of four patterns of cooperative walking divided into two groups: cooperative walking with and without mutual inhibition between left and right neural oscillators. The synchronization gain was increased to 0.3 and 0.5 for each group. The values of 0.3 and 0.5 meant lower and higher synchronization respectively. Each walking experiment was implemented for 1 min, where the oscillating amplitude gradually increased for the first 5 s as the subject began to walk and gradually decreased in the last 5 s as the subject came to a stop; the middle 50 s were taken for cooperative walking. The steps and time when walking in a straight line were recorded to calculate the speed.

Muscle activity and mutual joint torque between the suit and human were measured for each walking pattern. Note that the mutual torque and muscle activity should become smaller if the robotic suit synchronizes with the human user's movement. The phase difference between the left and right hip joints and fluctuations of the stride interval were calculated for each walk pattern. Mutual joint torque was used as an evaluating indicator for synchronization behavior analysis; muscle activity, step length and speed for assist effect analysis; and phase difference and fluctuations of the stride interval for walk stability analysis. The muscle activity, return map and fluctuations of stride interval were calculated as follows.

We employed electromyography to measure muscle activity (the root-mean-square signal) at four sites on the leg when the user moved independently and together with the robotic suit. The experimental scene is shown in Fig. 7.3.3. We used 100% maximal voluntary contraction to show physical strength. Maximum muscle activity for four muscles was measured beforehand by asking the subject to exert maximum force. The higher the muscle activity ratio, the greater the physical power consumed. To measure the stride interval, a micro force-sensitive switch was taped to the lateral-side back part of the right shoe. When the heel struck the ground, the DC voltage (5 V) became zero. Voltage data were recorded by a computer via an analog-to-digital transformer to compute the stride interval. One example of the stride periods measurements is shown in Fig 7.3.4. The phase differences between the left and right hip joints were analyzed using a return map. A two-dimensional return map was obtained by plotting the phase differences in a space where the x-axis is $\Delta x(n)$ and the y-axis is $\Delta x(n+1), n = 1,2,\cdots,N$. Here,

$$\Delta x(n) = \theta_{right\_post.}(n) - (-\theta_{left\_ant}(n)) + 180 - 2\theta_p \quad , (7.2)$$

N is the observation time, $\theta_{right\_post}(n)$ is the maximum angle of the right hip joint in the posterior direction at the nth observation, and $\theta_{left\_ant}(n)$ is the maximum angle of the left hip joint in the anterior direction at the nth observation. θ_p is the offset for emulating the natural motion of the hip joint.

7.3.3 Synchronous and stable assistance

Figure 7.3.5 shows the changes in mutual joint torque (of the right hip joint) with (Fig. 7.3.5(a)) and without (Fig. 7.3.5(b)) mutual inhibition for the 10 subjects. Figure 7.3.5 shows the average of the absolute value of the mutual joint torque. In both situations, mutual joint torque decreased as the synchronization gain increased. Note that the mutual joint torque decreased as the suit's synchronization gain increased because of the mutually synchronous actions. Therefore, we conclude that the robotic suit is capable of outer synchronization. What is more important is that even with mutual inhibition, the neural oscillators achieve outer synchronization freely. This result verifies our design of the inhibitory weight. This was discussed in more detail in section 7.1.

We compared the user's normal hip joint trajectory (shown in Fig. 7.3.6) with that of a cooperative walk while wearing the robotic suit (shown in Fig. 7.3.7). The normal trajectories of the subject were measured approximately by asking the subject to walk normally wearing the suit, which was very compliant, and the maximum resistance torque measured by the torque sensors was about 1.0 Nm. Figure 7.3.6 shows the normal trajectories of a user approximately measured via built-in encoders of the robotic suit. Figure 7.3.7 shows the desired and actual trajectories of the robotic suit in a cooperative walk with higher synchronization level (C = 0.5) and with mutual inhibition. The frequency of trajectories in Fig. 7.3.7 coincides with that in Fig. 7.3.6. There is reverse direction existing in-between the mutual joint torque and desired angle, shown in gray region, and the reverse direction of the input-output of neural oscillator results in the attenuation of its oscillation, thus the shape of output-desired angle of the suit becomes more compliant and more reasonable for walk assist. Figure 7.3.8 and Fig. 7.3.9 shows an example of compliant desired trajectory, where, C=0.5. The gray region represents where the reverse direction exists, and the "attenuation" mode occurred to enable the robotic suit to provide friendlier assist.

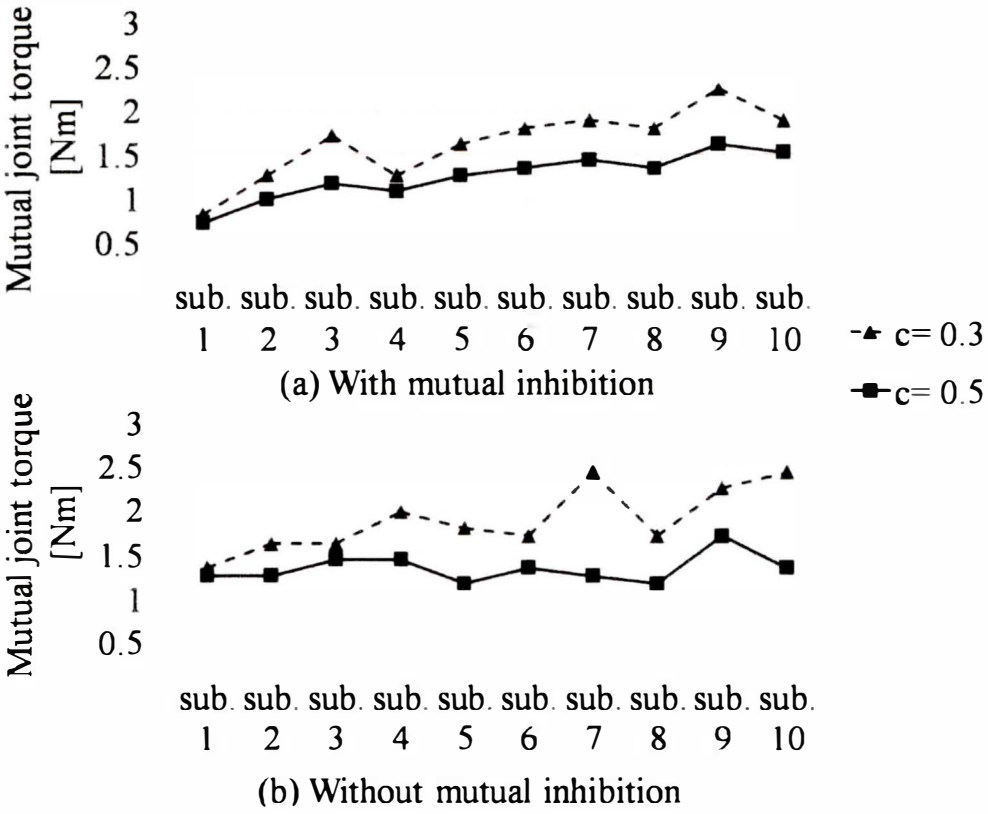

Fig.7.3. 5 Relationship between synchronization gain and mutual torque for each subject

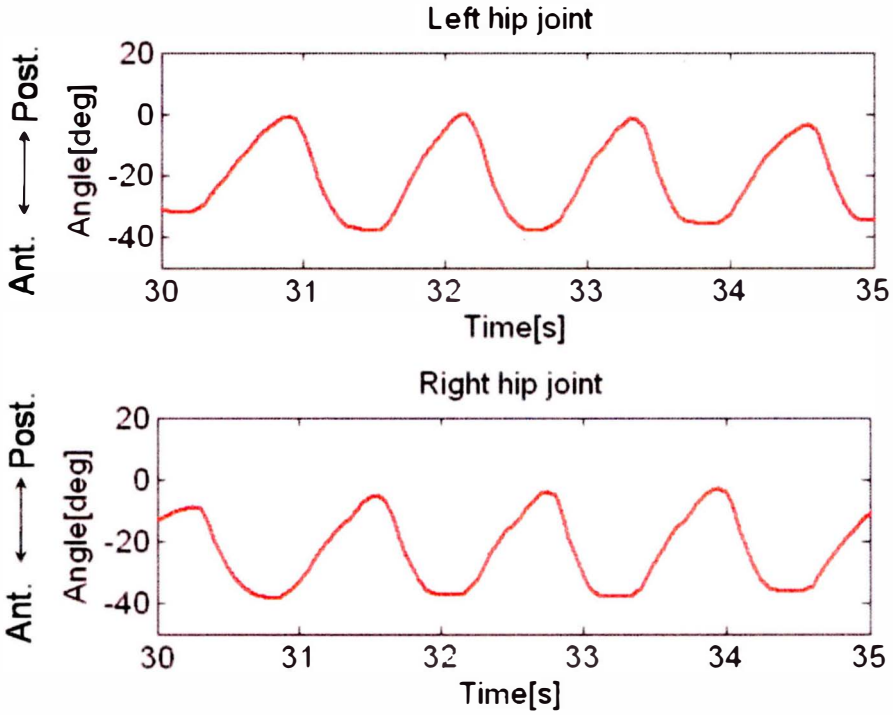

Fig.7.3. 6 Normal trajectories of a subject' left and right hip joints. Ant. means anterior direction, and Post. means posterior direction.

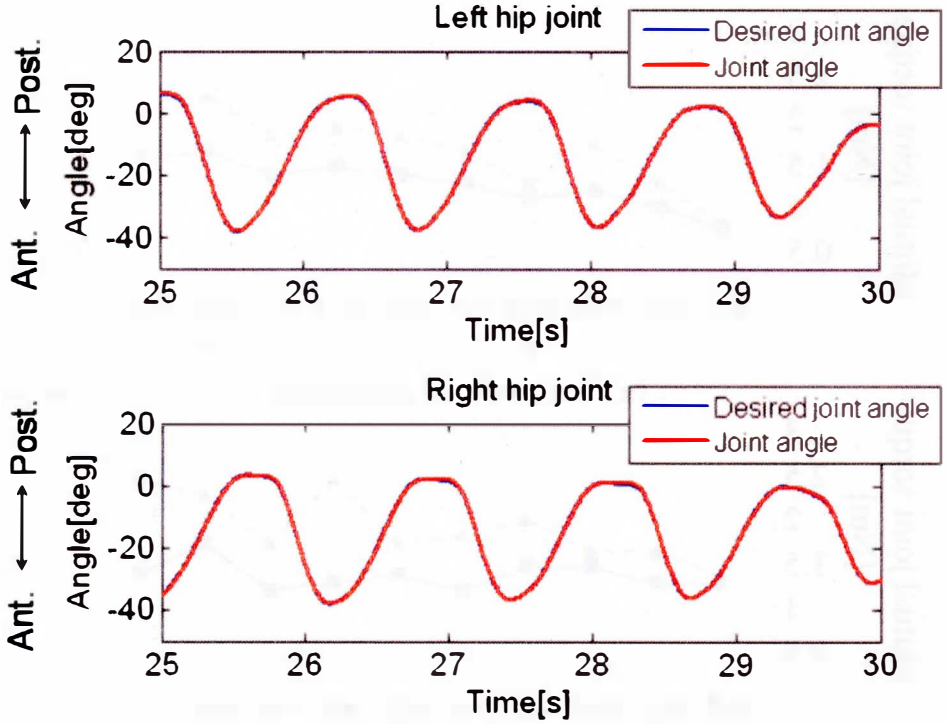

Fig.7.3. 7 Trajectories of the suit's left and right hip joints in a cooperative walk where c = 0.5. Blue lines represent the desired joint angles and red lines the joint angles, Ant. refers to the anterior direction and Post. the posterior direction.

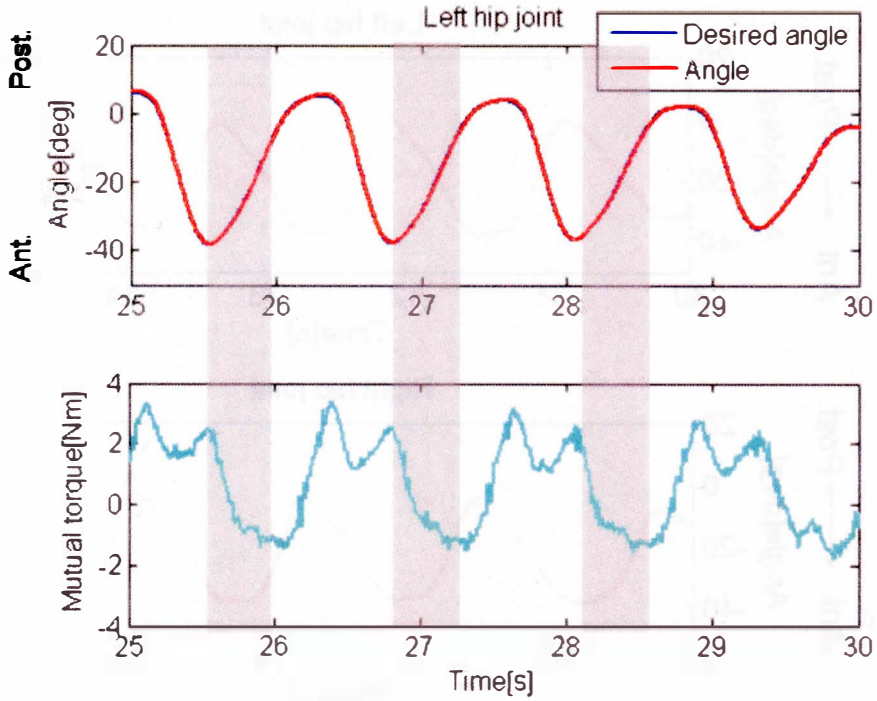

Fig.7.3. 8 Input/output(mutual joint torque/desired angle) of neural oscillator at the left hip joint when C=0.5

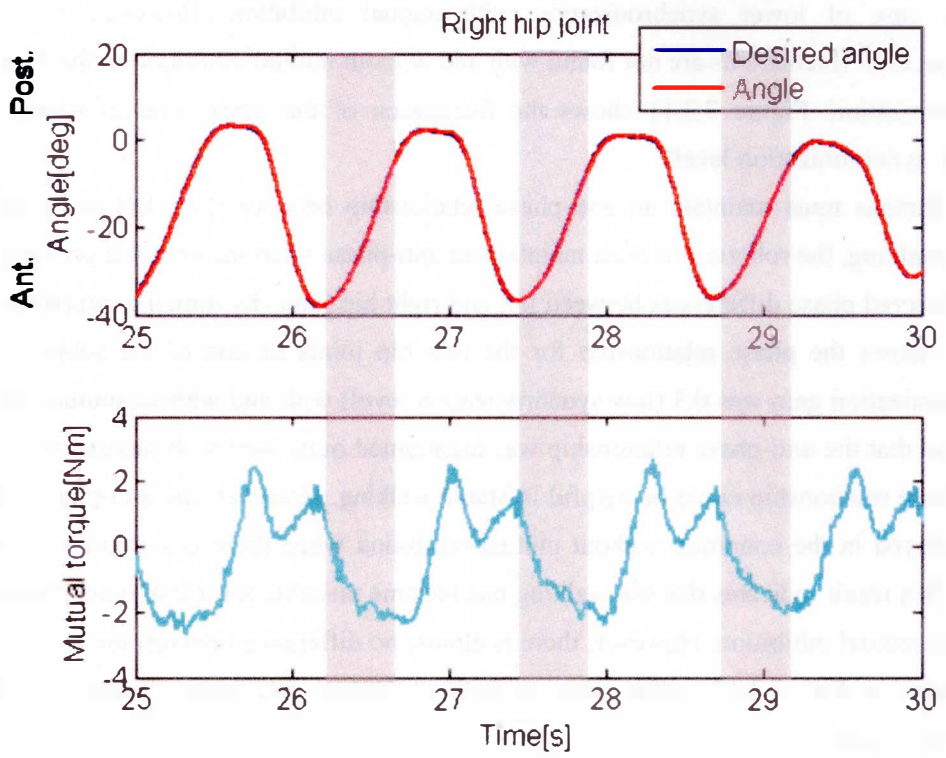

Fig.7.3. 9 Input-output(mutual joint torque-desired angle) of neural oscillator at the right hip joint when C=0.5

To demonstrate the necessity of mutual inhibition between neural oscillators on the left and right hip joints for stable walk assistance, we conducted pairs of walking experiments using the robotic suit with and without mutual inhibition. The synchronization gain was 0.3 and 0.5 for each group. The original movements of the robotic suit and the subject were the same as those in the last section. Walk stability was evaluated with the phase difference between the left and right hip joints using a return map and the fluctuations of the stride interval.

Figure 7.3.10 shows the time series of the stride interval of one of the subjects in the walking experiments when the synchronization gain is 0.3 with and without mutual inhibition. The lower part of Fig. 7.3.10 shows the stride interval calculated using the timing of each heel strike against the time cue, and the upper part is the power spectrum analysis of each heel strike according to the information of the micro switch. Compared with the case with mutual inhibition, the fluctuations without mutual inhibition are significant. Fluctuations of the stride interval in short periods of time could be an indicator of walk stability. The smaller the fluctuation, the more stable the walk. Greater fluctuation may suggest disturbed walking. Therefore, from the results shown in Fig. 7.3.10, we conclude that stability was well maintained

in the case of lower synchronization with mutual inhibition. However, these dramatic differences in fluctuations are not found with and without mutual inhibition in the case of higher synchronization. Figure 7.3.11 shows the fluctuation of the stride interval where $C = 0.5$ (higher synchronization level).

As humans must maintain an anti-phase relationship between their left and right legs for stable walking, the robotic suit must maintain an anti-phase relationship while providing support. We observed phase differences between left and right hip joints by drawing return maps. Figure 7.3.12 shows the phase relationship for the two hip joints of one of the subjects when the synchronization gain was 0.3 (low synchronization level) with and without mutual inhibition. It is found that the anti-phase relationship was maintained quite well with mutual inhibition. This anti-phase relationship could be helpful in stable walking. However, the anti-phase relationship is destroyed in the condition without mutual inhibition when there is a small synchronization gain. This result indicates that the walking has become unstable for a low synchronization level without mutual inhibition. However, there is almost no difference between the two return maps, as shown in Fig. 7.3.13, either with or without mutual inhibition, in the case of greater synchronization ($C = 0.5$).

We have drawn the phase portraits of the natural walking, each cooperative walking (C=0.3, C=0.5) with and without mutual inhibition. Figure 7.3.14 shows the phase portrait of the natural walking. Figure 7.3.15 (C=0.3) and Figure 7.3.16 (C=0.5) show the phase portraits of the cooperative walking without mutual inhibition. Figure 7.3.17 (C=0.3) and Figure 7.3.18 (C=0.5) show the phase portraits of the cooperative walking with mutual inhibition. The upper parts of those figures show the phase portrait of the left hip joint, and the lower parts show the phase portrait of the right hip joint. Comparing to the phase portraits in Fig. 7.3.15 and Fig. 7.3.16, the phase portraits in Fig 7.3.17 and Fig. 7.3.18 specify that the cooperative walking with mutual inhibition is robust and stable. In addition, the phase portrait of the left and right hip joint has the same qualitative dynamic behavior under the condition with mutual inhibition. However, the phase portrait of the left and right hip joint appears to indicate different qualitative dynamic behavior under the condition without mutual inhibition (see Fig 7.3.15). This different qualitative dynamic behavior between the left and right hip joint is the reason why the cooperative walking is unstable under the condition without mutual inhibition.

The experimental results presented in the last three paragraphs verify our assumption that mutual inhibition helps maintain stability for a low synchronization level.

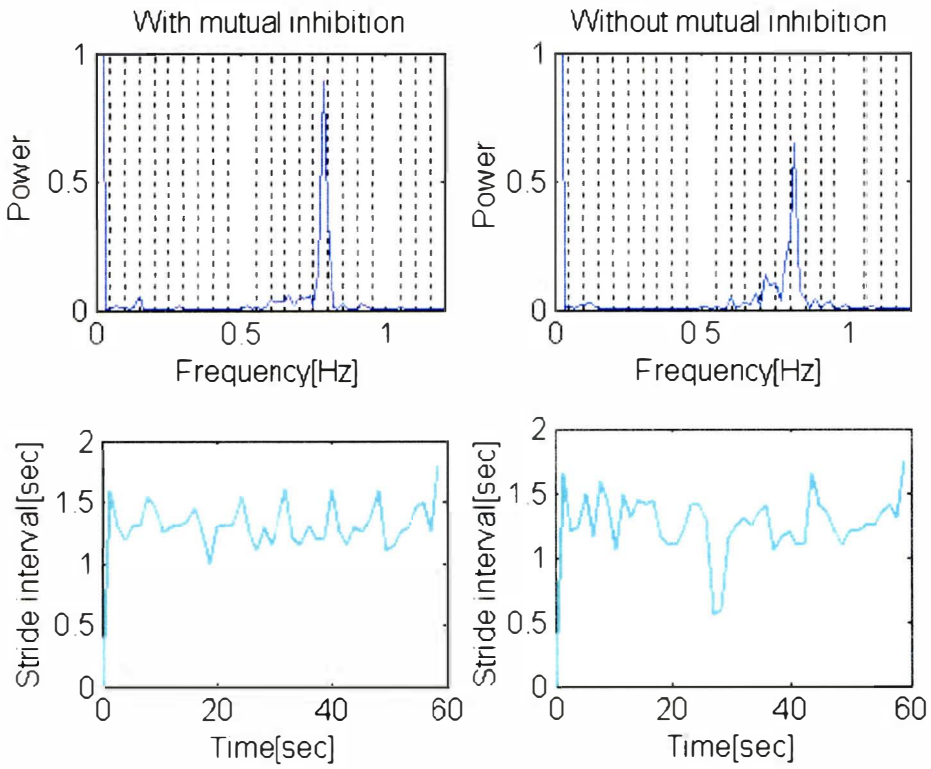

Fig.7.3. 10 Time series of the stride interval and its spectral analysis when c = 0.3; left: with mutual inhibition, right: without mutual inhibition

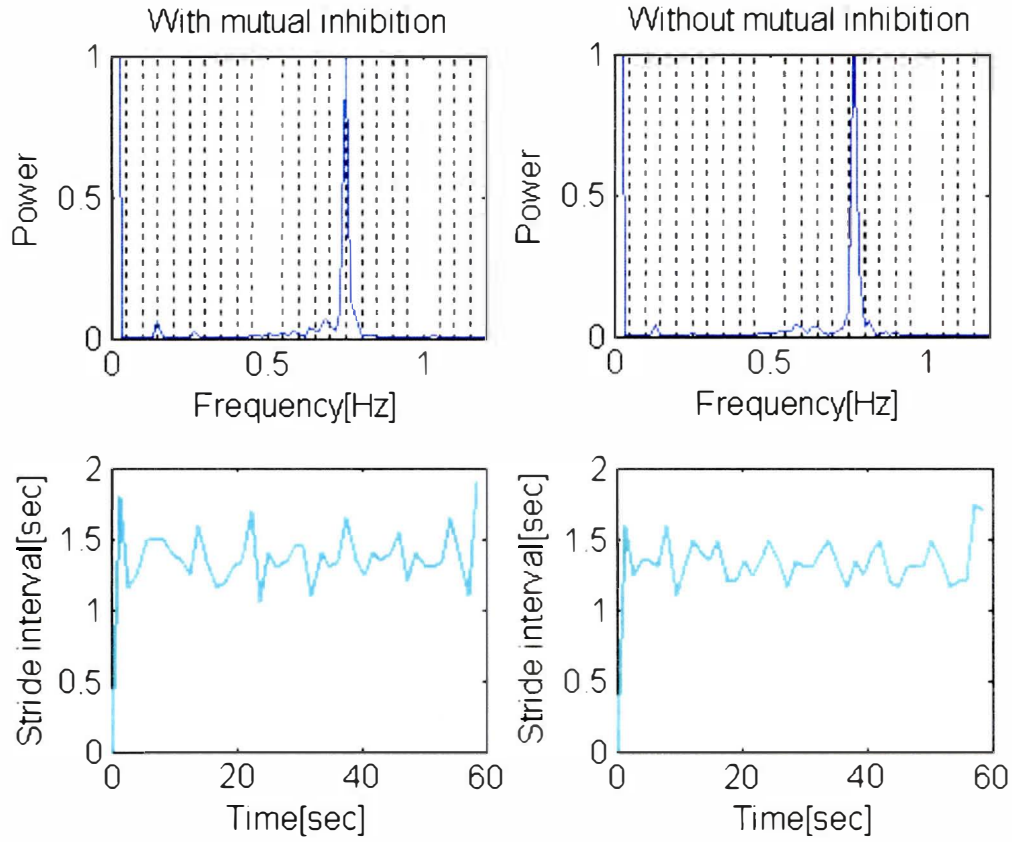

Fig.7.3. 11 Stride interval time serious and its spectrum analysis when c=0.5: the left part is with mutual inhibition, and the right part is without mutual inhibition

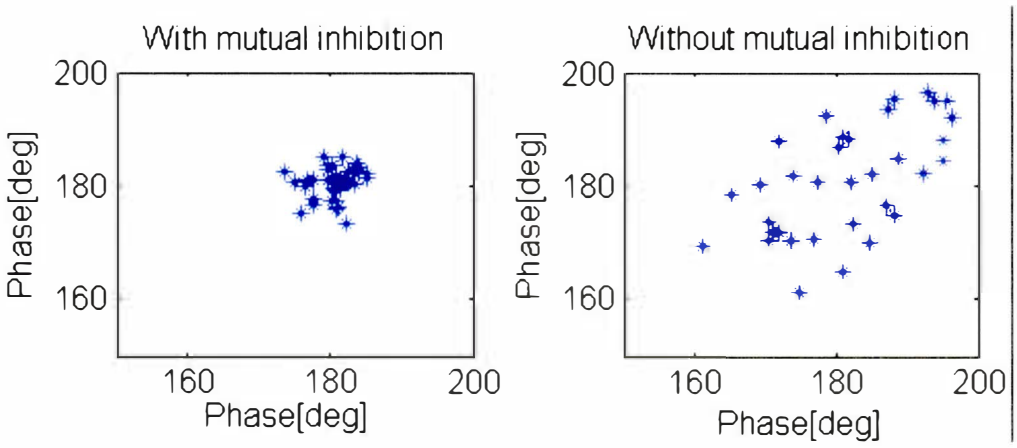

Fig.7.3. 12 Return maps for the relationship of the phase differences between left and right legs when c = 0.3

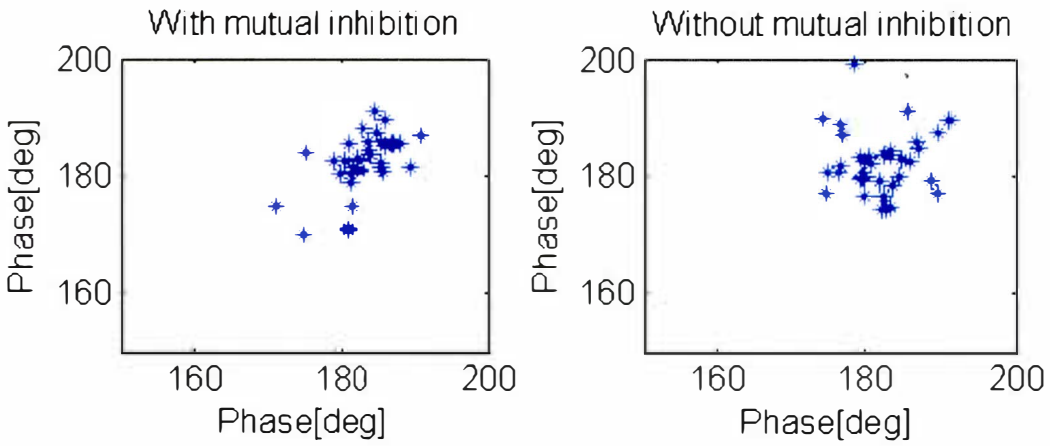

Fig.7.3. 13 Return maps for the relationship of the phase differences between left and right legs when c = 0.5

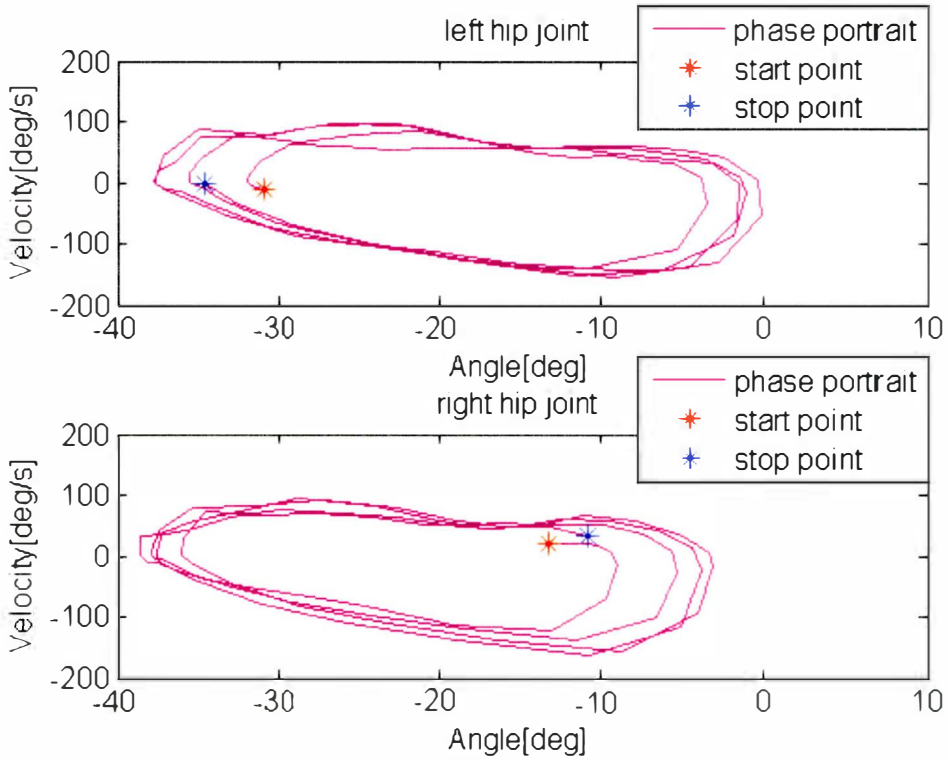

Fig.7.3. 14 Phase portrait of the natural walking

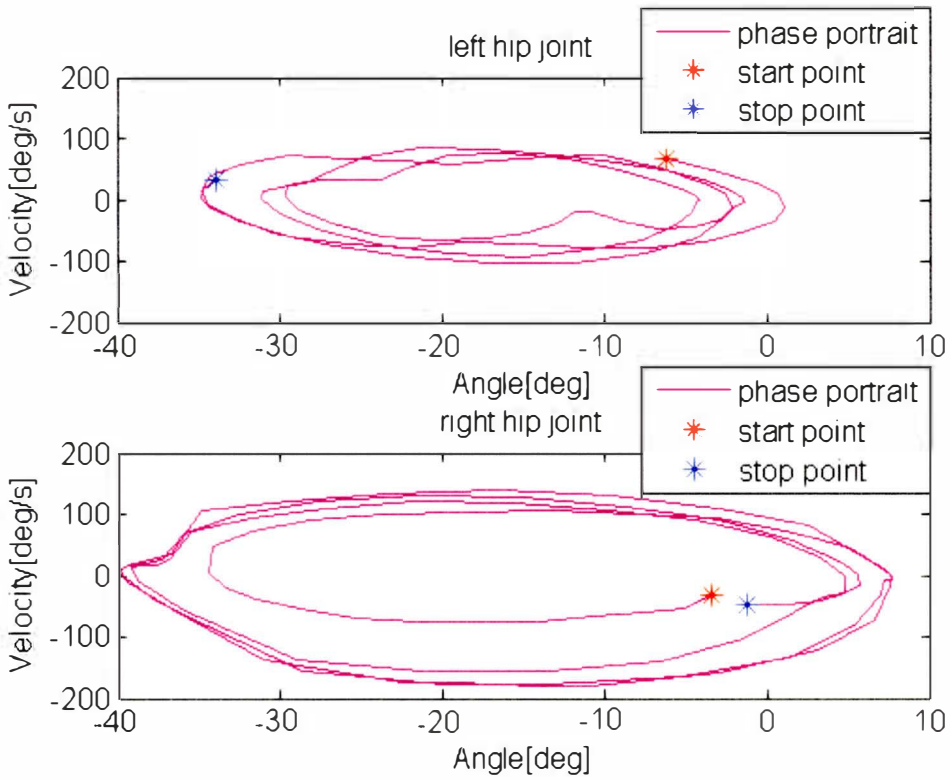

Fig.7.3. 15 Phase portrait of the cooperative walking (C=0.3) without mutual inhibition

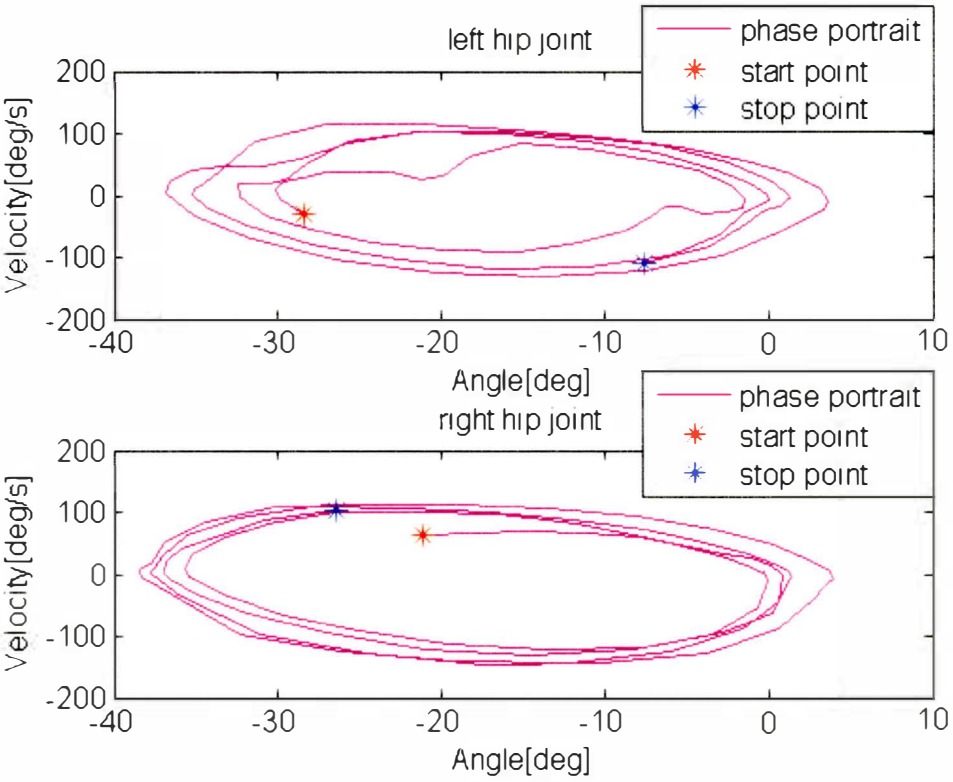

Fig.7.3. 16 Phase portrait of the cooperative walking (C=0.5) without mutual inhibition

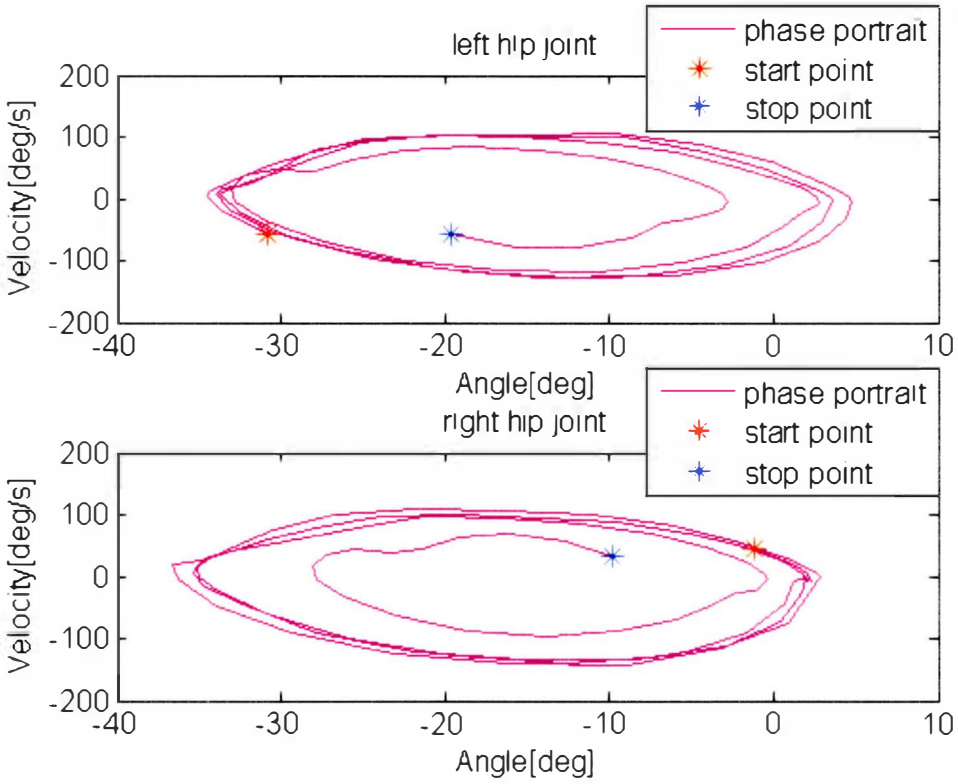

Fig.7.3. 17 Phase portrait of cooperative walking (C=0.3) with mutual inhibition

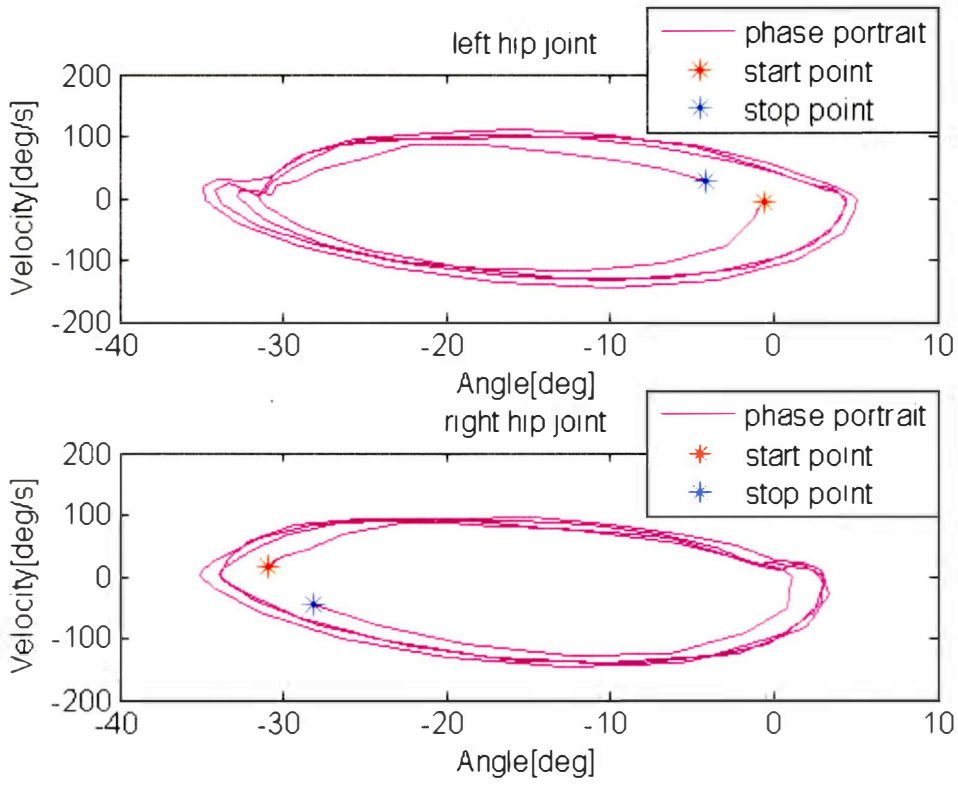

Fig.7.3. 18 Phase portrait of cooperative walking (C=0.5) with mutual inhibition

7.3.4 Walking assist effect

The walking assist effect is defined in this paper as easier mobility (e.g., lengthened step or increased speed) with less physical effort. Therefore, the assist effect was evaluated by changes in step length, speed and muscle activity relative to those of normal walking without wearing the robotic suit.

・Lengthened step and increased speed

In the scenarios where 10 subjects walked synchronously with the robotic suit, the step length was found to have lengthened. Figure 7.3.19 shows the ratio of the step length of cooperative walking with synchronization gain of the suit set at 0.3 and 0.5 to the step length of independent walking for each subject. Figure 7.3.19 shows that the step lengths of eight of the ten subjects increased. The result for the walking speed in Fig. 7.3.20 was found to be similar to that for the step length. Step length increased greatly in both cases of cooperative walking with $C = 0.3$ (two-tailed t-test, $t\ (18) = -3.534$, $P < 0.01$) and $C = 0.5$ (two-tailed t-test, $t\ (18) = -2.365$, $P < 0.05$). The speed also significantly increased in both cases of cooperative walking with $C = 0.3$ (two-tailed t-test, $t\ (18) = -3.095$, $P < 0.01$) and $C = 0.5$ (two-tailed t-test, $t\ (18) = -2.925$, $P < 0.01$).

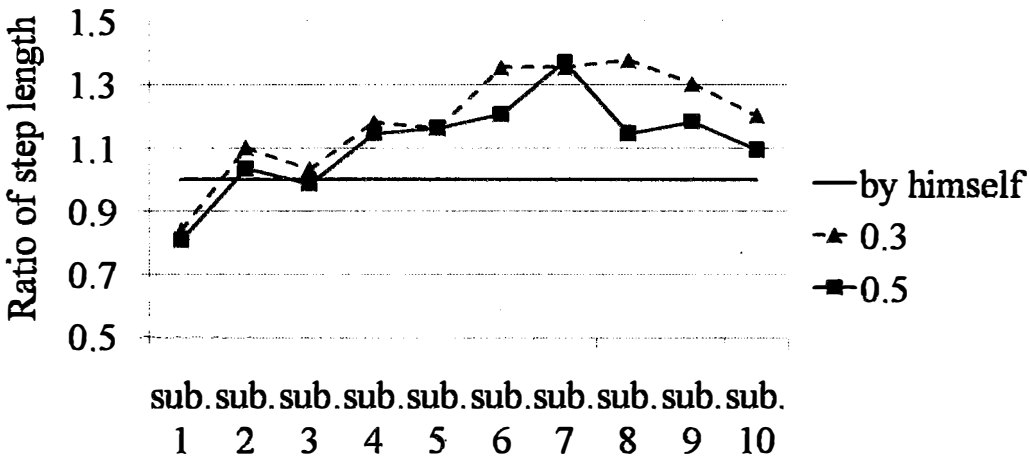

Fig.7.3. 19 Ratios of the step length when walking cooperatively to that when walking independently. The dotted line represents ratios of the step length when $C = 0.3$, and the solid line represents those when $C = 0.5$.

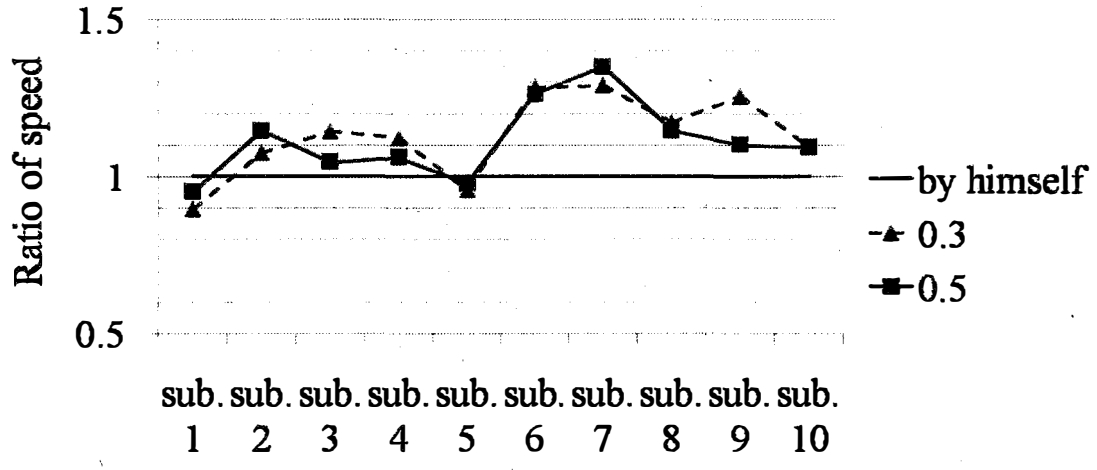

Fig.7.3. 20 Ratios of the speed when walking cooperatively to that when walking independently. The dotted line represents ratios of the step length when c = 0.3, and the solid line represents those when c = 0.5.

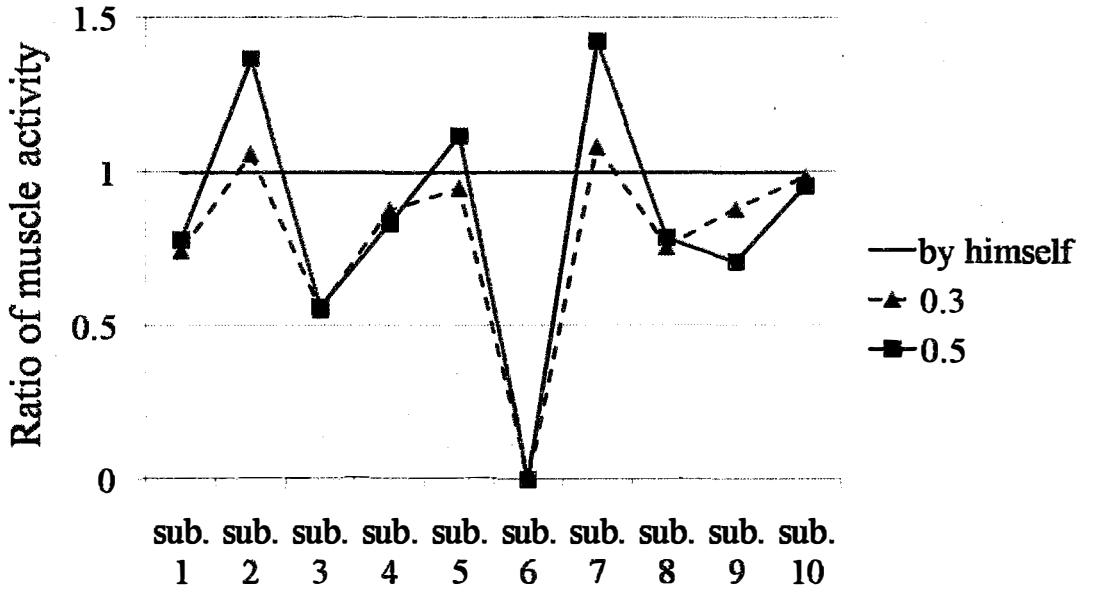

Fig.7.3. 21 Ratios of the muscle activity when walking cooperatively to that when walking independently. The dotted line represents ratios of the step length when c = 0.3, and the solid line represents those when c = 0.5.

• Physical consumption

Physical consumption was estimated by observing muscle activity. Figure 7.3.21 shows the result of the ratio of muscle activity of cooperative walking with a synchronization gain of the suit set to 0.3 and 0.5 to that of independent walking. Figure 7.3.21 suggests that most of the 10 subjects had less muscle activity in the case of cooperative walking, two or three had greater muscle activity, and there was one invalid datum (subject #6). Muscle activity greatly reduced for cooperative walking with $C = 0.3$ (two-tailed t-test, $t\ (18) = 2.216$, $P < 0.05$). However, we failed to find a significant difference using the t-test in the case of $C = 0.5$. We conclude from these results that the reduction in muscle activity is a verified assist effect.

7.3.5 From walk to stop

The subjects were asked to stop one time and re-start walking at any time he wanted in the walk experiment. The stopping motion of three subjects A, B, C are shown in Fig 7.3.22-7.3.27. The upper part of Fig 7.3.22-7.3.27 shows the angle of the left and right hip joints respectively, and the lower part shows the mutual joint torque of each hip joint. It can be found that when the user tried to stop, the robot stopped immediately, and restarted the walk when the user restarted to walk.

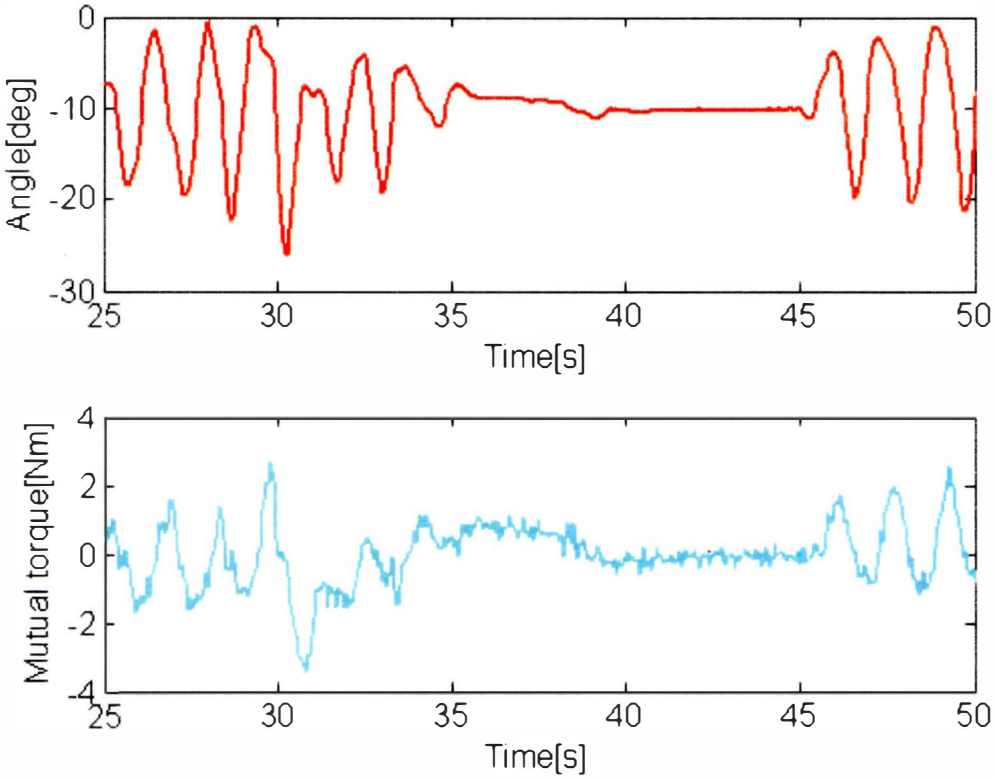

Fig.7.3. 22 Stop and re-start motion of the left hip joint of subject A

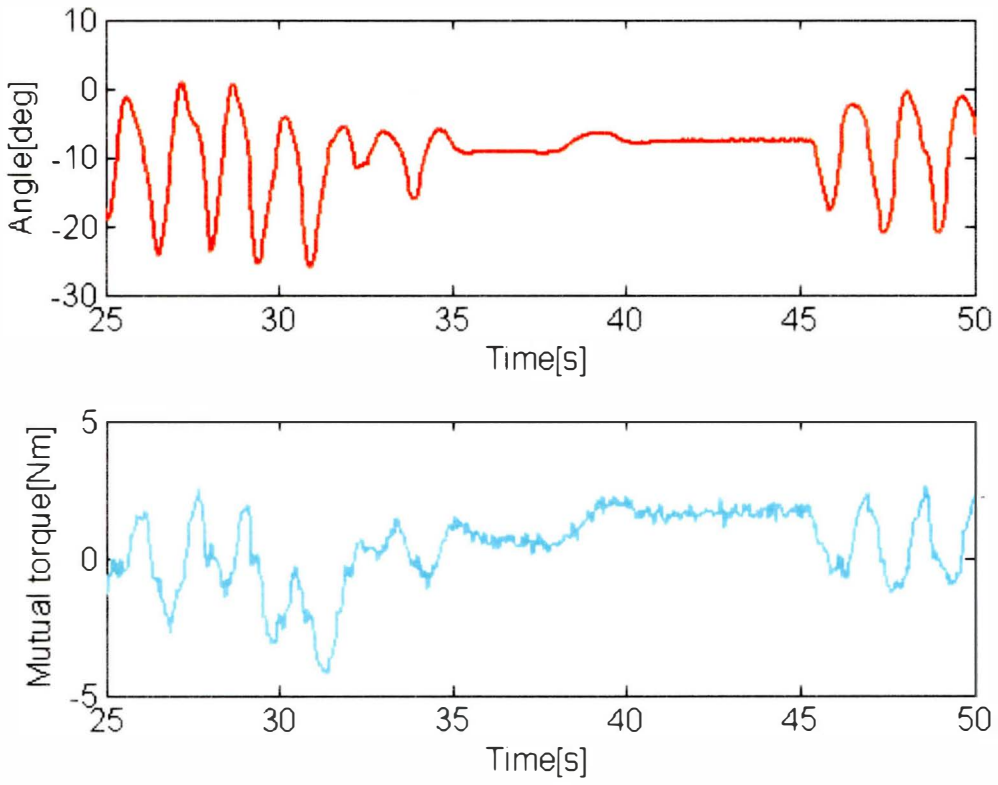

Fig.7.3. 23 Stop and re-start motion of the right hip joint of subject A

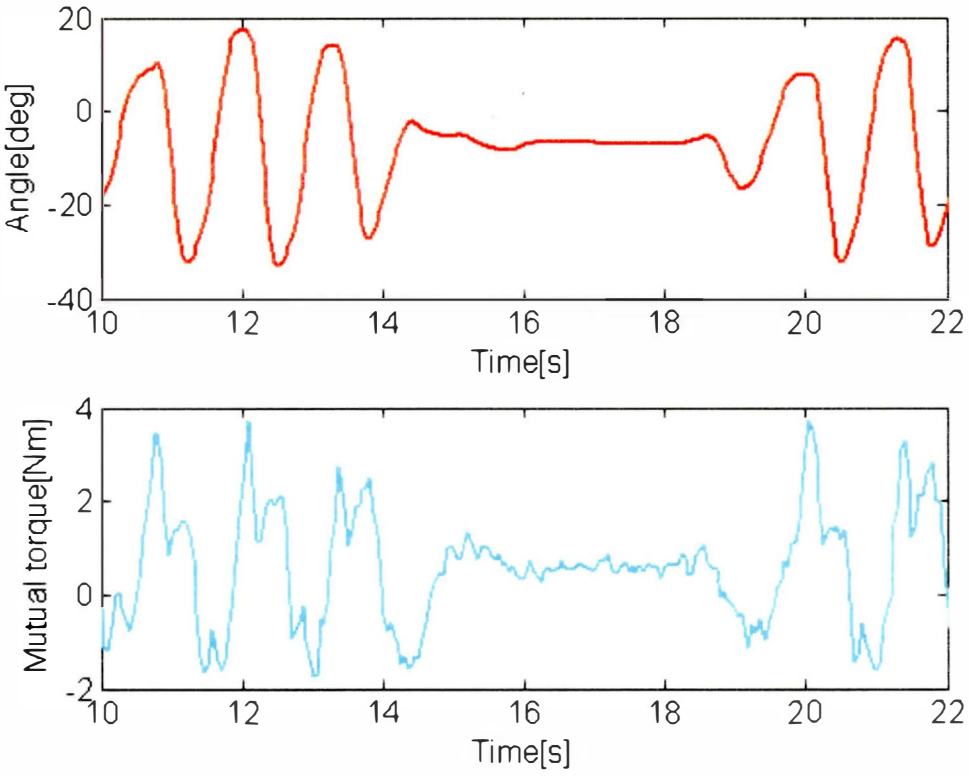

Fig.7.3. 24 Stop and re-start motion of the left hip joint of subject B

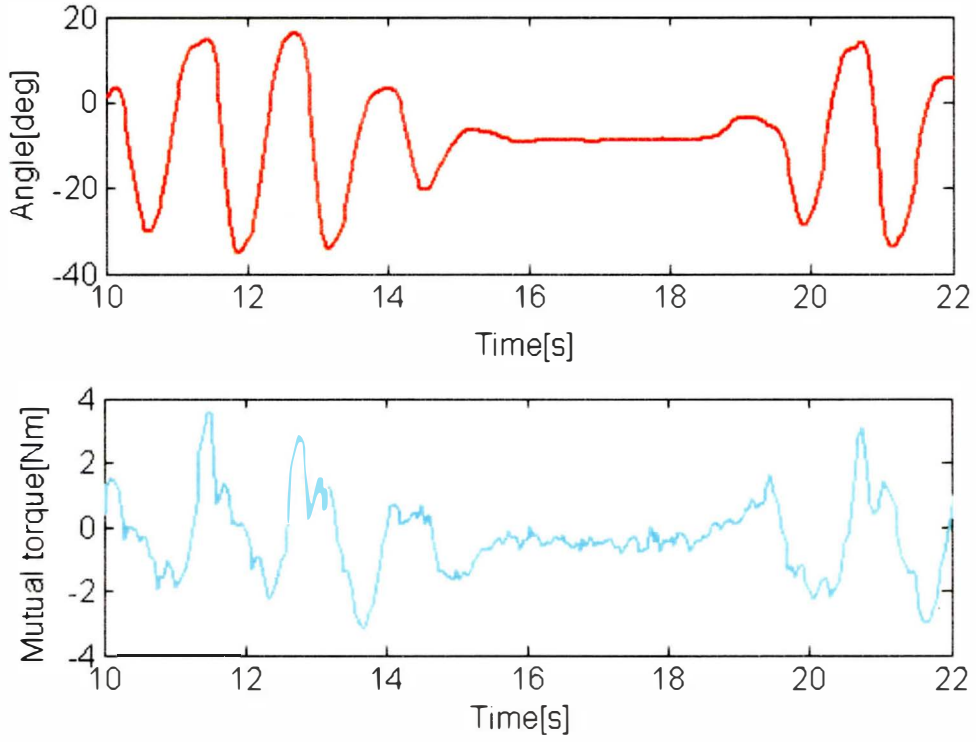

Fig.7.3. 25 Stop and re-start motion of the right hip joint of subject B

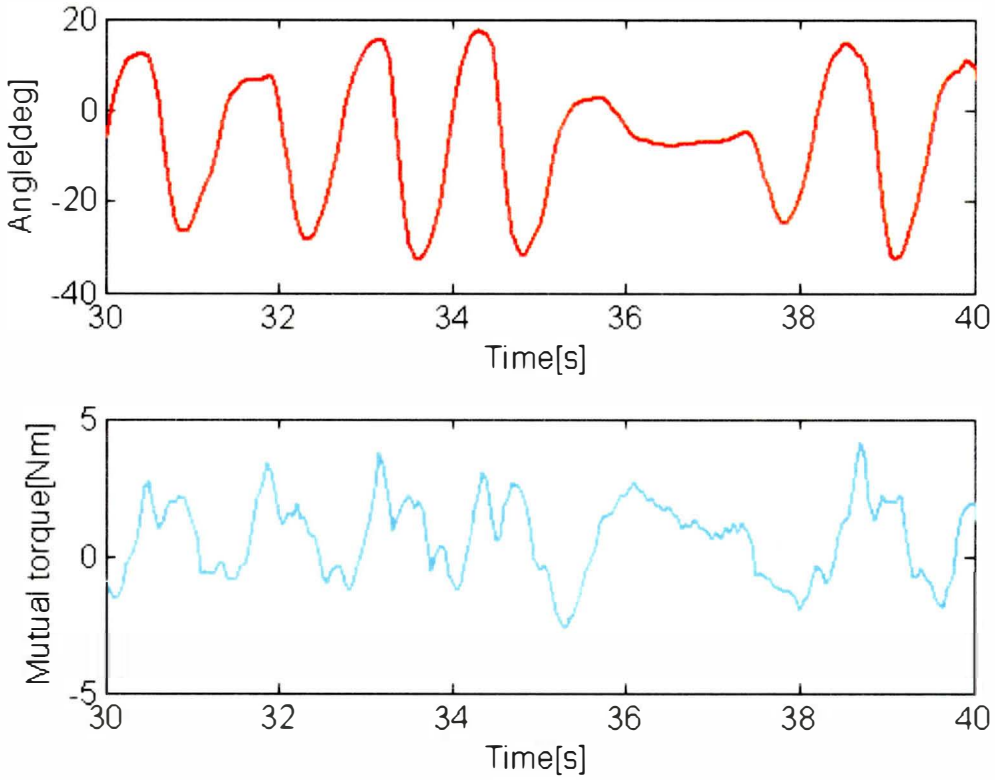

Fig.7.3. 26 Stop and re-start motion of the left hip joint of subject C

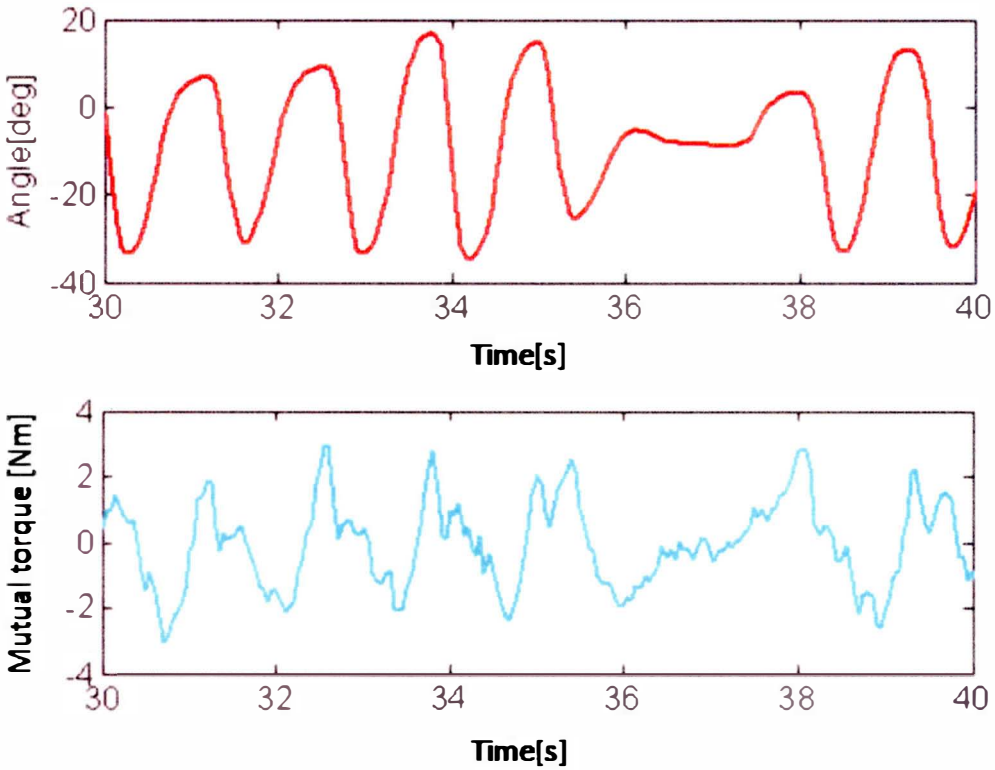

Fig.7.3. 27 Stop and re-start motion of the right hip joint of subject C

7.3.6 Psychological evaluation

Following the work of Bradley, we evaluated the psychology of three walking patterns: (a) walking independently, (b) walking cooperatively with the robotic suit with mutual inhibition, and (c) walking cooperatively with the robotic suit without mutual inhibition. We asked the subjects which walking pattern they considered the easiest and which they considered the most unstable. The views of the 10 subjects are presented in Tables 7.3.1 and 7.3.2. The tables present the number of subjects who consider the walking listed in the left column to be easier (Table 7.3.1) or more unstable (Table 7.3.2) than the walking listed in the top row. The results showed that many subjects considered walking pattern (b) to be easiest and walking pattern (c) to be the most unstable. Table 7.3.3 lists evaluation scale values and χ_0^2 . For both questions of ease and stability, the inequality $\chi_0^2 > \chi^2(2,0.1) = 4.6$ is satisfied. The statistical test using the χ^2 distribution function shows differences in rank among the three samples, indicating that our proposal is helpful for stable walking assistance.

Table7.3. 1 Ease of walking

	a	b	c	total
a	–	2	5	7
b	9	–	6	15
c	5	3	–	8

Table7.3. 2 Instability while walking

	a	b	c	total
a	–	6	3	9
b	4	–	2	6
c	7	8	–	15

Table7.3. 3 Interval scale and χ_0^2

	π_a	π_b	π_c	χ_0^2
Easy walk	0.19	0.6	0.21	5.31
Unstable walk	0.25	0.16	0.59	5.89

7.4 Conclusion and discussion

We proposed a synchronization-based motion assist method for a robotic suit for walking assistance purposes using neural oscillators. To enable the robotic suit to confer stability for walking assistance, we proposed a framework of mutual inhibition between neural oscillators on the left and right hip joints to maintain cooperative anti-phase movement of the robotic suit. The inhibitory weight was properly determined. We examined the validity and feasibility of our proposal with a lower-limb two-DOF robotic suit. A series of walking experiments and a psychological evaluation were conducted for the mutual-torque-detecting assist suit with cancellation of the gravity term. Results show that 1) synchronization was achieved; 2) the synchronization-based trajectory generation method works for walking assistance; and 3) stable assistance can be provided with our design of mutual inhibition between neural oscillators connected to the robotic suit. The basic idea in this chapter was to propose an interaction approach for controlling a robotic suit, thus providing walking assistance (by increasing the step length and lowering physical effort). Furthermore, this chapter presented our first attempt towards maintaining stable assistance using the mutual inhibition of neural oscillators.

We have developed a four-DOF robotic suit, depicted in detail in Chapter 6, which includes a knee joint. We are working towards the implementation of our proposal for the robotic suit and the combination of neural oscillators to achieve cooperative movement. Next Chapter will be the experimental walking results of the four-DOF robotic suit.

References

[1] Xia Zhang, Minoru Hashimoto, "Synchronization-Based Trajectory Generation Method for a Robotic Suit Using Neural Oscillators for Hip Joint Support in Walking," *Mechatronics,* in print

[2] Xia Zhang, Minoru Hashimoto, "Inhibitory Connections between Neural Oscillators for A Robotic Suit," *2011 IEEE Int. Conf. on Robotics and Automation (IEEE ICRA2011),* Shanghai, China, pp. 4182-4187, May, 2011

Chapter 8

Walking experiments using four-DOF robotic suit

Chapter 8 Walking experiments using four-DOF robotic suit

We worked towards implementing the proposal to the four-DOF robotic suit. The design of the prototype is depicted in detail in Chapter 6. For supporting the whole lower limb, the coordination motion among the suit's multiple joints becomes an important issue to concern. We investigated the phase relationships among multiple joints of normal walking. In order to realize the complex phase relationships among multiple joints, we proposed symmetrical and unsymmetrical inhibitory connections among neural oscillators. In section 8.1, phase differences among joints in natural walk and the change of amplitude were investigated. In section 8.2, we proposed the unsymmetrical inhibitory connections among neural oscillators to reproduce the phase differences. However, it was found that cooperative walking where wearing the robotic suit was lack of flexibility for the amplitude was not so natural. In order to solve this problem, in section 8.3, we considered the measures of regulating amplitude. In section 8.4, we investigated whether the proposed method was valid to realize the trajectories of walking by conducting walking experiments.

8.1 Phase differences among multi-joints in normal walk

We investigated the phase differences among multi-joints, which were calculated using joint angles. The normal trajectories of a subject were measured approximately and indirectly through measuring the robotic suit's trajectories, by asking the subject to walk normally wearing the four-DOF robotic suit, which was very compliant, and the maximum resistance torque measured by the torque sensors was about 1.0 Nm. Figure 8.1.1 shows the natural trajectories of walking. The upper part of Fig. 8.1.1 represents joint angles of the left leg, and lower part represents those of the right leg. Take the left leg as the analysis object. The blue line in Fig. 8.1.1 represents the hip joint angles, and the red line is the knee joint angles. "Post." represents the posterior direction at sagittal plane, and "Ant." represents the anterior direction. By comparing the trajectories, firstly, we found that the flexion-extension motion of the knee joint had been done twice while the hip joint finished single flexion-extension motion. Secondly, and more complicatedly, the amplitude of the first flexion-extension motion was different with that of the second flexion-extension of the knee joint. Thirdly, the center lines of the first and second flexion-extension were divided. The first flexion-extension motion of the knee joint takes place

in swing phase for stepping forward, and the second flexion-extension motion of the knee joint takes place in the heel striking phase for helping absorb the impact force and the Gravity of Center rotate to move forward [1].

We used return map to analyze the phase differences between the left and the right hip joint, the hip joint and the knee joint (first and second time flexion-extension), and the first and second flexion-extension motion of the knee joint. The result is shown by return map in Fig. 8.1.2. It can be found that there are anti-phase relationship between the left and right hip joint, about 1/4 π phase difference between the left hip and the knee joint's first time flexion-extension, about 1.1 π phase difference between the left hip and the knee joint's second time flexion-extension, and about 0.8 π phase difference between the first and second flexion-extension motion of the knee joint. Joints of the right leg shares the same relationships with that of the left leg.

So far, the anti-phase has been realized by incorporating mutual inhibition (symmetrical inhibition) between the left and right neural oscillator, which has been depicted in-detail in Chapter 7. The realization of other complicate phase relationships is the task that is hopefully resolved in the current study.

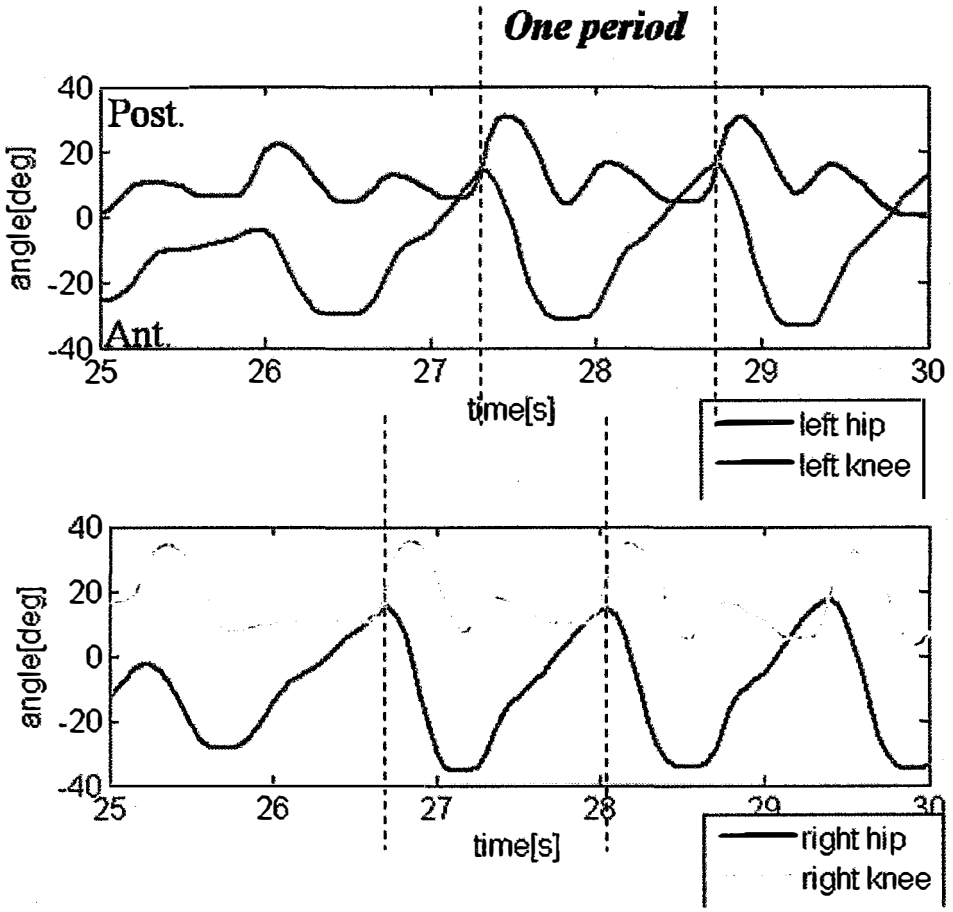

Fig.8.1. 1 Trajectory of each joint in normal walk

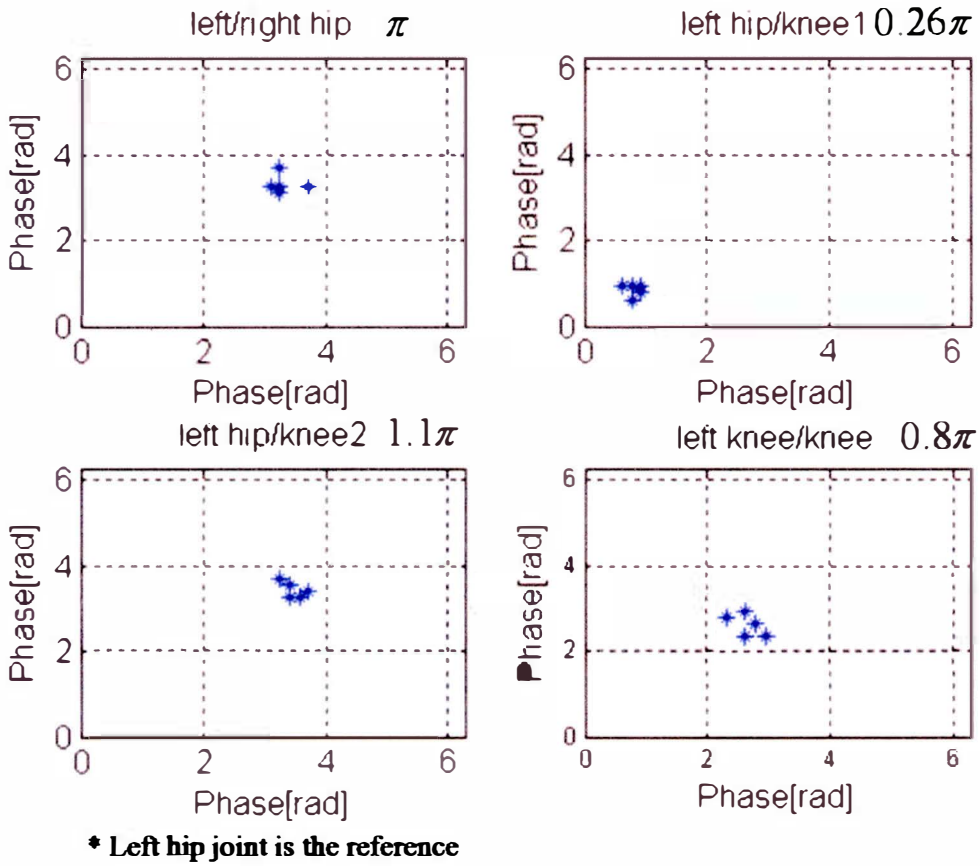

Fig.8.1. 2 Phase differences among multiple joints in normal walk

8.2 Connections among neural oscillators

Following the work of Matsuoka in 1985, we proposed using unsymmetrical inhibitory connections between neural oscillators at the hip and knee joint to realize the 1/4 phase difference between the hip-knee joint (first time flexion-extension). Matsuoka presented a "cyclic inhibition" (unsymmetrical inhibition) model which consists of four neurons (two neural oscillators) [1]. The unsymmetrical model is illustrated in Fig. 8.2.1. With the unsymmetrical inhibition, the four neurons activate subsequently. Consequently, the neural oscillator consisting of the neuron 1, 2, and the neural oscillator consisting of the neuron 5, 6 oscillate subsequently with a 1/4 π phase difference. The whole coupling of the four neural oscillators of the robotic suit are shown in Fig. 8.2.2.

In order to double the frequency of the knee joint flexion-extension motion, we assigned the time constant of the neural oscillator in the knee joint as $T_r = 0.06$ $T_a = 0.3$, which is the half

of that of the neural oscillator in the hip joint.

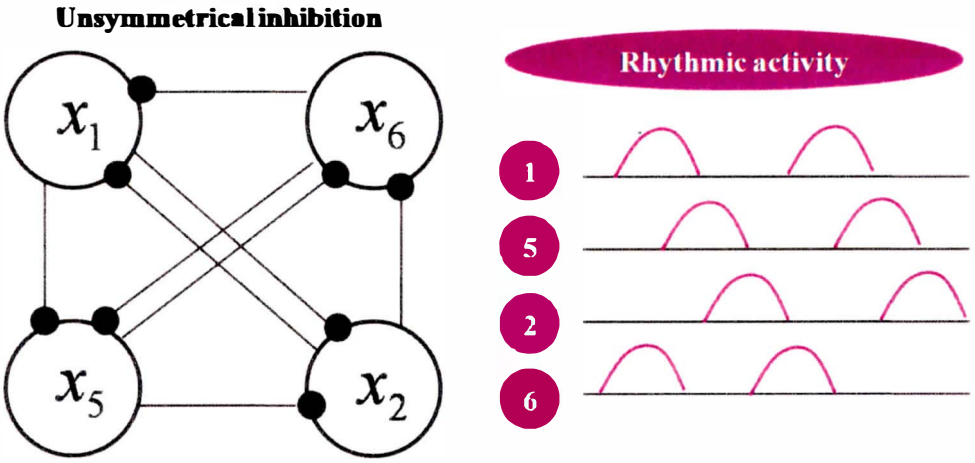

Fig.8.2. 1 Unsymmetrical inhibition among neurons

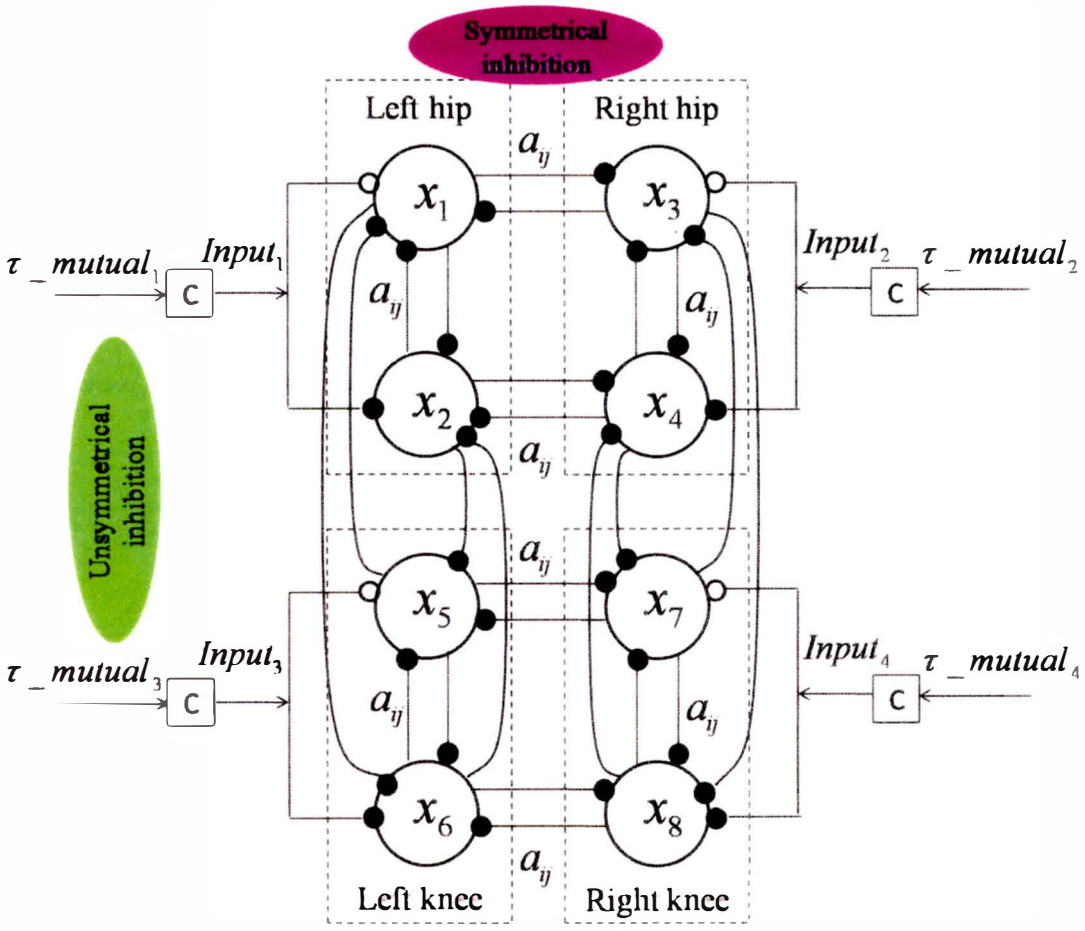

Fig.8.2. 2 Symmetrical & unsymmetrical inhibitions among neurons

We investigated whether the proposed model is valid for reproduction of the phase difference among the multiple joints by walking experiments.

A university student wore the robotic suit and was asked to walk synchronously with the robotic suit. In walk experiments, the synchronization gain for the hip and knee joints were increased to 0.5, which meant high synchronization level. The trajectories of the left leg in cooperative walk were shown in the upper part of Fig. 8.2.3, of which the red line represented the hip joint, and the blue line represented the knee joint. Although it can be found that the frequency of the knee joint motion is twice of that of the hip joint motion, by comparing to Fig. 8.1.1, the amplitude of the first and the second flexion-extension of the knee are not flexible as supposed. In addition, the lower part of Fig. 8.2.1 shows that large mutual joint torques have taken place, about 5 Nm at the hip joint and about 7 Nm at the knee joint, which could be considered as resistant forces. That is, the cooperative walking wasn't easy with the large resistant forces. Also, return maps were plotted to analyze the phase relationships among joints, and the results are shown in Fig. 8.2.4. It can be found that there are some errors between the phase differences appeared in the normal walk and the corporative walk, that is about 0.3π phase difference between the left hip and knee joint (first time flexion-extension), about 1.3 π phase difference between the left hip and knee joint (second time flexion-extension), and about 0.9 π phase difference between the first and second flexion-extension motion of the knee joint.

The subject participating in the walking experiments reported that it felt restrained and not freely during the corporative walking, and it felt heavy to move forward. The errors in phase differences and the lack of flexibility of amplitude in the knee joints could be considered as resulting in the un-natural walk. It is considered that the large amplitude of the second flexion-extension motion of the knee joint resists the Gravity of Center rotate to move toward, and because of that, the subject may feel heavy to move forward.

Next, we consider the measures of regulating amplitude at the knee joints.

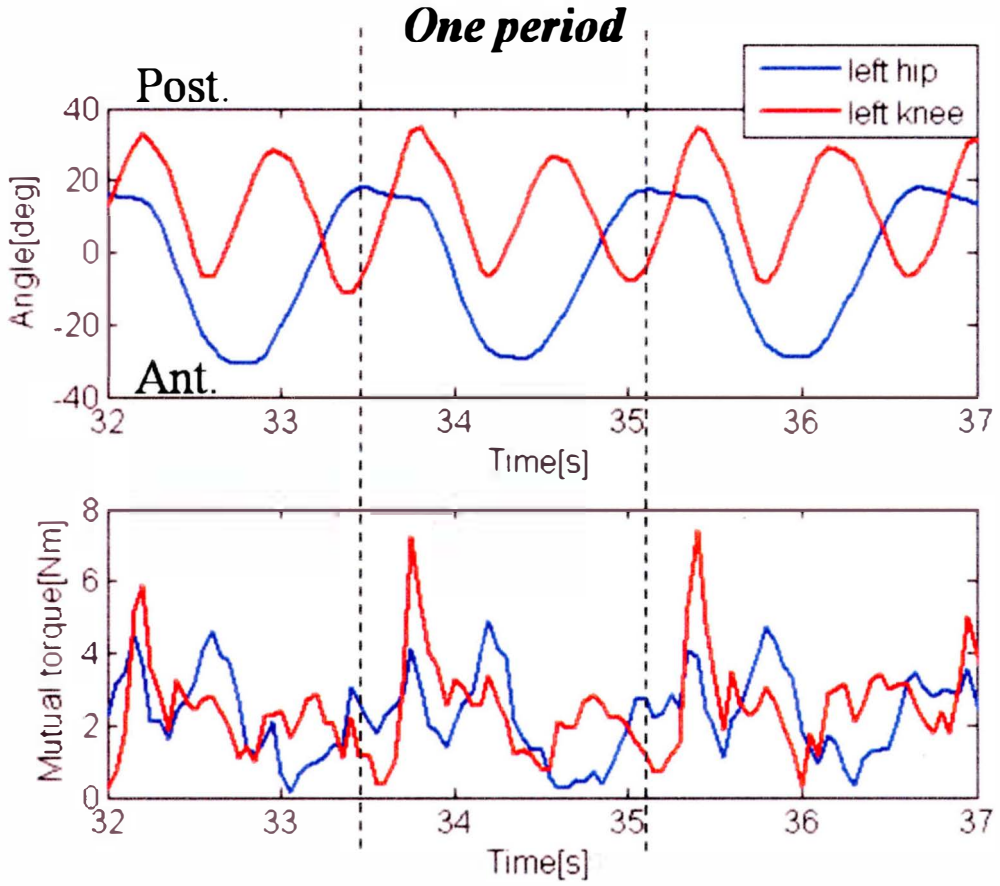

Fig.8.2. 3 Left hip and knee joint trajectory and mutual joint torque in cooperative walk

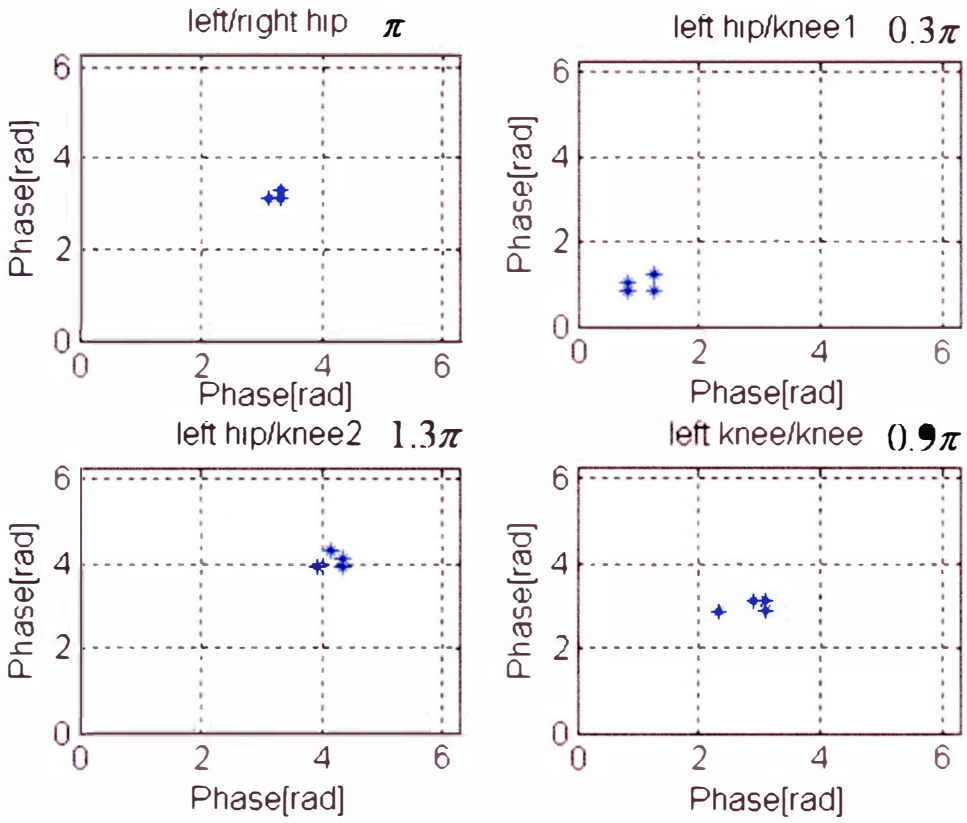

Fig.8.2. 4 Phase differences among multiple joints in cooperative walk

8.3 Amplitude regulation

As reported in the above sections, the amplitude of the first flexion-extension motion and that of the second motion of the knee is different, and it is necessary to regulate the amplitude to realize natural walking. In order to change the amplitude corresponding to each flexion-extension motion, we use the algorithm shown in Eq. (8.2). θ_{hip} in Eq. (8.1) represents the hip joint angles, and θ_{knee} in Eq. (8.2) represents the knee joint angles. $g(x_{ij})(i = 1,\cdots,4,\ j = 1,2)$ represents the output of the j th neuron of the i th neural oscillator. $\theta_{i\ cent}$ is an offset for emulating the natural motion of the hip and knee joint, and it is determined from experiments trails. f_{flex} is a constant to determine the amplitude of flexion motion. f_{ext} is a constant to determine the amplitude of extension motion. For the knee joints,

the constants $f_{flex.}, f_{ext.}$ will be regulated corresponding to the first/second flexion-extension motion at the knee joints. If it is the first flexion-extension motion, the constant of the first flexion motion will be designed as four-time larger than that of the second motion. The first and the second flexion-extension motion were judged using the inclination of the hip joints angle. The logic is: if the left hip joint is in flexion and the right hip joint is in extension, it is the first flexion-extension at the left knee joint and the second flexion-extension at the right knee joint; if the left hip joint is in extension and the right hip joint is in flexion, it is the second flexion-extension at the left knee joint and the first flexion-extension at the right knee joint.

$$\theta_{hip} = (f_{flex.} g(x_{i1}) - f_{ext.} g(x_{i2})) - \theta_{i\_cent.} \quad f_{flex.} = f_{ext.} \qquad (8.1)$$

$$\theta_{knee} = (f_{flex.} g(x_{i1}) - f_{ext.} g(x_{i2})) - \theta_{i\_cent.} \qquad (8.2)$$

$$if \quad \text{first} \quad f_{flex.} = 4 f_{ext.}$$

$$if \quad \text{second} \quad f_{flex.} = f_{ext.}$$

The designed trajectories of the four joints basing on Eq. (8.1) and Eq. (8.2) were shown in Fig. 8.3.1. Comparing to Fig. 8.1.1, it can be found that the designed trajectories are more similar to the natural trajectories in walking: firstly, the flexion-extension motion of the knee had been done twice while the hip joint finished single flexion-extension motion. Secondly, the amplitude of the first and the second flexion-extension motion of the knee joint were differentiated. Thirdly, the center lines of the first and second flexion-extension were divided successfully.

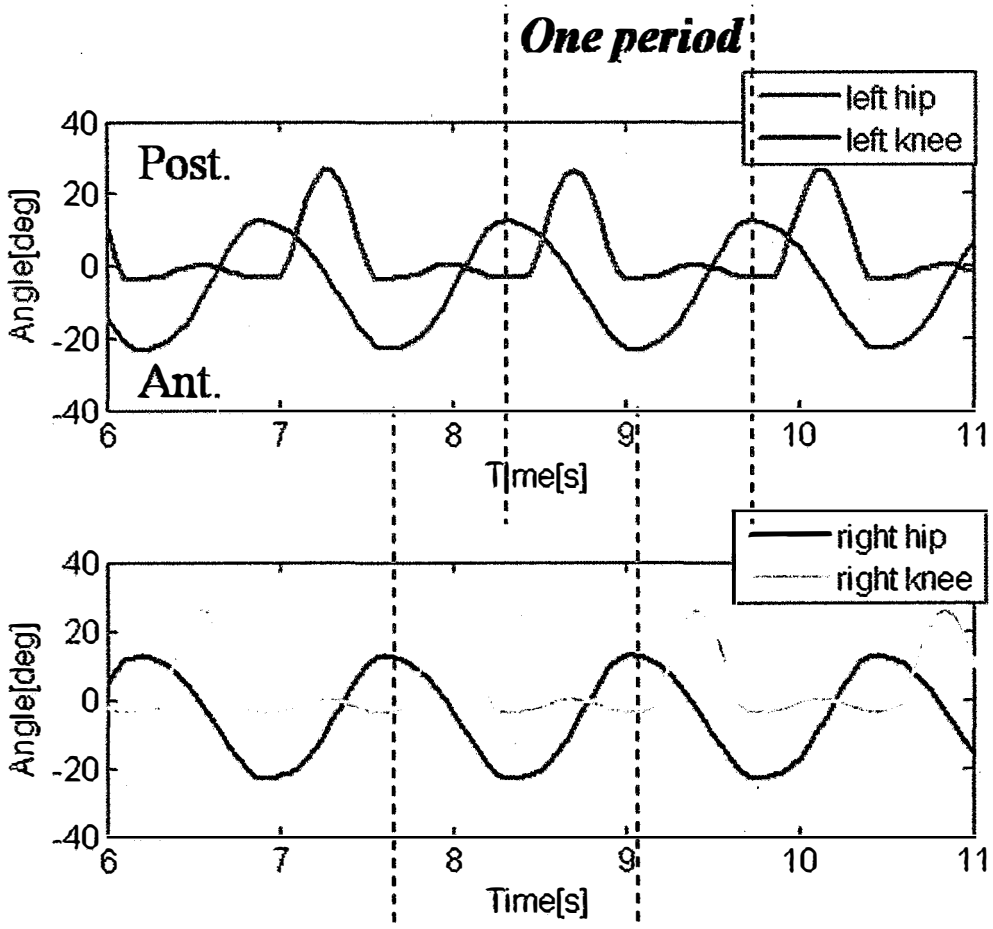

Fig.8.3. 1 Trajectories with amplitude adjustment

8.4 Wearing experiment

A university student wore the robotic suit and was asked to walk synchronously with the robotic suit. The synchronization gains of all the four neural oscillators were determined to be 0.5, which means high synchronization level. The basic movement of the robotic suit is shown in Fig. 8.3.1.

The walking experiment was implemented for 20 s, where the oscillating amplitude gradually increased for the first 5 s as the subject began to walk and gradually decreased in the last 5 s as the subject came to a stop; the middle 10 s were taken for cooperative walking.

Mutual joint torque between the suit and human were measured.

The upper part of Fig. 8.4.1 showed the trajectories of the left hip and knee joints in cooperative walking, and the lower part showed the mutual joint torques. It can be found that the mutual joint torque were not so large comparing to those shown in Fig. 8.2.3, about 2 Nm at

the hip joint and 3 Nm at the knee joint. This indicated the resistant forces became much smaller after implementing the amplitude regulation algorithm. The participant also reported that it felt much lighter and easier during the cooperative walking comparing to the one without amplitude regulation.

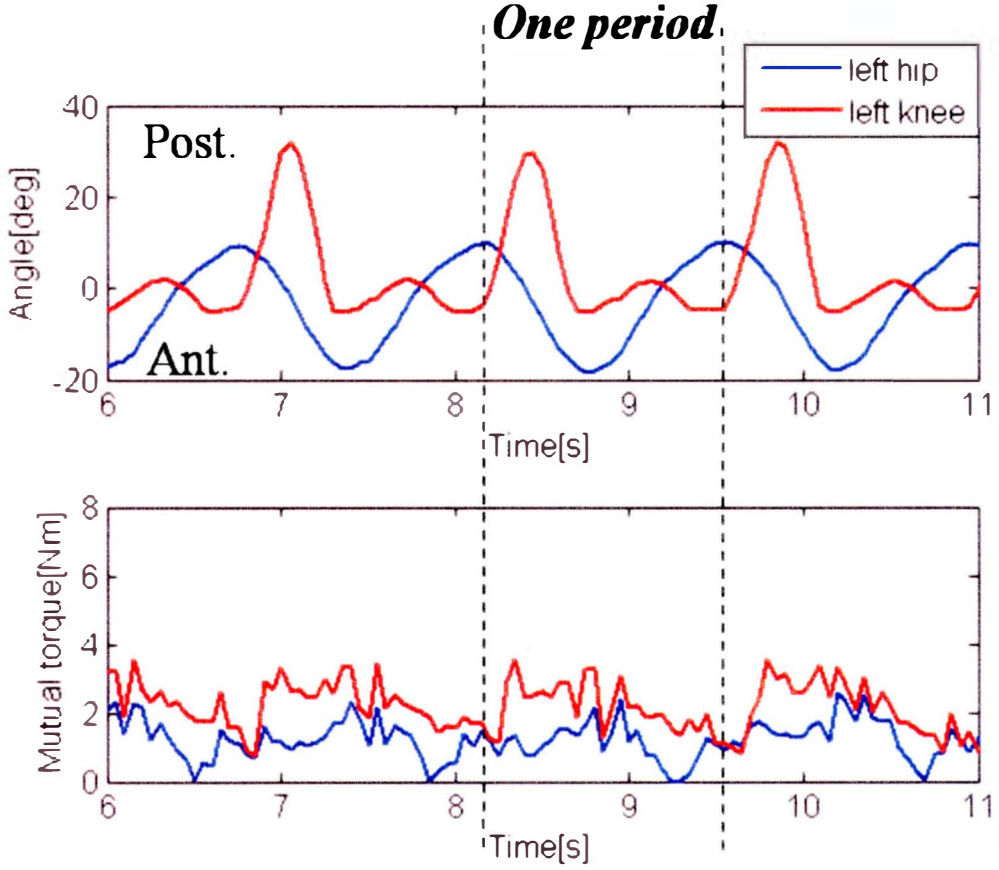

Fig.8.4. 1 Left hip and knee joint trajectory and mutual joint torque in cooperative walk after using amplitude adjustment

8.5 Discussions

We implemented our control system to the four-DOF robotic suit designed for walking assist. We proposed the symmetrical and unsymmetrical inhibitory connections among neural oscillators to reproduce the phase differences of natural walking. To realize natural walking, we considered regulating amplitude corresponding to the knee joint's first/second flexion-extension motion. We verified that our proposed model was valid for realization of the anti-phase relationship between the left-right legs and about 0.25 π phase differences between the hip-knee joints on the ipsilateral side, and we verified that the amplitude regulation algorithm helped to realize the trajectories of normal walking by conducting walking experiments.

8.5.1 Failures in judgment algorithm

Although we discussed the success of cooperative walking in section 8.4, there were failures in the experiments due to the judgment algorithm using the hip joints inclination. Figure 8.5.1 shows one of the examples of judgment failures. Comparing to the blue line which represents the left hip joint, the purple line representing the right hip joint appeared to be with more twists and turns when changing the inclination direction, and these are considered as natural phenomenon in walking. However, as we used the inclination direction as the judgment index of the knee joint's first/second flexion-extension motion, the twists and turns are the essential factor that resulting to the failure of judgment. Due to the failure of judgment, there were some twists and turns at the knee joint took place, and the designed knee joint trajectories were not so smooth (see the yellow line in Fig.8.5.1). Consequently, the cooperative walking where wearing the robotic suit was uneasy and sometimes the walking was forcibly suspended for the joint angle over speed. Therefore, a more reliable judging index and algorithm are necessary in the future walking experiments. Using a reaction force sensor may be helpful for exact judgment of the knee joint motion. Next step will make a reliable sensor which is easy to use.

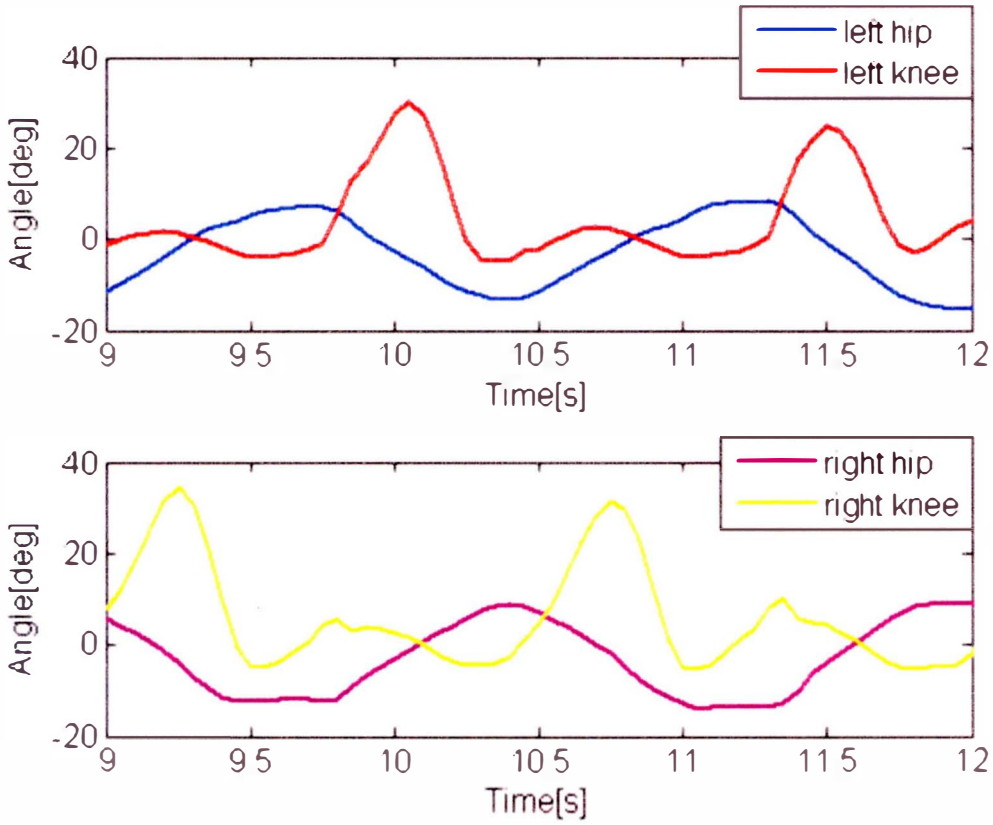

Fig.8.5. 1 Failure case of the judgment algorithm

8.5.2 Remained work

1, Due to the current system, the connection among neural oscillator made about 1.3 π phase difference between the left hip and the second knee joint flexion-extension. However, the natural phase difference was about 1.1 π according to our measurement. The errors of phase difference between the natural walking and designed trajectory should be re-considered, and its effect on the cooperative walking should be investigated in the following work.

2, In this study, we only investigated the walking in the straight direction. The turning movement should be investigated as a next step in the following work.

3, So far, we only discussed the possible potential of our proposal for walking assist, that is, the robotic suit was able to move passively to assist walking with a high synchronization level. However, the robotic suit with a low synchronization level could move actively to provide motion training. The latter possible potential will be examined in the following work.

References

[1] 石井慎一郎, "歩行動作における動作支援のバイオメカニクス, "理学療法, 27 巻 1 号, pp.56-65, 2010

[2] Kiyotoshi Matsuoka, "Sustained Oscillations Generated by Mutually Inhibiting Neurons with Adaptation," *Biological Cybernetics,* vol.52,pp.367-376,1985.

Chapter 9

Conclusion

Chapter 9 Conclusion

In this study, we proposed synchronization-based control using neural oscillators for a wearable robotic suit designed for walking assist. In order to realize synchronization between a human user and the robotic suit, a neural oscillator is connected to each joint of the suit to synchronize the robotic suit's motion with that of human user. In addition, we introduced a gain to switch the neural oscillator to be synchronous and non-synchronous status with the input, thus the robotic suit could switch its assist model to be synchronous or non-synchronous for different assist requirement. Furthermore, coordination movement among the suit's multiple joints is achieved by the incorporation among neural oscillators.

We proposed two ways that can be thought to realize synchronization-based assist using the neural oscillator, one is synchronization-based motion assist and the other is synchronization-based power assist. We investigated the mechanism of the two kinds of synchronization-based assist methods using simulations and experiments. Basing on the results, we compared the two kinds of control methods, and finally chose the synchronization-based motion assist method in further study for walking assist, for its simple system, which also helps the robot act synchronously and provide assist. In addition, the attenuation of neural oscillator makes the desired angle of the robot to be generated more reasonably for motion assist, and the assist action to be more compliant.

Firstly, in the preliminary simulations and experiments on the knee joint flexion–extension movement assist, we verified the validity of our proposal and concluded the following: by using synchronization based control, firstly, the synchronization motion can be realized; secondly, the motion assist effect has been obtained; We also compared our proposal to the conventional impedance control to verify that this approach has a good usability.

Secondly, a series of walking experiments were conducted with a two-DOF robotic suit that assists by supporting hip joint movement and maintaining an anti-phase relationship in walking. We proposed incorporation of mutual inhibition between neural oscillators for the walking stability assistance of a robotic suit by maintaining anti-phase movement of the left and right hip joints. The validity of incorporation between neural oscillators for walking stability was discussed and confirmed using walking experiments with the two-DOF robotic suit. Results

show that 1) synchronization was achieved; 2) the synchronization-based motion assist method works for walking assistance; and 3) stable assistance can be provided with our design of mutual inhibition between neural oscillators connected to the robotic suit.

We have designed a four-DOF wearable robotic suit to assist a user to walk. The robotic suit has three new features. First, a new control architecture was developed to enable the robotic suit synchronize with a user. Second, utilizing Harmonic Drive Gear and its built-in torque sensor, a compact structure of the robotic suit with relative high power is realized. Third, the synchronization-based control was developed that controls the robotic suit through measurements of the mutual joint torque, thus there is no need to apply any sensor to a user body to get the user's move intension.

We implemented our proposal to the four-DOF robotic suit designed for walking assist. We proposed the symmetrical and unsymmetrical inhibitory connections among neural oscillators to reproduce the phase differences of natural walking. To realize natural walking, we considered regulating amplitude corresponding to the knee joint's first/second flexion-extension motion. We verified that our proposed model was valid for realization of the anti-phase relationship between the left-right legs and about 0.25π phase differences between the hip-knee joints on the ipsilateral side, and we verified that the amplitude regulation algorithm helped to realize the trajectories of natural walking by conducting walking experiments. Evaluations on the assist effect and the usability of the four-DOF robotic suit haven't yet been done in the current study.

The basic idea in this thesis was to propose an interaction approach for controlling a robotic suit, thus providing flexible walking assist (by increasing the step length and lowering physical effort). Furthermore, this thesis presented our first attempt towards maintaining stable assistance using the inhibitory connections of neural oscillators.

Acknowledgement

This work was supported by a Grant-in-Aid for Global COE Program awarded by the Ministry of Education, Culture, Sports, Science, and Technology of Japan. Support was also provided by Kakenhi (19560255). Harmonic Drive Systems Company provides actuators.

The research achievements reported in this thesis is the result of the combined efforts of all colleagues who have been working hard to give me generous support.

First and foremost, I would like to appreciate the advice offered by Prof. Atsushi Nishikawa, Associate Prof. Takashi Kawamura, and Associate Prof. Hiroaki Yoshida and their efforts that went into reviewing this thesis.

I would like to express my heartfelt respect to my supervisor, Prof. Minoru Hashimoto, for his rigorous instruction with professional knowledge to help me throughout the whole process of accomplishing this thesis.

I would like to express my grateful respect to my tutor, Prof. Hirohisa Morikawa, for his advice and kind help every time I inquired him about the solutions to difficulties that I encountered.

I would like to show my heartfelt thanks to Japanese government for the scholarship supporting me during the whole study period in Japan.

I would like to thank my colleagues in our laboratory for their generous assistance in every aspect in my life and warm encouragement during my study in Japan.

Finally, thank my dear family from the bottom of my heart for their full support, understanding and encouragement.